DELAY AND COLLISION REDUCTION IN WIRELESS NETWORKS

by

Seyedmohammad Salehi

A dissertation submitted to the Faculty of the University of Delaware in partial fulfillment of the requirements for the degree of Doctor of Philosophy in Computer Science

Winter 2020

ACKNOWLEDGEMENTS

I would like to express my gratitude to my Ph.D. supervisor, Professor Chien-Chung Shen for guiding me through each step of the way, and spending countless hours to read and revise my work. I also would like to thank my Ph.D. committee members for their insightful remarks and support, our collaborators from Cisco Systems for the funding and guidance, and other kind people at the University of Delaware without whom I could not have finished my Ph.D., Dr. Mary Martin, Dr. Andrew Roosen and Dr. Bryan Youse.

I also would like to thank my beautiful family members who encouraged, supported, and guided me not only during my PhD years but throughout my life: my parents, my grandparents, my sisters, my aunts and my uncles. I also would like to thank Dr. Hossein Cheraghi for his guidance and support, my close friends Vahab, Ahad, and Navid for their encouragements, and my colleagues, Li, Hao, and Guangyi for their companionship and helpful discussions. Finally, special thanks to my wife, Tiphanie, whose constant support made me accomplish this goal.

To my mother, Monireh.

TABLE OF CONTENTS

Chapter

LIST OF TABLES

LIST OF FIGURES

GLOSSARY

AC	Access Category
AIFS	Arbitration Inter-Frame Spacing
AMPDU	Aggregated MAC Protocol Data Unit
AMSDU	Aggregated MAC Service Data Unit
ASV	Autonomous Surface Vehicle
AUV	Autonomous Underwater Vehicle
BA	Block Acknowledgement
BER	Bit Error Rate
BEB	Binary Exponential Backoff
BSR	Buffer Status Report
BSRP	Buffer Status Report Poll
BSS	Basic Service Set
CS	Carrier Sensing
CSMA/CA	Carrier Sense Multiple Access with Collision Avoidance
CSMA/ECA	Carrier Sense Multiple Access with Enhanced Collision Avoidance
CSMA/ECA-DR	Carrier Sense Multiple Access with Enhanced Collision Avoidance and Distributed Reservation
CW	Contention Window
DBFD	Destination Based Full Duplex
DCF	Distributed Coordination Function
DR	Distributed Reservation

DL	Downlink
ED	Energy Detection
EDCA	Enhanced Distributed Channel Access
FD	Full Duplex
HD	Half Duplex
HMD	Head Mounted Display
IBFD	In-Band Full Duplex
IP	Internet Protocol
OBSS	Overlapping Basic Service Set
OFDM	Orthogonal Frequency Division Multiplexing
OFDMA	Orthogonal Frequency Division Multiple Access
NAC	Number of Active Contenders
NAV	Network Allocation Vector
MAC	Medium Access Control
MIMO	Multiple Input Multiple Output
MPDU	MAC Protocol Data Unit
MPDU	MAC Service Data Unit
MU-MIMO	Multi-User Multiple Input Multiple Output
PHY	Physical layer
PLCP	Physical Layer Convergence Protocol
PPDU	PLCP Protocol Data Unit
PSDU	PLCP Service Data Unit
QoE	Quality of Experience
QoS	Quality of Service
RF	Radio Frequency
RTS/CTS	Request To Send / Clear To Send

SBFD	Source Based Full Duplex
SINR	Signal to Interference plus Noise Ratio
SIR	Signal to Interference Ratio
TB	Trigger Based
TDD	Time Division Duplex
ToS	Type of Service
TF	Trigger Frame
TXOP	Transmission Opportunity
VOIP	Voice over IP
WLAN	Wireless Local Area Network
UASN	Underwater Acoustic Sensor Network
UL	Uplink

ABSTRACT

With the ever-increasing wireless data demand and limited wireless spectrum resources, to increase the capacity of wireless networks and to make more efficient use of the wireless spectrum have become two key challenges. On the one hand, new technologies are invented to increase the data rate and capacity of wireless networks. On the other hand, new data-hungry applications (e.g., interactive high-resolution video games and augmented and virtual reality) and delay-sensitive applications (e.g., real-time voice over IP and virtual reality) need more bandwidth and more frequent channel access, respectively. Medium access control (MAC) protocols located at the second layer of the Internet protocol stack (i.e., Link layer) are responsible for coordinating transmissions of different wireless stations to reduce end-to-end delay, collisions, and battery consumption, and to increase the overall throughput of the wireless networks. Since different layers of the Internet protocol stack are isolated from each other (to facilitate innovation in each layer separate from the others), when a new wireless communication technology requires enhancements in some criteria, new MAC protocols can be designed to address the needs.

In this dissertation, we design new MAC protocols for different wireless communication technologies so as to reduce the collision and end-to-end delay among stations while increasing the overall throughput of the wireless network. To that end, we develop innovative access mechanisms, scheduling techniques, and architectures, and with simulations, measure the performance of networks working with these protocols based on the popular metrics of throughput, delay, and jitter among others. Finally, we compare the performance of the proposed protocols with state-of-the-art solutions.

For wireless local area networks (WLANs), since the scheduling of packet transmissions solely relies on the collision and/or success a station may experience, we propose a distributed reservation mechanism for the Carrier Sense Multiple Access Extended Collision Avoidance (CSMA/ECA) MAC protocol, termed CSMA/ECA-DR. In CSMA/ECA-DR, stations collaboratively achieve higher network performance by avoiding anticipated collisions. In addition, proper Contention Window (CW) size will be chosen based on the instantaneously estimated number of active contenders in the network. Moreover, as the technology of full-duplex (FD) wireless communications (transmit/receive at the same time on the same frequency) has become feasible, and is orthogonal to other technologies in terms of increasing the capacity of wireless networks, we design a novel FD MAC protocol based on CSMA/ECA-DR.

Furthermore, a new standard of IEEE 802.11 (i.e., WLAN), 802.11ax, has been standardized in late 2019. The new standard incorporates the technology of orthogonal frequency-division multiple access (OFDMA) to reduce collisions among stations and better satisfy the quality of service (QoS) for different types of traffic. Although OFDMA is not a new technology, due to intricacies associates with OFDMA usage in IEEE 802.11ax, new MAC scheduling algorithms are required to work with this Wi-Fi standard. We design a station selection algorithm and a scheduler for 802.11ax that can satisfy QoS requirements of different traffic types even in dense deployments. We further enhance the designed mechanisms to support virtual reality (VR) applications with IEEE 802.11ax.

For underwater acoustic networks (UANs), we study the problem of energy-efficient acoustic networking. In addition, we design a new hybrid architecture that can increase the throughput while reducing the end-to-end delay between different pairs of autonomous underwater vehicles (AUVs). Furthermore, we design an FD MAC protocol that is capable of multi-targeted transmissions and adjusting transmitting

power based on distances between nodes.

Chapter 1

INTRODUCTION

1.1 Background

Wireless communications and networking have enabled mobile users and devices to be connected to their destinations to transmit and receive data. In general, wireless networks can be divided into two classes: (1) *infrastructure-based* networks in which transmissions are to/from a pre-existing base station, and (2) *ad hoc* networks in which devices can communicate with each other directly without any base station. Depending on the situations and use cases, the types of wireless networks to be used are different. For instance, ad hoc networks are suited in emergency situations such as natural disasters or military conflicts where no pre-existing infrastructure exists.

Resources are limited in wireless networks. For example, wireless spectrum is scarce and wireless devices are usually battery-powered. With the ubiquity of wireless devices and ever-growing data demand with different quality of service (QoS) requirements, increasing the capacity of wireless networks and coordinating efficient transmissions among wireless devices became two key challenges. Although new technologies have emerged to increase the capacity of wireless networks, efficient usage of these technologies calls for new techniques in resource scheduling to maximize the battery life of, and minimize delay and interference among wireless devices.

With the new technologies, scarcity of wireless resources, increasing data demand and delay-constrained applications, efficient MAC protocols are needed to satisfy users' and applications' QoS requirements. In this dissertation, we propose to investigate different methods to reduce delay and collisions in wireless networks. Specifically,

1

for terrestrial wireless networks, Chapter 2 presents a distributed reservation protocol, termed CSMA/ECA-DR to reduce frame collision among stations in wireless local area network (WLAN). A novel full-duplex MAC protocol based on CSMA/ECA-DR is presented in Chapter 3 to make use of the full-duplex transmission capability. In Chapter 4, we propose a learning mechanism for transmission intervals, a station selection algorithm and a scheduling mechanism for the IEEE 802.11ax (Wi-Fi 6) standard. In Chapter 5, the station selection mechanism and the scheduling framework are further enhanced to support VR applications with IEEE 802.11ax. For underwater acoustic networks, a new hybrid acoustic-Wi-Fi architecture is proposed in Chapter 6 which significantly reduces the end-to-end delay among autonomous underwater vehicles (AUVs). Chapter 7 discusses the energy consumption of acoustic communications and presents a full-duplex, energy-efficient MAC protocol for underwater acoustic sensor networks (UASNs) and Chapter 8 concludes the thesis with future research directions. In the remainder of this chapter, we summarize the motivations, goals and problem statements of our research.

1.2   Research Motivation, Goals, and Problem Statements

1.2.1   Traffic Differentiation in Dense WLANs with CSMA/ECA-DR MAC Protocol

Increasing data demand with stringent QoS requirements has densified the deployments of wireless base stations. However, the performance of carrier-sense multiple access with collision avoidance (CSMA/CA), the standardized medium access control (MAC) protocol for wireless local area networks (WLAN), degrades with increasing number of stations. There is extensive research to improve the performance of CSMA/CA. One recent success is carrier-sense multiple access with enhanced collision

avoidance (CSMA/ECA), a protocol to replace CSMA/CA's random backoff with deterministic backoff after successful transmissions. In saturated scenarios with the single traffic type case, CSMA/ECA can reach a collision-free schedule even in dense deployments [2]. However, with traffic differentiation comprising both voice and video, due to the unsaturated behavior of these traffic types, CSMA/ECA is not able to achieve a collision-free schedule, which results in higher delay for delay-constrained traffic in dense deployments.

In this research effort, we identify issues of the binary exponential backoff (BEB) algorithm that is used in both CSMA/CA and CSMA/ECA. Specifically, choosing a random backoff from the minimum contention window (CW_{min}) after receiving a packet in transmit queue and doubling the CW after each collision do not always lead to the best results. We propose a new MAC protocol, CSMA/ECA with distributed reservation (termed CSMA/ECA-DR). In CSMA/ECA, a station chooses a deterministic backoff after a successful transmission which is computed from the CW_{min} and the transmitting backoff stage. Therefore, if a transmitting station includes the transmitting backoff stage in its transmission, owing to the broadcast nature of wireless transmissions, each station receiving the transmission can compute the next transmission of the transmitting station (in terms of time slots) and avoid choosing a backoff value that might collide with that transmission. CSMA/ECA-DR also employs the idea of adaptive CW selection for different traffic types based on the instantaneous traffic load of the network. Simulation results demonstrate that CSMA/ECA-DR can achieve significantly higher performance than both CSMA/CA and CSMA/ECA, even in dense deployments with traffic differentiation.

1.2.2   Full-Duplex MAC Protocol based on CSMA/ECA-DR

Today's wireless communications are half-duplex (HD), where a station can either transmit or receive, but not both at the same time. Recently, full-duplex (FD) communications, where a station can simultaneously transmit and receive at the same time over the same frequency, have been made possible by canceling the interference that the transmission of a station has on its own reception. FD technology can increase the capacity of wireless networks and is orthogonal to other technologies (i.e., FD can be used alongside other technologies). However, unlike HD communications that only engage two stations, FD communications can be among three stations or a chain of stations. Hence, HD MAC protocols cannot fully utilize the benefits of the FD technology and new MAC protocols are needed. Since simultaneous transmission and reception would happen at the same time, recently proposed FD MAC protocols use the RTS/CTS mechanism to choose the same backoff slots (i.e, synchronize) to form an FD communication. However, in traffic differentiation comprising small packets, the four-way handshake used in RTS/CTS can waste the channel time and incur higher delays for some applications (e.g., voice).

This research focuses on adapting the CSMA/ECA-DR MAC protocol for wireless FD communications. Since each station can compute the time of the next transmission of a transmitting station, stations can refrain from transmitting that might collide with the transmitting station, except the recipient of the transmission (the destination station) that will choose a backoff equal to the computed time of the next transmission of the transmitting station and will form an FD transmission (either to the transmitting station or to another station). Thus, in FD CSMA/ECA-DR, the expensive RTS/CTS mechanism is no longer needed. Simulation results show that network throughput increases significantly with FD CSMA/ECA-DR.

1.2.3 Uplink OFDMA Framework for IEEE 802.11ax (Wi-Fi 6)

Wi-Fi is the most popular WLAN technology based on the IEEE 802.11 standards. Unlike former standards of Wi-Fi (e.g., a/b/g/n/ac) in which resources are allocated only in time domain, in the new Wi-Fi standard, 802.11ax or Wi-Fi 6, resources are allocated in both time and frequency domains which is called orthogonal frequency-division multiple access (OFDMA). In OFDMA, multiple stations can receive and transmit from/to access point (AP) simultaneously using different chunks of the bandwidth. Because of the intricacies associated with OFDMA scheduling, both downlink and uplink resource allocations are performed by the base station. Although OFDMA has been used in cellular networks, such as Long Term Evolution (LTE) and IEEE 802.16 (i.e., WiMAX), for a long time, it has only been recently adopted into IEEE 802.11ax. Due to the fundamental differences in scheduling between Wi-Fi and cellular networks, schedulers designed for LTE cannot be directly applied to IEEE 802.11ax. Hence, new schedulers need to be designed to efficiently schedule resources for different stations based on their traffic requirements.

Ideally, a scheduler is required to maximize the Quality of Service (QoS) of stations with delay-sensitive traffic (such as voice and video) while being fair to stations that have best effort traffic. In this research, we divide the problem of scheduling and resource allocation in 802.11ax into station selection, scheduling and duration computations, and design techniques for each part. For station selection mechanism, based on the ability of MAC protocol to impose intervals on the transmission of different access categories, we design a learning technique whereby the AP can learn these intervals and serve stations when they actually have pending frames for the AP. For scheduling, we defined utility functions based on the station's rate, type of service, and queue depth and design a recursive algorithm that assigns to each station a proper size resource unit. For duration computations, we formulate an optimization function that

takes into account the frame durations and overheads.

1.2.4 Extending Channel/QoS-aware Scheduler to support VR traffic

Recently, virtual reality (VR), augmented reality (AR) and the combinations of them termed "mixed reality" (MR) have attracted a lot of attention. In particular, the wide range of VR applications in military, healthcare, education, business, entertainment, and engineering, to name a few, made this technology one of the top research topics in both industry and academia. However, compared to other video traffic types, VR traffic has larger frames and much lower delay-budget. Therefore, VR head mounted displays (HMDs) are usually wire-connected to the computers to which the video rendering is delegated. However, there are two serious issues with this approach: (1) the lack of user mobility, and (2) the need for advanced, expensive video cards. With the rise of Edge computing (also known as Fog computing), rendering of video can be transferred to the edge. Also, mobility can be supported with wireless communications. However, with the current contention-based Wi-Fi technology, protocol optimizations across all the layers of the network stack can only support a few VR devices in low interference situations. Therefore, other communication technologies such as mmWave (WiGig and 5G New Radio) have become the options to support VR. However, they both require their specific base stations. Moreover, 5G is not free.

By making the best use of OFDMA, in this study, we investigate the possibility of supporting VR traffic with its stringent QoS requirements in the context of 802.11ax. We enhance our proposed station selection algorithm and the scheduling mechanism to reduce the delay of VR traffic in both uplink and downlink transmissions. In recursive scheduling, we found that if stations of different access category are divided equally in both sides of the bandwidth tree, the scheduler is able to allocate the proper size resource unit to the station with higher priority. Therefore, splitting should happen

6

when high priority traffic with large queue length is considered for scheduling.

1.2.5 Hybrid Infrastructure for AUV Operations

Coordinated sampling via autonomous underwater vehicles (AUVs) is a major trend in ocean monitoring and exploration. However, the current underwater communication and networking technologies are still primitive, as they cannot provide the needed reliability and data rates for the navigating AUVs. As the main means for information exchange, underwater acoustic communications suffer from limited bandwidth and large propagation delay. Therefore, compared to terrestrial wireless networks, the efficiency of direct underwater communications is very low.

In this research, we design a hybrid network infrastructure to support communications and networking among multiple AUVs. As an alternative to direct AUV-to-AUV acoustic communications, the hybrid architecture uses autonomous surface vehicles (ASVs) that are connected by the radio-frequency (RF) wireless links as a high data rate backbone above the sea surface. At the same time, ASVs serve as mobile acoustic base stations to meet the communication needs of the navigating AUVs. This architecture uses a fleet of ASVs to increase the achievable network throughput and to reduce latency. Moreover, direct AUV to ASV communications reduce the refraction and multi-path effect because of close-to-vertical communications to achieve higher data rates in practice. Through extensive simulations using the ns-3 network simulator, we compare network throughput and end-to-end delay of different scenarios between hybrid and pure acoustic networks.

1.2.6 Full-Duplex MAC Protocol for Underwater Acoustic Communications

Due to resource constraints in underwater acoustic communications, MAC protocols should maximize the performance of underwater acoustic networks (UANs) by

taking into account the energy consumption of nodes and reducing transmission collisions and end-to-end delay between the underwater nodes. The ideal goal is to transfer information with no collisions. However, due to the fact that nodes are mobile with the sea current and might frequently join and leave the network, building a collision-free network, if not impossible, is an arduous task. Recently, proposed MAC protocols try to incorporate different learning techniques to reduce collisions and increase the throughput of underwater acoustic networks but there is no protocol that reduces the energy consumption with the multi-targeted transmissions.

In this research, we design a new MAC protocol that incorporates multi-targeted transmissions in the MAC layer. For instance, if a node is transmitting an acknowledgement frame, it can aggregate a request-to-send (RTS) to another node. Additionally, to enable FD communications, the protocol takes into account and adjusts the transmitting power of each node to reduce interference in multi-node FD transmissions. The protocol retains the performance of an underwater acoustic network with higher energy efficiency in half-duplex communications and efficiently increase the performance in full-duplex scenarios.

Chapter 2

TRAFFIC DIFFERENTIATION IN DENSE WLANS WITH CSMA/ECA-DR MAC PROTOCOL

2.1 Introduction

Recently, the usage of wireless networks have surpassed the wired networks and as forecast by Cisco's Visual Networking Index (VNI), global IP traffic is expected to increase three-fold reaching an annual run rate of 3.3 zettabytes by 2021, and 53% of such traffic will be accessed via Wi-Fi [3]. In addition, as depicted in Fig. 2.1, Machine-to-Machine (M2M) communications will be the fastest-growing category of devices and connections [3]. Unlike previous generations, the intent of 5G will not be solely to standardize new innovations, but be mostly as a platform to aggregate existing and future technologies and to enable their efficient coexistence [4]. To increase throughput and satisfy QoS requirements of increasing number of mobile devices, one solution is to replace/accompany macro cells by/with micro cells (nano, femto, and pico cells). However, this approach would cause more transmission contentions. Therefore, there is an excessive urgency for upper layers in the network stack (MAC and cross-layer protocols), to efficiently coordinate data transmissions and adapt to the network traffic changes.

Although innovations have been made at the physical (PHY) layer of the 802.11 family, such as MIMO, MU-MIMO, massive MIMO, beamforming, and OFDMA, the underlying CSMA/CA algorithm of Wi-Fi's medium access control (MAC) layer is almost intact from one standard to another [5]. To share wireless spectrum among contending Wi-Fi stations, Distributed Coordination Function (DCF) employs CSMA/CA
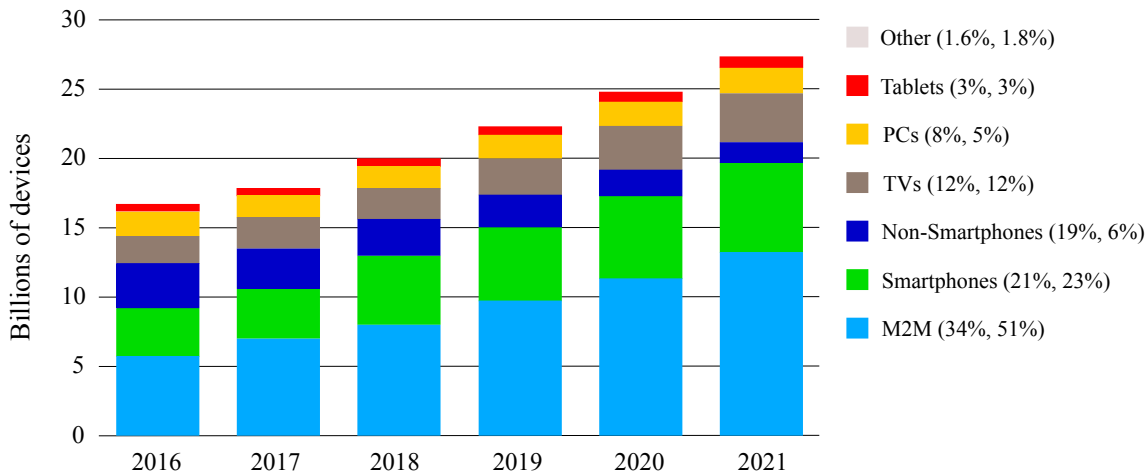
Figure 2.1: Cisco's forecast of devices and connections. By 2021, M2M connections will be 51% of the total devices and connections.

with Binary Exponential Backoff. For traffic differentiation, Enhanced Distributed Channel Access (EDCA) specializes DCF parameters for different traffic Access Categories (ACs) as well as giving more channel access time to high priority ACs by giving them different Arbitration Inter-Frame Spacing (AIFS) values and TXOP durations based on IEEE 802.11e.However, in dense scenarios, performance of EDCA severely degrades with increasing number of contenders and resultant collisions [2]. In particular, to satisfy QoS requirements, delay-sensitive traffic will blindly be given more channel access time, which may further increase the collision probability, and hence negatively affect the overall efficiency of the channel and QoS/QoE in dense scenarios [6].

Recently, there have been several efforts to improve CSMA/CA for emerging Wi-Fi standards [2, 6–13]. Specifically, to address high collision rates in dense scenarios, different techniques have been developed to achieve collision-free schedules or reduce collisions by choosing optimal CW values. In particular, using CSMA Enhanced Collision Avoidance with Hysteresis and Fair Share (CSMA/ECA$_{Hys+FS}$) [2, 6, 7], upon

a successful transmission, a station chooses the 'expected value' of the Contention Window (CW) in which it just transmitted as its next backoff value (termed *deterministic backoff*). This will gradually create a collision-free schedule in single traffic scenarios but is unable to achieve collision-free schedule in traffic differentiation.

Our goal is to further reduce collisions in both saturated and unsaturated dense scenarios with traffic differentiation. To achieve this goal, we extend CSMA/ECA$_{\text{Hys+FS}}$ [6] to propose CSMA/ECA$_{\text{Hys+FS}}$ with *Distributed Reservation* (termed CSMA/ECA-DR$_{\text{Hys+FS}}$), where stations add their transmitting backoff stage (a 3-bit field) into transmitted MAC frame headers. Owing to the broadcast nature of wireless transmissions, other stations overhearing the transmitted frame(s) are also able to extract the current backoff stage of the transmitting station. Since in CSMA/ECA$_{\text{Hys+FS}}$, the current CW is derived from both backoff stage and CW_{min}, other stations can compute the future transmissions of the transmitting station (in terms of time slots) to avoid future 'predicted' collisions with their own transmissions. CSMA/ECA-DR$_{\text{Hys+FS}}$ also employs Kalman filter [14] to adjust the CW size of different traffic categories based on the estimated number of active contenders. Through extensive simulations, we show that CSMA/ECA-DR$_{\text{Hys+FS}}$ (hereafter, referred to as ECA-DR) outperforms CSMA/ECA$_{\text{Hys+FS}}$ (hereafter, referred to as ECA) in both saturated and non-saturated dense scenarios.

The rest of this chapter is organized as follows. Related research is summarized in Section 2.2. Section 2.3 describes ECA-DR in detail. Section 2.4 presents simulation settings and traffic models used for the simulations followed by simulation results and evaluation. Section 2.5 summarizes this chapter with future research directions.

2.2 Related Work

The closest work to ECA-DR is EBA [15] which is a distributed reservation mechanism designed to improve CSMA/CA with a single type of traffic. Using EBA, a station announces to other stations its future random backoff value and current offset (so that recipients can synchronize their reservation windows) in a 24-bit field piggy-backed on each transmitted MAC frame header. A receiving station should keep a reservation window to compute its next backoff value based on the announcement overheard and choose the offset if it is not an active transmitter (i.e., no packet[1] in its queue). However, the backoff value is chosen randomly and, hence, would not help to reduce collisions among a large number of contenders.

Instead, a station using ECA-DR shares its *backoff stage* value with other stations, in a **3-bit** field added to the MAC frame header. Since ECA-DR is based on ECA, a station chooses the expected value of CW in which it transmitted its frames and hence, other stations overhearing the transmitting station could compute *both* the future transmission time of the transmitting station *and* the number of frames to be transmitted. Instead of keeping a reservation window as in EBA (which incurs higher memory usage and computational cost), each station, using ECA-DR, only keeps the prohibited backoff values, decreases them with its own backoff values (if it has packets to transmit), and avoids choosing them for its future transmissions.

In addition, adaptive selection of optimal CW size based on different measured criteria in the network has been shown to improve the performance of CSMA/CA. Such criteria can be the number of contenders estimated based on Conditional Collision Probability (P_{cc}) [9, 14]; the number of contenders and average idle slots [10]; the channel utilization ratio and retransmit counts [11]; the channel Bit Error Ratio (BER), backoff parameters and contention level [12, 16]; the delay deviation and

---

[1] Packet and frame are used interchangeably in this work and both refer to MAC layer PDU (M-PDU).

channel congestion status [13], etc. Specifically, ECA-DR uses P_{cc} to approximate the number of active contenders and selects the appropriate backoff stage for different traffic categories both between two unsuccessful transmissions and when the backoff stage is supposed to be reset to zero.

2.3 Description of ECA-DR

Algorithm 1[2] without the blue lines represents ECA with traffic differentiation. It is important to note that usage of AIFS violates the assumption that all backlogged stations simultaneously decrease their backoff values after each slot, and hence, AIFS is not practical in ECA and ECA-DR [17]. Unlike CSMA/CA in which successive transmissions of a station have no correlation with each other (even after successful transmissions, the backoff stage (k_i) will be reset to zero), ECA would relate successive successful transmissions of a station by the "Hysteresis" mechanism (i.e., choosing the expected value of the transmitting CW as the next backoff value, line 31). The issue of fairness among stations that wait longer to transmit is also addressed by the "Fair Share" mechanism which relates the number of transmitting frames to the transmitting backoff stage, k_i (line 21).

———————————————————

[2] This algorithm is borrowed from [2] and adapted to traffic differentiation using ECA-DR.

Algorithm 1 ECA-DR with Traffic Differentiation

1: **while** the device is on **do**
2:     $R \leftarrow 6; K \leftarrow 5; AC \leftarrow 4;$
3:     $BIV = 1;$ ▷ BOS increase value
4:     $CW_{min}[AC] \leftarrow [32, 32, 16, 8];$
5:     **for** $i \leftarrow 0$ to $AC - 1$ **do**
6:         $r_i \leftarrow 0; k_i \leftarrow 0;$
7:         $B_i \leftarrow \mathcal{U}[0, 2^{k_i}CW_{min}[i] - 1];$
8:     **end for**
9:     **while** there is a packet in Q_i to transmit **do**
10:         **repeat**
11:             **while** $B_i > 0$ **do**
12:                 Wait 1 slot;
13:                 $B_i \leftarrow B_i - 1;$
14:                 **if** overheard a packet (p) **then**
15:                     $NT \leftarrow (2^{p.b}CW_{min}[p.AC])/2 - 1;$
16:                     **if** $B_i = NT$ **then**
17:                         $B_i \leftarrow \mathcal{U}[0, 2^{k_i}CW_{min}[i] - 1];$
18:                     **end if**
19:                 **end if**
20:             **end while**
21:             Transmit 2^{k_i} packet(s);   ▷ Fair Share
22:             **if** collision **then**
23:                 $r_i \leftarrow r_i + 1;$
24:                 Choose BIV based on Estimated NAC;
25:                 $k_i \leftarrow \min(k_i + BIV, K);$
26:                 $B_i \leftarrow \mathcal{U}[0, 2^{k_i}CW_{min}[i] - 1];$
27:             **end if**
28:         **until** $(r_i = R)$ or (success)
29:         $r_i \leftarrow 0;$
30:         **if** success **then**
31:             $B_i \leftarrow (2^{k_i}CW_{min}[i])/2 - 1;$ ▷ Hysteresis
32:         **else**
33:             Discard 2^{k_i} packet(s);
34:             $k_i \leftarrow 0;$
35:             Choose k_i based on Estimated NAC;
36:             $B_i \leftarrow \mathcal{U}[0, 2^{k_i}CW_{min}[i] - 1]$
37:         **end if**
38:     **end while**
39:     Wait for a packet in Q_i to transmit;
40:     $k_i \leftarrow 0;$
41:     Choose k_i based on Estimated NAC;
42:     $B_i \leftarrow \mathcal{U}[0, 2^{k_i}CW_{min}[i] - 1];$
43: **end while**

ECA only reaches a collision-free schedule in saturated single traffic scenarios, since almost all contenders will converge to the same CW. However, ECA is unable to converge to a collision-free schedule in traffic differentiation or unsaturated scenarios within dense deployments. In traffic differentiation, delay-sensitive access categories (AC) require frequent transmissions and hence shorter transmission intervals (and CW sizes). However, among the deterministic backoff values computed by Algorithm 1 (i.e., 3, 7, 15, 31, 63, 127, 255, 511), 15 is divisible by 3 (AC[VO], the voice AC, in backoff stage 0) and 63 is divisible by 7 (AC[VO] in backoff stage 1 and AC[VI], the video AC, in backoff stage 0). Thus, AC[VO] and AC[VI] might collide with other traffic categories or the same traffic categories with larger deterministic backoff values.In unsaturated scenarios, due to frequent queue flushes, a station might not retain its deterministic backoff value for a long time. This is followed by choosing random backoff values with resultant collision increase in dense scenarios. The proposed distributed reservation mechanism of ECA-DR correctly identifies these collisions and prevents them from happening.

2.3.1   Distributed Channel Reservation

The blue-colored section in Algorithm 1 depicts the general inner workings of ECA-DR and its integration with ECA. To compute the next transmission time (in terms of time slots) of a transmitting station, an overhearing station requires the knowledge of the type of overheard traffic, its CW_{min} and the transmitting backoff stage. The type of traffic can be extracted from the "TID" subfield of the "QoS Control" field in the MAC header (denoted by p.AC in line 14) and CW_{min} for that type of traffic is based on IEEE 802.11e. Also, the added 3-bit field to the MAC frame header contains the transmitting backoff stage (p.b). Line 14 shows the computation of the next transmission time of an overheard frame. After computing the next transmission

time, the overhearing station compares the next transmission time with its own backoff values of backlogged traffic categories (line 15). If a collision is predicted with any of the station's traffic categories, the station should choose another random backoff value.

The 3-bit field can represent numbers 0 to 7 in binary, but the maximum backoff stage will not exceed 5 or 6 (5 in our simulations). If a station finds its queue empty, it will announce its queue status (similar to setting the "More Data" subfield of the "Frame Control" field) by setting the 3-bit field to 7 (i.e., 111 in binary) in order not to prevent other stations from choosing the station's deterministic backoff value computed in Algorithm 1 as NT. If the backoff stage value is less than 7, the next transmission (NT) will be added to the list of prohibited backoff values kept by each station. If a station requires a random backoff value for any of its traffic categories (new packet in an empty queue or after collision), it avoids choosing the prohibited values. Note that once a prohibited value is added to the list of prohibited values of a station, a station should count it down with its own backoff values for each passing time slot. If the station does not have any packet in its queues, it should still count down the prohibited values for each passing time slot.

In our simulations we put this 3-bit field in the Address 4 field of MAC frame header so as to avoid any MAC frame header overhead. Including transmitting backoff stage into the MAC frame header also plays the role of RTS control frame. In order to avoid hidden terminals in multi-hop and overlapping basic service set (OBSS) scenarios, a receiver should also include this field in the ACK control frame to also play the role of CTS control frame. Unlike RTS/CTS that reserves the channel for a transmission that follows CTS, the distributed reservation mechanism of ECA-DR only instructs the overhearing stations to refrain from transmission at the next transmission of a transmitting station (i.e., the overhearing stations may transmit before or after). Therefore, distributed reservation does play the role of RTS/CTS without four-way

handshake which is important for short frames and delay-sensitive applications.
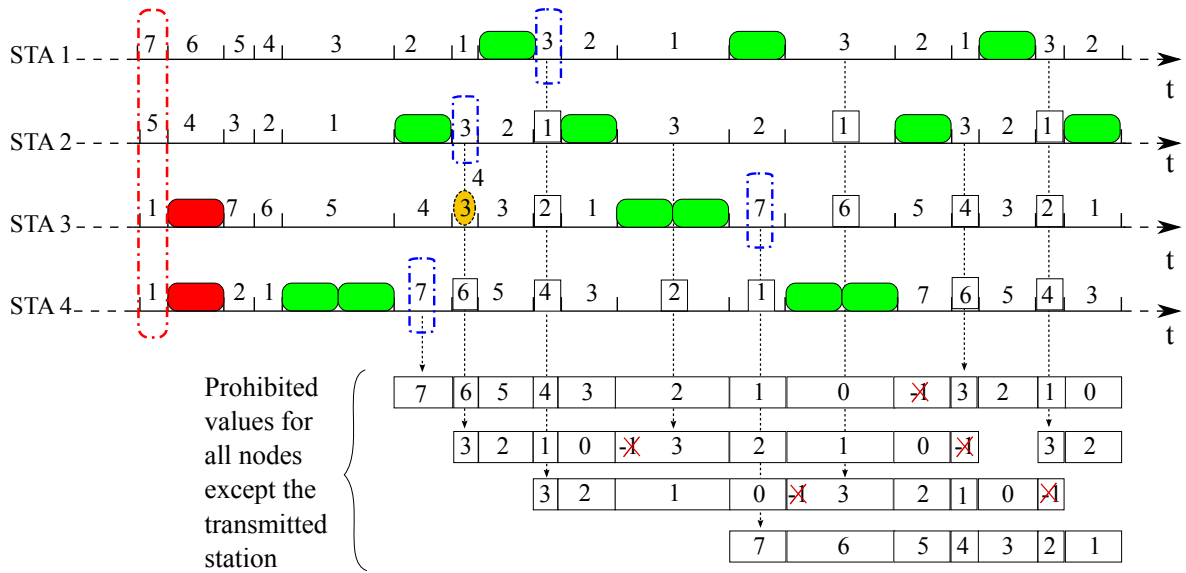
Figure 2.2: An example of the ECA-DR protocol. STAs collaborate to reduce the anticipated collisions which helps keep the delay of high priority application within their QoS requirements even in dense network deployments.

Figure 2.2 illustrates an example of our proposed ECA-DR protocol. Consider four STAs in this example (STA-1 and STA-2 with voice traffic and STA-3 and STA-4 with video traffic) choose random backoffs from their CW_{min} ranges (8 and 16, respectively), the values 7, 5, 1, 1. After one time slot, STA-3 and STA-4 would transmit one frame as their backoff reaches zero. Since the simultaneous transmissions lead to a collision, they increase their backoff stage (k) to 1, and hence, from a doubled CW, they choose another random backoff, 7 and 2, respectively. However, upon reaching zero, they would transmit 2^k, two frames which will be transmitted using an aggregated MPDU. Meanwhile, STA-1 and STA-2 count down to zero and transmit one frame each. Upon each successful transmission, the next backoff is chosen based on the expected value of the transmitting CW (line 31 in Algorithm 1). The distributed reservation mechanism is shown as values under the timeline. After each successful transmission, all STAs that receive the frame would check if they have a backoff that

would collide with the next transmission of the transmitting STA. If so, they would choose another random variable to not cause collision. In the Figure, STA-3 has a random backoff of 3 that would collide with the next transmission of STA-2. Thus, STA-3 chooses another random backoff that is not 3 and 7 (sensed from the transmission of STA-4), and continues its operation.

2.3.2 Backoff Stage Selection

Conditional Collision Probability (P_{cc}) is the probability of occurring packet collisions that are only caused by transmissions. Based on [14], P_{cc} will remain constant irrespective of the number of packet retransmissions by a station and can be used to infer the number of active contenders (NAC) in the network. P_{cc} can be computed by dividing the number of busy and collision slots (a station overhears) by the total slots:

$$P_{cc} = \frac{Slot_{busy} + Slot_{Collision}}{TotalSlots} \tag{2.1}$$

Also we noticed in dense networks, always resetting backoff stage to zero (after receiving packet in an empty queue or packet drop after reaching the maximum retry limit) highly contributes to the overall collisions and performance degradation. Thus, a station can compute P_{cc} to choose the proper CW when it is supposed to reset its backoff stage. In Algorithm 1, ECA-DR uses P_{cc} to estimate the NAC and choose the proper CW (1) between two consecutive transmissions of a station if the first transmission results in a collision by computing the backoff stage increae value (lines 20) and (2) where the station has to reset its backoff stage (line 30 and line 34).

Optimal CW selection cannot be used with the "hysteresis" mechanism of ECA because deterministic backoff values chosen after successful transmissions might divide each other which may cause more collisions in dense networks. Thus, to compute

18

Table 2.1: Other parameters for the simulations

Parameters	Value
Physical channel rate	65 Mbps
Channel width	20 MHz
Number of streams	2x2 MIMO
Empty slot duration	9 μs
DIFS	28 μs
SIFS	10 μs
Maximum retransmission attempts	6
Packet size	1470 Bytes
MAC queue size	2000 Packets

'proper' CW for AC[BE] and AC[BK], ECA-DR chooses the backoff stage (k_{AC} and BIV) based on Eq. 2:

$$2^{k_{AC}} CW_{min}[AC] > NAC^2 \cdot P_{cc} \tag{2.2}$$

Due to stringent delay requirements of delay-sensitive traffics, CW for AC[VO] and AC[VI] is chosen equal to half of the value computed by Eq. 2.

2.4 Simulation and Analysis

We extend [6] to implement ECA-DR in the COST simulator [18]. Simulations are carried out in a single hop scenario where all stations are in transmission range of each other and the channel is assumed to have no errors.

2.4.1 Simulation settings

To resemble dense traffic scenarios, each station is simulated to have four types of traffic (i.e., AC[VO], AC[VI], AC[BE] and AC[BK]). AC[VI] source traffic is based on H.264/Advanced Video Coding (H.264/AVC) with compression mechanism and resulting rate-variability. AC[VO] is chosen based on Internet Low Bit Rate Codec (iLBC) with silent detection (payload of 38 bytes with 20 ms intervals). For more information about the detail of Voice and Video codecs, we refer the readers to [6].

In *saturated* settings, MAC queues of AC[BE] and AC[BK] always have packets to transmit with packet arrival rate of 65 Mbps which is larger than the throughput they can attain. In *unsaturated* traffic scenarios, the packet arrival rate to the MAC queues of AC[BE] and AC[BK] is 1 Mbps that will result in frequent queue flushes.

Simulations are based on 10 repetitions with different seeds that simulate 60 seconds of different protocols (i.e., ECA and ECA-DR). Other simulation parameters are illustrated in Table 2.1. Since the goal is to use the proposed distributed reservation mechanism instead of the expensive RTS/CTS mechanism in the conventional ways, all simulations are carried out without RTS/CTS. Thus, in saturation scenarios, the transmission duration of a successful frame can be computed by:

$$T_{success} = T_{frame} + SIFS + T_{BlockACK} + DIFS + T_{\sigma}, \tag{2.3}$$

where T_{σ} is the duration of an empty slot. T_{frame} and $T_{BlockACK}$ are computed from Eqs. 2.4 and 2.5, respectively, as follows.

$$T_{frame} = T_{PHY} + \left\lceil \frac{SF + k(MD + L_{MH} + L_{data}) + TB}{OFDM\ Rate} \right\rceil T_{sym} \tag{2.4}$$

In Eq. 2.4 T_{PHY} is 32 μs, Service Field (SF) is 2 bytes, k is the transmitting backoff stage that gives the number of aggregated MAC frames (A-MPDUs), MPDU Delimiter (MD) is 4 bytes, length of MAC header (L_{MH}) is 36 bytes including 3-bit field, Tail Bits (TB) is 6 bits and the duration of OFDM symbol T_{sym} is 4 μs. OFDM Rate is computed based on the number of subcarriers (234 for 20 Mhz bandwidth), the number of bits per OFDM symbol (6), coding rate (3/4) and antenna settings (MIMO).

$$T_{BlockACK} = T_{PHY} + \left\lceil \frac{SF + L_{BlockACK} + TB}{OFDM\ Rate} \right\rceil T_{sym} \tag{2.5}$$
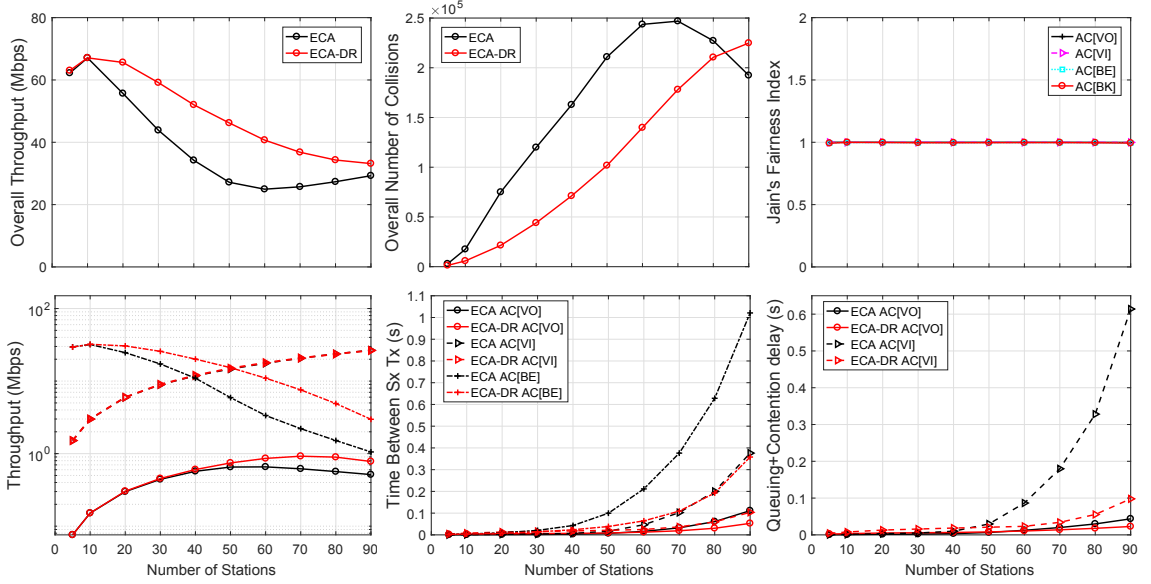
Figure 2.3: Results of saturated scenario for 5-90 stations each with 4 ACs. Overall network throughput, collisions, and Jain's fairness index are shown on top. Results for different ACs are shown on the bottom. Legend of throughput per AC can be inferred from the next sub-figure.

Length of Block Acknowledgement (L_{BlockACK}) is 32 bytes.

2.4.2   Analysis of simulation results

Fig. 2.3 depicts the results of ECA-DR in saturated scenarios.

The top 3 sub-figures show the overall statistics. The overall number of collisions in ECA-DR is less than half of that in ECA for up to 50 users. Not only does ECA-DR achieve higher throughput than ECA (top-left sub-figure), it also reduces the average delay of delay-sensitive traffic (bottom-right sub-figure). This will give the chance to support larger numbers of Voice (AV[VO]) and real-time Video AC[VI] users. Average queuing delay and time between successful transmissions of AC[VO] remain below 10 ms for up to 70 users and for AC[VI], remain below 100 ms for up to 90 users. ECA can only satisfy delay requirements of 60 AC[VO] users and 60 AC[VI] users.

Real-world scenarios are mostly represented by *non-saturated* scenarios. AC[BE] and AC[BK] represent web-surfing, email and file download (not all the users constantly

21
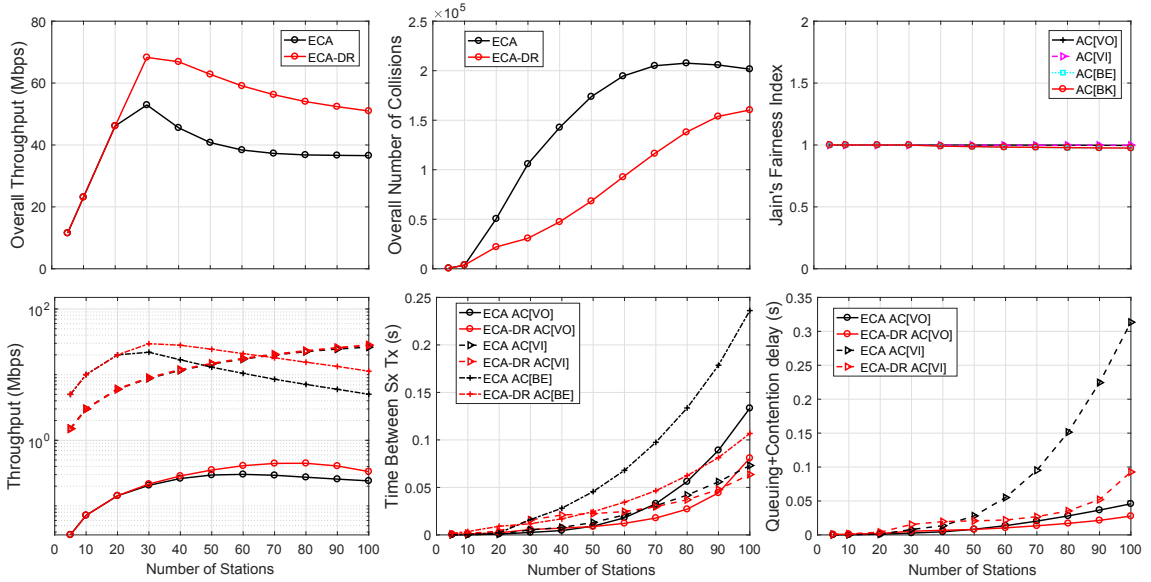
Figure 2.4: Results of unsaturated scenario for 5-100 stations each with 4 ACs. Overall network throughput, collisions, and Jain's fairness index are shown on top. Results for different ACs are shown on the bottom. Legend of throughput per AC can be inferred from the next sub-figure.

saturate these ACs). Packet arrival rate to the MAC queue of these traffics is 1 Mbps. Fig. 2.4 illustrates the network statistics based on different network metrics. Like saturated scenario, ECA-DR outperforms ECA in achieving both higher throughputs and lower delays. In unsaturated scenarios, ECA-DR satisfies delay requirements of 100 AC[VI] and 60 AC[VO] users. ECA can only satisfy delay requirements of 70 AC[VI] and around 55 AC[VO] users.

2.5   Chapter Summary

Three features of CSMA/CA that cause network performance degradation in dense networks are (1) prioritization of delay sensitive traffics by blindly giving them more channel access time, (2) doubling of CW after collision to reduce further collisions without considering the number of active contenders, and (3) scheduling of packet transmissions by solely relying on the collision or success a station may experience. Choosing optimal CW based on instantaneous estimated number of active contenders

has been shown to improve the efficiency of CSMA/CA-based MAC protocols. However, optimal CW selection cannot be used with the "hysteresis" mechanism of ECA due to asynchronous stations decisions. In this chapter, we introduced a distributed reservation mechanism for ECA, termed ECA-DR, based on which stations can collaboratively achieve higher network performance. To be able to use ECA with proper CW, ECA-DR chooses the CW based on estimated number of active contenders. Simulation results demonstrate that ECA-DR can greatly improve the efficiency of WLANs and, hence, support larger numbers of voice and real-time video users.

Chapter 3

FULL-DUPLEX MAC PROTOCOL FOR DENSE WLANS BASED ON CSMA/ECA-DR

3.1 introduction

As discussed in previous chapters, enormous data demand and traffic differentiation with delay-constrained traffics call for (1) efficient transmission coordination and (2) increase in capacity of wireless networks. Spectrum reuse and advanced air interfaces are two categories of enhancements in increasing the capacity of wireless networks. In-band full-duplex (IBFD) communication is one of the advanced air interface technologies that have attracted a lot of attention recently. The main challenge of IBFD (hereafter referred to as FD) is "self-interference" that is the interference that transmission of a station (STA) has on its own reception. In the physical layer (PHY), analog and digital cancellation techniques are used to reduce this self-interference to a great extent (almost to the power of noise floor) so as to enable simultaneous transmission/reception. Since this simultaneous transmission/reception can be among two or more STAs, regular half-duplex MAC protocols are unable to fully utilize the benefits of FD technology. Besides, enabling FD transmissions should depend on the STAs' locations and channels. Hence, new MAC protocols are required to efficiently coordinate transmission of STAs and adaptively select HD or FD transmissions based on the network conditions and STAs locations.

Figure 3.1 shows different transmission modes in FD communications. As shown in Figure 3.1a, in half-duplex transmissions, when primary receiver (PR) is receiving a
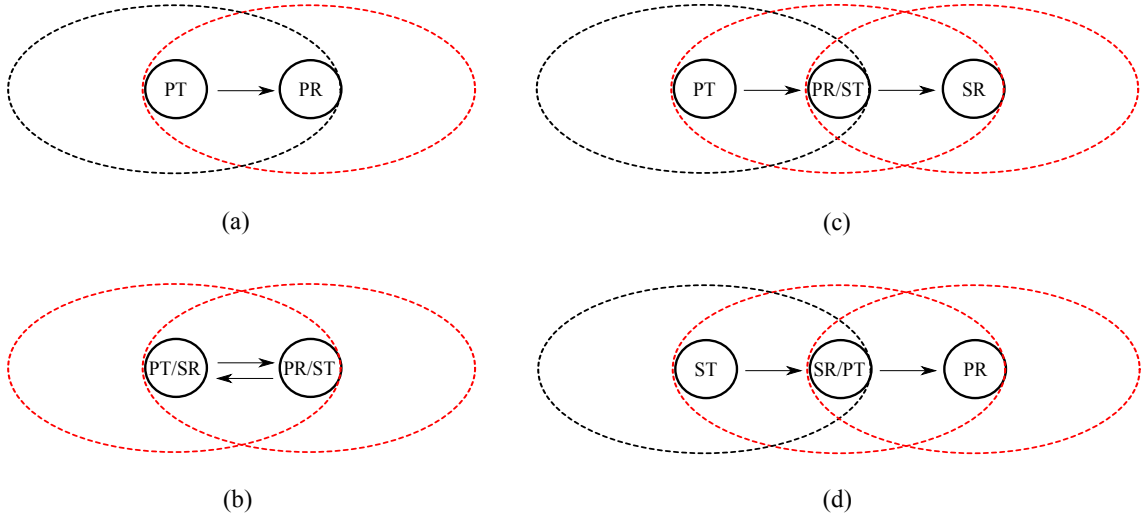
Figure 3.1: Full-duplex transmission modes (a) half-duplex (HD); (b) bi-directional FD (BFD); (c) source-based FD (SBFD); (d) destination-based FD (DBFD)

frame from primary transmitter (PT), only one transmitting STA can be in the interference range of PR, shown in red dashed circle. Otherwise, two frame transmissions are received at the same time in PR (frame collisions), and since PR is unable to decode them properly, both frames get dropped. In other FD transmission modes, since an STA can perform self interference cancellation (SIC), it can transmit to the source STA (PT) while receiving from it, Figure 3.1b, or it can transmit to another station, named secondary receiver (SR) while receiving from PT, Figure 3.1c. Furthermore, as it is illustrated in Figure 3.1d, the PT can receive from another STA while transmitting to the PR.

Transmissions in a wireless network can be asynchronous (not synchronized in time) and asymmetric (different frame sizes). Also, the queues might not always be saturated. Therefore, to reduce inter-station interference (ISI) and efficiently utilize the spectrum, the decision to choose the FD mode of operation, the size of frames to transmit, and the access mechanism should be based on the type of traffic, number of active contenders and the inferred channel between STAs.

MAC protocols for half-duplex contention-based communications have only one

mode of operation, see Figure 3.1a. To reserve the channel and reduce the collisions caused by hidden terminals, the MAC protocols would activate the RTS/CTS mechanism. In wireless networks with traffic differentiation comprising small, delay-constrained frames, the four-way handshake employed in the RTS/CTS mechanism is known to waste the channel time [16,19] and is only activated for large frames. However, with increase in the number of STAs, the number of collisions will also increase. In this situation, we noticed that for traffic differentiation in the UL direction, the benefit of RTS/CTS overcomes its overhead and is beneficial to be activated. So, not only does RTS/CTS activation depend on the size of packets, but it also depends on the number of active contenders and the type of traffic (DL/UL) which calls for an adaptive RTS/CTS activation threshold for both DL/UL.

Some of the proposed FD MAC protocols employ some mechanisms for sharing a random backoff [20] but since STAs might belong to different contention domains this method might not be beneficial. Other methods of channel reservation [21–23] report less collisions and higher throughput gains. Another category of proposed FD MAC protocols rely on the fact that as soon as one STA receives the MAC header, it can decide to transmit back to the sender or to a third STA. To protect these transmissions, they employ a busytone signaling to prevent hidden terminal problem. Choosing the packet-to-transmit right after receiving a packet header can be longer than DIFS because of PHY-MAC turn around time which puts the practicality of this method under question [24]. Moreover, as mentioned before, random access in dense networks causes excessive amount of collisions which limits the scalability of these solutions.

In Chapter 2, we proposed a protocol that instead of utilizing the expensive RTS/CTS mechanism, employs a distributed reservation mechanism to reduce the frame collisions even in traffic differentiation. Owing to the periodic transmission of

frames imposed by this protocol, and the ability to compute the exact next transmission of a transmitting STA (in terms of time slots), this protocol can be extended to be used in FD communications. Since after a successful transmission, a STA would choose the expected value of its transmitting contention window (deterministic backoff), and other STAs would refrain from choosing the same backoff value, the destination of the transmission has the ability to transmit at the same time with the next transmission of that STA. Owing to periodic transmission of information, distributed reservation and optimal contention window selection, we expect the efficiency of this protocol to be higher than other proposed MAC protocols for FD communications.

The rest of this chapter is organized as follows. Section 3.2 gives a summary of the benefits of using FD communications as well as challenges in designing an efficient FD MAC protocol. In Section 3.3, an in-depth analysis of the state-of-the-art protocols proposed for FD communications is presented. In Section 3.4, we propose FD-CSMA/ECA-DR, a novel FD MAC protocol based on techniques of CSMA/ECA-DR. In Section 3.5 we present the results of simulating FD ECA-DR MAC protocol and we summarize this chapter in Section 3.6.

3.2 Benefits and Challenges of FD communications

In this section, we summarize the most notable benefits of using FD communications along with some challenges that should be addressed when designing an FD new MAC protocol.

3.2.1 Benefits of FD communications

As self interference cancellation is proved to be achievable, following benefits make FD technology an interesting and promising technology for the near future [25]:

1. exploiting FD technology is orthogonal to other technologies and hence it can be combined with them to achieve higher throughputs.

2. In a point-to-point link with perfect SI cancellation, full-duplex can double the spectral efficiency compared with conventional half-duplex.

3. Knowing the channel conditions and interference level, best FD mode can be chosen to increase overall throughput of the network.

4. In centralized networks, with increase in number of contenders associated with the AP, a bottleneck occurs at the AP as it should transmit/receive packets to/from all STAs [24]. FD communications can solve this problem as AP can transmit simultaneously with the STAs, and hence increase the overall throughput of the network and reduce the end-to-end delay.

5. Bidirectional full-duplex mode can mitigate hidden node problem since STAs around the transmitter and receiver listen to their transmissions and refrain to transmit simultaneously.

6. If the network is capable of working in different frequency channels, an STA that is receiving and has nothing to transmit, can transfer the channel information (interference, occupancy, etc) to other neighboring STAs if they are not in receiving state.

7. FD systems can reduce feedback and end-to-end delays. Control frames can be piggybacked to the data frames sent to the destination or be sent when the destination is transmitting. In relay networks, a STA (ST in figure 3.1c) can simultaneously transmit (to SR) while receiving from PT.

8. Since listening to a full-duplex communication will give a complex mixed signal, higher security in transmission can naturally be achieved.

9. Also a node that is transmitting can simultaneously get RF energy to charge.

3.2.2 Design challenges at the MAC layer

Because of possible different modes of operation in FD networks, different packet sizes in traffic differentiation, and traffic changes there are considerations to take in to account when designing a new FD MAC Protocol:

1. **Asynchronous Contention:** wireless STAs might belong to different contention domains and not synchronized in time slots. For FD transmissions, two stations must transmit exactly at the same time. Thus, STAs can use RTS/CTS mechanism to reserve the channel, synchronize in time slots (e.g., share the same backoff slots), and be aware of each engaging STAs in a multi-node FD transmission. However, RTS/CTS frame use the lowest data rate and hence, the four-way handshake used in RTS/CTS is known to waste the channel time in traffic differentiation comprising small, delay-constrained frames. Most of today's networks have traffic differentiation, therefore, other mechanisms are required to reserve the channel, share the backoff slots and assign participating STAs in a FD transmission.

2. **Selecting FD transmission modes and STAs:** in an FD network, the receiver of the first transmission selects the best mode depending on available frames in its MAC queues. There are some techniques to select STAs already in the literature such as creating interference history by header snooping [20]. To coordinate the transmissions and reduce collisions some techniques are proposed: reservation mechanisms [22,23] and RTS/CTS based mechanisms [21]. There are also techniques to select the FD transmission modes such as click formation [20], channel inference [22,23] etc.

3. **Fairness:** in a wireless network, STAs that experience more interference because of their locations (i.e., have more STAs in their interference area) have less chance

to transmit. This is doubled in FD communications. Therefore, designed FD MAC protocols should take this into account to be fair among STAs.

4. **Prioritize Bi-directional FD by buffer:** when backlogged, STAs choose their transmission destinations by the Head of Line (HOL) frame in their queue. Depending on the network conditions, prioritizing full-duplex opportunities by searching the buffer might be beneficial. If PT is transmitting to PR and the HOL frame of PR is a frame destined to another STA that might experience interference from PT, PR can prioritize other frames in its buffer to transmit to other STAs in DBFD mode or transmit back to PT in BFD mode.

5. **Residual Hidden node problem:** in BFD mode, if either of simultaneous transmissions ends sooner than the other, the rest of the transmission time is susceptible to hidden node problem. In this case, the transmitter that has finished its transmission sooner can transmit busy tone until the other finishes the transmission [22, 23, 26]. Although busytone reduces the hidden terminal issue, it wastes the channel time and energy of STAs.

3.3 Related Work

In this Section, we compare some of the proposed FD MAC protocols for different wireless networks. The classification is based on multiple criteria that are important in the design of a new practical FD MAC protocol. These criteria include access mechanism, number of activated FD modes, network type, traffic type, inter-symbol interference (ISI) consideration, key features, and performance metrics to evaluate their work. Table 3.1 illustrates this comparison.

Table 3.1: IBFD MAC Protocol Comparisons

Reference	Year	Access	FD Modes	Type	Traffic	ISI	Performance Metric(s)	Key Feature(s)
ContraFlow [27, 28]	2009 2011	Random Access	BFD DBFD	Distributed	Synchronous	No	Throughput Fairness	Weighted list Receiver Selection, Busytone
PRT [24]	2011	Random Access	BFD DBFD	Centralized	Synchronous	No	Throughput Fairness	Simultaneous ACK, Busytone, Compared with MIMO
FD-MAC [20]	2011	Random Access	BFD SBFD	Centralized	Asynchronous	No	Throughput	Shared Random Backoff, Header Snooping Virtual Contention
Janus [29]	2013	Cycle Based	BFD DBFD SBFD	Centralized	Asynchronous	Yes	Throughput Fairness	Adaptive FD activation, Load- and Rate-aware Scheduler
Goyal et al. [23]	2013	MAC Header Coordination	BFD DBFD SBFD	Distributed	Asynchronous	Yes	Throughput	Adaptive FD activation, OFDM-OFDMA Integration
RCTC [22]	2013	PN Coordination	BFD DBFD	Centralized Distributed	Asynchronous	Yes	Throughput Fairness	Exposed node activation, History-based Receiver Selection
RTS/FCTS [21]	2013	RTS/CTS	BFD DBFD	Centralized Distributed	Asynchronous	No	Throughput	p-persistent CSMA-based Analytical Model, Full-Duplex Efficiency Metric

3.3.1 Random Access Protocols

The protocols of this section [20, 24, 27] use basic access of CSMA/CA protocol to enable FD communications. They might also add some fields to the MAC header or create FD headers to facilitate FD operations. The general idea is as follows: considering Fig. 3.1, when PR receives the MAC frame header from the PT, if it has a frame for PT, it can form a BFD by transmitting simultaneously to PT. If PR has packets for another STA (Fig. 3.1c), it starts transmitting to SR simultaneously. While receiving, if PR does not have a frame to transmit or its transmission is shorter than the other ongoing transmission (asymmetric traffic), it should transmit a busytone to prevent possible collision from hidden terminals. In the case of asymmetric traffic (very common with frame aggregation and traffic differentiation) utilizing busytone would waste the channel time and energy of the STAs. Moreover, due to possible collisions from multiple STAs, these protocols are unable to activate SBFD mode.

In [24], achieving FD communications is based on implementing per-destination transmission queues. So, the number of queues at the AP is the number of associated

STAs which is not scalable. Authors compare the FD results with MIMO in half-duplex. They report that in DL, MIMO is better but in DL/UL (bidirectional) traffic FD is better. MIMO HD is better in low SNR regime and FD is better in high SNR. This capacity gain is because of devices power constraints (it allows FD to use twice as much energy as HD per unit of time). Hence, a protocol that combines MIMO and FD is also interesting.

FD-MAC [20] adds a 6-byte FD header to the MAC header of CSMA/CA for different FD functionalities. STAs perform *header snooping* on each other's transmissions to estimate their local topology and to check if the ongoing transmission between AP and other STAs form a clique or hidden terminal with themselves. So, if a STA finds a transmission between AP and another STA to be hidden to itself, it can simultaneously transmit to AP while AP is also transmitting to the other STA. FD-MAC assumes that DBFD mode is infeasible due to the limited coherence time of self interference channel state estimation but Contraflow [28] show that it is possible to activate DBFD.

3.3.1.1 Other notable features:

Consider Figure 3.1c when PR is receiving a frame from PT. If PR has packets for other STAs rather than the PT, random selection of SR might result in collision. This collision might be because of the interference from the PT or from hidden terminals. To select the SR, Contraflow [27] employs history-based receiver selection. Contraflow addresses fairness issues among the STAs by providing fair channel access time.

To keep fairness among STAs, FD-MAC uses *shared random backoff*, a 10-bit field in the FD header of two nodes that have more packets for each other. By *virtual contention resolution*, FD-MAC also prioritizes BFD mode by searching the buffer

instead of serving the HOL packet.

3.3.2 Reservation-based Protocols

Protocols of this section enhance coordination among FD STAs with control frames exchanges prior to the actual data transmissions [21–23]. RCTC [22] employs pseudo-random noise to generate unique signatures for each STA in the network along with other signatures for half-duplex and full-duplex transmissions. Other STAs in the vicinity of PT and PR can overhear the control packet exchanges and keep quiet for the FD duration. For the asymmetric traffic, RCTC also uses busytone transmission. SR selection in RCTC is history-based like Contraflow.

Goyal *et al.* [23] proposed a FD protocol that can activate all FD modes opportunistically. To that end, authors propose to add two fields to the MAC header; a two-bit field, full-duplex acknowledgment (FDA), for BFD and DBFD modes, and a 1-bit field for SBFD called transmission flag (TF). The PT splits its transmission into two parts: it first transmits the MAC header followed by busytone while waiting for the response from the PR. Upon receiving the MAC header, PR transmits the 2-bit field showing its chosen mode (0:BFD, 1:DBFD, 2:HD, and 3:transmission not allowed). Once PT receives the 2-bit field, it stops the busytone, transmits the 1-bit field to show its updated mode to its neighboring STAs and

1. If SBFD: transmits to PR while waiting for other STAs' transmission on different subchannels, and responds to the selected one with a busytone on that subchannel splitting its transmission to the PR.

2. If DBFD: continue the rest of its transmission

Meanwhile, If PR has packets for another STA and wants to perform DBFD, it transmits its MAC header to the SR followed by busytone and waits for the confirmation of

SR. If there is asymmetric traffic, STA with shorter traffic should transmit busytone to suppress hidden terminals.

Some studies have added some fields to the RTS/CTS mechanism to communicate with other nodes in the network by informing them of the chosen mode and transmission duration to prevent hidden and exposed terminal problems. In [21], authors propose the addition of duration and participating STAs in primary transmission (PT-PR) and secondary transmission (ST-SR) to the Full-duplex CTS (FCTS) control frame. Since in both BFD and DBFD, FCTS frame should be transmitted twice, it prolongs the handshaking process from 4-way handshake to 5-way handshake which reduces the network efficiency. RTS/FCTS is unable to activate SBFD and does not take into account the ISI between STAs participating in a FD transmission (PT, SR).

3.3.2.1 Other notable features:

For ISI measurement in DBFD, SR should measure the signal-to-interference ratio (SIR) from PT and ST based on Figure 3.1 and if the SIR is above a threshold (Δ), it will permit the transmission from ST to itself. The question arises as to what data rate should ST use to transmit information to SR? In other words, shouldn't this SIR be sent back to the ST to choose the data rate based on it? In [23], the data rate chosen will be the lowest data rate in the network.

$$SIR_{SR} = \frac{P_{ST-SR}}{P_{PT-SR}} = \frac{P_{ST}|h_{ST-SR}|^2}{P_{PT}|h_{PT-SR}|^2} > \Delta, \tag{3.1}$$

where P_{ST-SR} and P_{PT-SR} are the received signal strength at the SR from ST and PT, respectively. P_{ST} and P_{PT} are the transmit powers of PT and ST and $|h_{ST-SR}|^2$ and $|h_{PT-SR}|^2$ are the channel power gains between ST/SR and PT/SR, respectively. For ISI measurement in SBFD, based on Eq. 3.1, the following equation should be

satisfied:

$$SIR_{PR} = \frac{P_{PT}|h_{PT-PR}|^2}{P_{ST}|h_{ST-PR}|^2} > \Delta \qquad (3.2)$$

However, in SBFD, ST is unaware of the channel between PT and PR. By using inverse power echo signal method introduced in [30], PR transmits only the FDA field (because it neither has packets for PT nor SR) with the power computed based on the Eq. 3.3:

$$P_{PR} = \frac{Z}{P_{PT}|h_{PT-PR}|^2}, \qquad (3.3)$$

where Z is a shared constant among the STAs. Therefore, ST receives the PR's FDA transmission with the power of 3.4:

$$P_{PR-ST} = P_{PR}|h_{PR-ST}|^2 = \frac{Z|h_{PR-ST}|^2}{P_{PT}|h_{PT-PR}|^2}. \qquad (3.4)$$

Thus, to satisfy the original SIR equation 3.1, the received power at ST should satisfy the following equation:

$$P_{PR-ST} = \frac{Z|h_{PR-ST}|^2}{P_{PT}|h_{PT-PR}|^2} < \frac{Z}{\Delta P_{ST}}. \qquad (3.5)$$

RCTC [22] employs a similar mechanism to [23] not for activating SBFD but to enable exposed terminals. Since the transmission of exposed terminal might interfere with the PR or SR and vice versa, by means of signal-to-interference ratio (SIR), the exposed node can make sure whether its transmission interferes with the ongoing transmission of (PT-PR). If received signal strength at PR is higher than a threshold, it can decode the signal using packet capture method.

$$SIR_{PR} = \frac{P_{TR-PR}}{P_{ER-PR}} = \frac{P_0|h_{TR}|^2}{P_0|h_{ER}|^2} = \frac{|h_{TR}|^2}{|h_{ER}|^2} > \Delta_d, \qquad (3.6)$$

where Δ_d is a constant related to data rate d. Since h_{TR} is not available to the exposed terminal, it should infer it by the received signal strength from the PR. PR also adjusts its transmission power based on h_{TR}:

$$P_{ST} = \frac{C_d}{P_{TR}}, \tag{3.7}$$

where C_d is also a constant related to date rate d. Received signal power at the exposed terminal is:

$$P_{RE} = P_{ST}|h_{TR}|^2 = \frac{C_d}{P_{TR}}|h_{TR}|^2 = \frac{C_d|h_{ER}|^2}{P_0|h_{TR}|^2}. \tag{3.8}$$

From Eqs. 3.6 and 3.8, the following eq. should satisfy at the exposed terminal:

$$P_{RE} = \frac{C_d|h_{ER}|^2}{P_0|h_{TR}|^2} < \frac{C_d}{P_0\Delta_d}. \tag{3.9}$$

Also, exposed terminal does not know the transmission data rate of PT, so if $C_d = C(P_0\Delta_d)$, where C is constant known to all STAs, Eq. 3.9 can re-written as:

$$P_{RE} < \frac{C_d}{P_0\Delta_d} = C. \tag{3.10}$$

3.3.3 Other Protocols

Janus [29] is a centralized polling-based protocol that works in variable-length cycles. In the beginning of each cycle, AP polls all the STAs to measure if they have packets to transmit. STAs willing to participate respond in their predefined time slot. Then, AP approximates an optimal FD scheduling by taking into account fairness (based on channel time) and adaptive data rates to maximize spectrum utilization and FD opportunities.

3.4 Description of Full-Duplex CSMA/ECA-DR

In this Section, we explain how FD ECA-DR gradually achieves a collision-free schedule. The design of ECA-DR protocol is based on periodic transmission of frames by the MAC layer of each STA. Following period transmissions, a harmony gradually gets formed in the wireless network which decreases the collisions. Thus, with distributed reservation, ECA-DR can operate without the RTS/CTS mechanism in dense network scenarios and achieve higher efficiency compared to that of CSMA/CA and CSMA/ECA.

One of the biggest challenges in designing an efficient FD MAC protocol is the transmission asymmetricity. This asymmetry is not only because of different frame lengths but is also because of different data rates. The data rate in a wireless network is chosen based on the channel between the transmitter and the receiver. The protocol should try to make the transmission durations close to each other as much as possible. If the data rates are the same, in single traffic with saturated queues this is possible but in practical scenarios due to different distances between STAs, varying channels and traffic differentiation, some mechanism is needed to address the issues of different transmission durations. In infrastructure-based FD MAC protocols, since the transmissions take place only between the AP and the STAs, the AP can compute both PT and PR transmission duration to minimize the traffic asymmetry [29]. It is also possible to first reserve the channel (e.g., by RTS/CTS) and choose the same duration frames based on the exchange of channel quality of each link.

Owing to interval-based transmissions of ECA-DR protocol (based on deterministic backoffs), when an STA (PT) transmits its frame, the destination of the transmission (PR) can compute the next transmission time of PT in time slots. If PT has more frames to transmit to the PR, and PR has frames to transmit (either to PT or SR), PR first measures the feasibility of the next FD transmission and if it finds

feasible, includes the FD Duration of its next transmission in the ACK frame. Note that PR chooses the destination of its transmission (SR) based on a history of previous successful transmissions, and compute the duration based on the data rate. In this case, not only STAs around the PR can compute its next transmission and refrain from transmitting at that time, the PT will also include the correct mode of operation in its next transmission and as a result hidden terminals are also aware of the next transmission.

Unlike other FD MAC protocols, if FD ECA-DR is used without RTS/CTS, the first transmission is always half-duplex. This is necessary because the recipient of first transmission might also belong to another collision domain and with simultaneous transmissions, the probability of collision will increase. Note that ECA-DR can be used with or without RTS/CTS mechanism. However, since the four-way handshake of RTS/CTS incurs additional delay on the small frames and other security issues related to using RTS/CTS mechanism, the distributed reservation of ECA-DR is preferred over RTS/CTS.

Algorithm 2 Pseudocode of Receiving Chain at the AP in Full-Duplex ECA-DR
___
1: **while** the device (d) is on **do**
2:     **if** Received a packet (p) **then**
3:         Record the pair of ID and Received SNR;
4:         $NT \leftarrow (2^{\text{p.b}}CW_{\min}[\text{p.AC}])/2 - 1$;
5:         **if** p.dst_add = d.src_add & has packets to transmit in Q_i **then**
6:             **if** FD mode is feasible **then**
7:                 (1) Select the FD mode and set the ID of FD STA;
8:                 (2) Choose the transmission duration equal to p.dur;
9:                 Create an ACK with (1) and (2);
10:                 $B_i \leftarrow NT$;
11:             **end if**
12:         **else if** p.dst_add = d.src_add & has no packets to transmit **then**
13:             (1) Select the FD mode as HD;
14:             (2) Select 0 as FD duration;
15:             Create an ACK with (1) and (2);
16:         **else if** p.dst_add $\neq$ d.src_add & has packets to transmit in Q_i **then**
17:             **if** $B_i = NT$ **then**
18:                 $B_i \leftarrow \mathcal{U}[0, 2^{k_i}CW_{\min}[i] - 1]$;
19:             **end if**
20:         **end if**
21:     **end if**
22: **end while**
___

3.5   Results and Discussion

In this Section, we present the results of FD ECA-DR in the context of an infrastructure-based network where there are both UL and DL traffic. Wireless STAs are random uniformly placed in an 50 m x 50 m area around the AP where AP is located in the middle of the area. The Pathloss (PL) is computed based on WINNER II for indoor environment with the following equation:

$$PL = 20 \times \log_{10}(d) + 46.4 + 20 \times \log_{10}(f_c/f_b) + L_w \times W, \tag{3.11}$$

where d is the distance between transmitter and receiver; $f_c = 5.180$ GHz is the center frequency, $f_b = 5GHz$ is the base frequency; L_w is wall loss and W is the number of Walls between transmitter and receiver. The AP is equipped with 4x4 antennas capable

Table 3.2: Other parameters for the simulations

Parameter	Value
Number of STAs (N)	5-60
STA's λ for Poisson arrival	20
AP's λ for Poisson arrival	$20 \times N$
Channel width	20 MHz
Number of Antennas AP	4x4
Number of Antennas STAs	1x1
CW_{min}/CW_{max} AP	8/16
CW_{min}/CW_{max} STAs	16/512
Empty slot duration	9 μs
DIFS	34 μs
SIFS	16 μs
Max retransmission attempts	6
Packet size	15k-50k Bytes

of MU-MIMO to the maximum of 4 stations but stations have only 1x1 antenna set. Other parameters are based on the Table 3.2.

In this research, to resemble a practical scenario, we assumed only AP being capable of full-duplex operations. Therefore, bidirectional full-duplex is not possible. For DBFD, as discussed in Section 3.3, since AP can infer the PT-SR channel from the known PT-AP and AP-SR channels, AP can decide if activation of simultaneous transmission will cause a collision at the SR. It is possible for AP to traverse the queue and choose the frame whose transmission will cause minimum interference with the PT at the PR. However, for the sake of simplicity, in this study, AP decides based on the HOL frame destination.

For SBFD, AP can decide which backoff to choose to transmit simultaneously with next transmission of another STA. Again, based on AP's HOL and each HD transmission of STAs, AP can find a STA whose simultaneous transmission will cause minimum interference at the receiving STA. Figure 3.2 compares the performance of
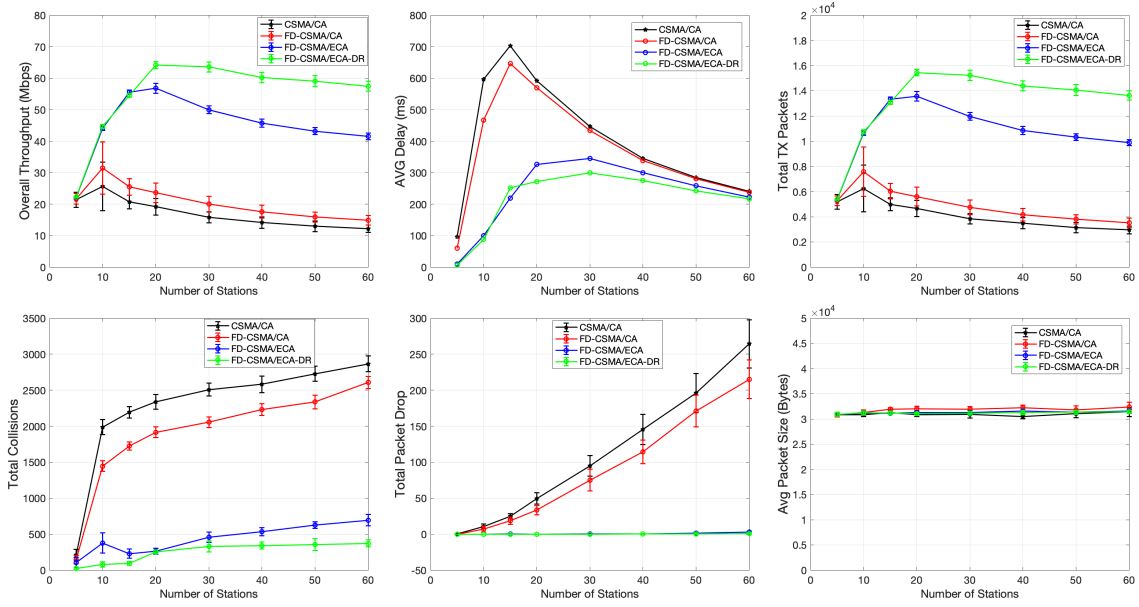
Figure 3.2: Comparative results of CSMA/CA, FD CSMA/CA, FD CSMA/ECA and FD ECA-DR for 5-60 stations. Overall network throughput, average delay, and transmitted frames on top. Total Collisions, packet drops and average packet sizes are shown in the bottom.

four protocols: CSMA/CA, FD CSMA/CA, FD CSMA/ECA, and FD CSMA/ECA-DR. Owing to the advantage of deterministic backoff, CSMA/ECA and CSMA/ECA-DR have higher performance over CSMA/CA. With the addition of FD capability, they will outperform CSMA/CA up 4 times in large number of STAs. Moreover, owing to superiority of CSMA/ECA-DR over CSMA/ECA, the performance of FD CSMA/ECA-DR is upto 38% higher than FD CSMA/ECA which translates to fewer collisions and lower delay.

It is important to note that the superior performance of FD ECA-DR like ECA-DR comes at the cost of constantly listening to the network and counting the number of passing slots to choose the optimal CW to decrease the collision probability. In the scenarios that the network is not saturated, the STA should measure the channel statistics right before transmission to save some battery.

3.6   Chapter Summary

In this research study, we propose a novel full-duplex MAC protocol based on the CSMA/ECA-DR protocol. We know that although RTS/CTS can decrease the collision probability caused by hidden terminals, its four-way handshake can increase the delay in the dense wireless deployments with traffic differentiation. Therefore, we need a reservation mechanism that achieves acceptable throughput and delay even with increasing number of STAs. In CSMA/ECA-DR, owing to the ability of STAs to compute the next transmission of a transmitting STA (primary transmitter), they can refrain from transmitting on the time slot that might collide with that except for the destination of that transmission (primary receiver) that can transmit simultaneously with the next transmission of primary transmitter. In FD ECA-DR, although the first transmission of a STA should be half-duplex, in single traffic situation and UL traffic, the STAs would reach a collision-free schedule quickly. In practical scenarios (both UL and DL and traffic differentiation), although ECA-DR cannot eliminate the collision, it reduces it to a great extent which is needed for densely deployed networks of future.

Chapter 4

PRACTICAL UPLINK SCHEDULING FRAMEWORK FOR IEEE 802.11AX

4.1 Introduction

To operate over unlicensed spectrum, the IEEE 802.11 standards have, from their origin, adopted a contention-based channel access scheme termed the distributed coordination function (DCF) which employs carrier sense multiple access with collision avoidance (CSMA/CA) and binary exponential backoff (BEB). Later, to facilitate traffic differentiation by satisfying the quality of service (QoS) requirements of different access categories, DCF was replaced by the enhanced distributed channel access (EDCA). On the one hand, EDCA is simple to implement and works well for a small number of stations. On the other hand, to support the continuing proliferation of wireless devices and their higher traffic demands with various QoS requirements, deployments of wireless networks have been densified with small cells. With more contenders and higher amount of traffic in a contention-based wireless network and hence inevitable increase in the number of collisions, the efficiency of EDCA degrades significantly [6, 31].

Although the standardized channel reservation mechanism of RTS/CTS brings down the collision duration to short control frames, such reservation introduces overhead to practical networks transmitting multiple traffic types and small frames, and is barely used in such scenarios [32]. Alternative enhancements to CSMA/CA have been proposed to increase the channel efficiency of contention-based wireless networks, which include dynamic contention window (CW) selection [9, 14], deterministic backoff in carrier sense multiple access with enhanced collision access (CSMA/ECA) [2, 6] and

other channel reservation schemes, such as *distributed reservation* for CSMA/CA [15] and CSMA/ECA [31]. However, the higher performance comes at the expense of higher computation overhead and energy consumption.

To address the inefficiency of using contention-based MAC protocols to arbitrate the transmissions of many wireless stations (STAs) over the entire channel, the IEEE TGax Task Group has adopted the technology of orthogonal frequency division multiple access (OFDMA) for both downlink and uplink (DL/UL) transmissions of IEEE 802.11ax (Wi-Fi 6) for high efficiency (HE) STAs. In 802.11ax OFDMA, the channel bandwidth is divided into smaller sub-channels of different, but fixed, bandwidth sizes termed resource units (RUs). Since multiple STAs can transmit or receive frames at the same time using different RUs, frames of different sizes can be transmitted by using RUs of appropriate sizes. In addition, compared to wide-band OFDM that suffers from frequency selectivity and hence lower average data rates, narrow bands exhibit flat fading which helps in achieving higher average data rates. Furthermore, since the transmission power of STAs is not allowed to exceed a threshold (e.g., 17 dBm) per antenna in any allocated bandwidth, on average, the transmission power spectral density (PSD) and, as a result, the selected modulation and coding scheme (MCS) index values of OFDMA STAs transmitting over subchannels are higher than that of OFDM STAs transmitting over the entire channel bandwidth [33].

Another enhancement in IEEE 802.11ax is its channel access mechanism. For backward compatibility and to support contention among different access points (APs) operating on the same/overlapping channels, EDCA is kept as a part of 802.11ax. In addition, a modified EDCA is designed for the channel access of HE STAs. For UL transmissions, two OFDMA-based mechanisms are standardized for HE STAs in IEEE 802.11ax, in which the AP allocates channel resources to different STAs for UL OFDMA transmissions. In particular, HE STAs should remain silent until the AP
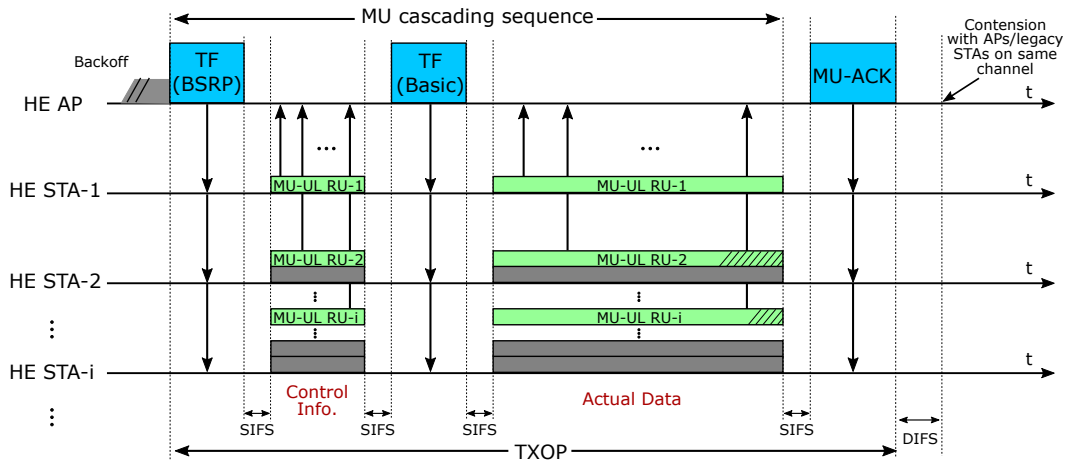
(a) Triggered response Scheduling (TRS).
All RUs are Scheduled Access (SA-RUs).
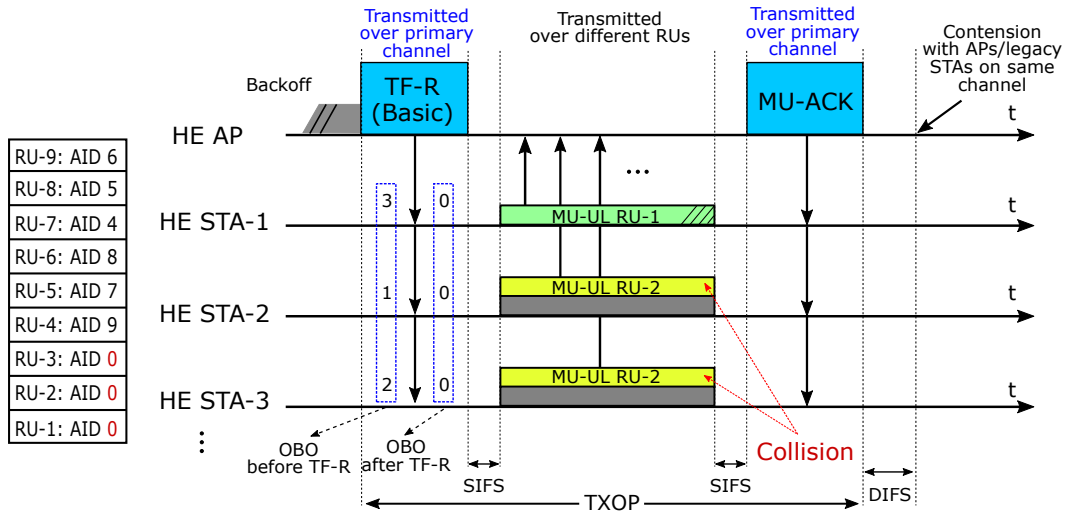
(b) Uplink OFDMA-based Random Access (UORA).
Some RUs might be advertised as Random Access RUs (RA-RUs).

Figure 4.1: OFDMA-based UL channel access mechanisms: (a) explicit channel access by polling in TRS, and (b) explicit and implicit channel access with modified EDCA in UORA; transmission collisions are possible among HE TB PPDUs. In both mechanisms, solicited and unsolicited BSR mechanisms are possible. MU cascading sequence is illustrated with TF-BSRP and TF-basic and HE TB PPDUs.

explicitly or implicitly allows them to transmit their UL frames. To synchronize the uplink transmissions of multiple STAs, transfer transmission parameters (RU assignment, power, duration, etc.) to STAs and initiate a time period termed transmission opportunity (TXOP), an HE multi-user PLCP[1] protocol data unit (HE MU PPDU) called trigger frame (TF[2]) is transmitted by the AP over the entire primary channel. STAs that receive the TF and are allowed to transmit their frames, start transmitting after a short interframe space (SIFS) time. The uplink transmissions after a trigger frame are called HE trigger-based PPDU (HE TB PPDU). Note that AP might transmit more than one TF in a TXOP to solicit multiple control and/or data frames from the STAs, which is called "MU cascading sequence". The purpose for MU cascading sequence is to allow an AP to transmit and receive as many control/data frames as possible subject to the maximum TXOP duration (5.484 ms) without contending again. Therefore an AP can

- perform optimizations on TB PPDU duration since for CSMA/CA to work correctly, HE STAs should transmit for the entire UL duration advertised in the TF and thus, STAs with less data duration should add padding to their UL MAC protocol data units (MPDUs);

- switch direction (UL/DL) if the amount of data in one direction is insufficient, which is similar to LTE-TDD.

Fig. 4.1 illustrates the two UL OFDMA access mechanisms. In the first mechanism, Fig. 4.1(a), referred to as triggered response scheduling (TRS), the AP in a TF, allocates one RU to selected STAs to either poll their control information or their

---

[1] Physical layer convergence protocol

[2] TF can have 8 different types, of which one is "basic" TF to solicit the actual UL data transmissions and the rest are "control" TFs that can be transmitted prior to the "basic" TF to solicit control information of STAs in order to achieve higher efficiency.

UL data. Thus, only RU-allocated STAs can transmit their control information or UL data. The shaded area at the end of some UL PPDUs indicates the padding. In the second mechanism, Fig. 4.1(b), termed uplink OFDMA-based random access (UORA), the AP allocates some of the RUs to certain HE STAs and advertises the rest as random access RUs (RA-RUs). HE STAs with allocated RUs would transmit their UL PPDUs without contention. Other HE STAs receiving a TF with RA-RUs (TF-R) may contend based on a modified EDCA access mechanism to transmit their UL PPDUs with one of the RA-RUs. The table next to Fig. 4.1(b) shows an example assignment of RUs to STAs in a TF for UORA, where the AP assigns an associated ID (AID) to each STA and an RU number to each RU (where RA-RUs have AID 0). HE STAs associated with the AP that receive the TF, have pending UL frames, and are not allocated a dedicated RU, decrease their OFDMA Backoff (OBO) values by the number of available RA-RUs, $\max(0, \text{OBO} - |\text{RA-RUs}|)$, where $|.|$ denote the set cardinality, and if reached zero, randomly choose one of the RA-RUs to transmit their frames[3]. As an example in Fig. 4.1(b), prior to a TF, STAs 1, 2 and 3 have OBO values of 3, 1, and 2, respectively. After receiving the TF, they decrease their OBO values by the number of RA-RUs (i.e., 3) and since all reach zero, randomly choose one of the RA-RUs to transmit their UL data. In this example, since both STA-2 and STA-3 choose the RA-RU # 2, it leads to a collision. Since an implementation of the UORA mechanism is not mandatory in Release 1 of the IEEE 802.11ax standard, in this research study, we only study the TRS mechanism.

Compared to Long Term Evolution (LTE) in which resource blocks (RBs) can be allocated to users in any pattern, the structure of RUs in IEEE 802.11ax is fixed and each STA cannot be allocated more than one RU. Thus, due to the differences in

---

[3] Note that if carrier sensing (CS) is required and carrier is not sensed free, although the OBO of an STA is zero, it cannot transmit and should choose another random OBO value from its minimum OFDMA contention window ($\text{OCW}_{\min}$).

rules and structures of sub-channels, scheduling algorithms designed for LTE cannot be applied directly to scheduling in IEEE 802.11ax. Moreover, existing scheduling algorithms proposed for UL OFDMA assume one traffic type for STAs and usually with saturated traffic load. However, in practical scenarios, STAs generate distinctive traffic types (voice, video, data, etc.) with various QoS requirements and their traffic loads are not always saturated (an exception can be data stream which can be bursty and/or saturated e.g., FTP). Therefore, an AP demands efficient mechanisms to obtain the number of STAs with traffic and their queue length. AP could poll STAs to learn their buffer, and if needed, channel quality. However, with increasing number of STAs, large delay and varying jitter become unavoidable for the high priority traffic. Therefore, a practical and effective resource allocation scheme should take into account the traffic types, channel quality and queue status of different STAs when scheduling UL resources.

In this paper, we formulate the UL OFDMA scheduling as a multi-objective optimization problem to maximize the data rate and queue serving and minimize the delay of high priority traffic, which are conflicting objectives. To solve this multi-objective optimization problem, we employ an *a priori* method and define utilities for different STAs based on their channel quality, type of service (TOS) and queue status. At each TXOP, the scheduler will maximize the instantaneous utility of the STAs with pending traffic for the AP.

In this paper, we propose an interval learning mechanism not only to satisfy the QoS requirements of high priority traffic but also to enhance the overall throughput of the network. Simulation results demonstrate higher efficiency of the proposed STA selection and RU allocation compared to the other state-of-the-art STA scheduling schemes.

The main contributions of this paper is summarized as follows:

- Based on the ability of the MAC layer to impose intervals on transmission of different traffic types, we propose a scheme in which AP can gradually learn the intervals and queue depth of each STA and serve them with proper RU size when they actually have pending frames for AP. This mechanism significantly reduces the amount of control frames exchanged.

- Since certain applications (e.g., voice) have larger delay budgets compared to interactive augmented/virtual reality (AR/VR) applications, we propose an adaptive algorithm based on the instantaneous number of active STAs to prioritize high priority traffic types.

- For RU allocation to the selected STAs, we propose a divide and conquer technique that considers the RU structure of IEEE 802.11ax and allocates proper RU size to STAs based on their traffic type, queue length, and channel quality.

The remainder of the paper is organized as follows. The next Section reviews the state-of-the-art protocols and schedulers proposed for OFDMA in general and 802.11ax in particular. In Section 4.3, we describe the structure of RUs along with equations to count them and compute the valid partitions. In Section 4.4, we describe STA selection as a part of scheduling or as a separate part with benefits of each scheme and propose our learning algorithm. Section 4.5 describes a multi-class channel and QoS-aware scheduler for 802.11ax. Simulation parameters and results are presented in Section 4.6. We conclude the paper with future research directions in Section 4.7.

4.2 Literature Review

Unlike the former WLAN standards, the operations of IEEE 802.11ax in DL and UL can be different. In DL OFDMA, the AP can directly transmit multi-user MAC protocol data units (MU-MPDUs) to different STAs at the same time using the basic

49

access mechanism. Alternatively, the AP can improve the probability of successful transmissions and avoid hidden terminals by first transmitting a multi-user request-to-send (MU-RTS) control frame and, after receiving clear-to-send (CTS) control frames on different chunks of the channel (i.e., RUs), transmit the actual data frames. Sharon and Alpert [34] analytically computed and compared the DL throughput in 802.11ax and 802.11ac networks with certain scheduling strategies.

Several studies have extended Bianchi's model [35] for performance analysis of the UOSA mechanism [36] and for the UORA mechanism when all the RUs are marked as RA-RUs [37]. Naik *et al.* [38] studied the performance of a High Efficiency WLAN (HEW) network under the UORA mechanism for a combination of SA-RUs and RA-RUs. Sharon and Alpert [39] analytically computed and compared the UL throughput of 802.11ax and 802.11ac networks with certain scheduling strategies. To achieve fairness in mixed scenarios, Khorov *et al.* [40] proposed different EDCA parameters for 802.11ax and legacy STAs. Since the addition of padding at the end of UL MPDUs would waste the channel access time and energy of the devices, Karaca *et al.* [41] proposed to minimize the padding overhead by dynamically adjusting the transmission duration of TXOP.

In general, there exists no optimal solution for resource allocation of large scale OFDMA networks. In the classical OFDMA resource allocation, different close-to-optimal algorithms have been proposed with the assumption that multiple subcarriers (not necessarily contiguous) can be assigned to each STA. These proposed algorithms jointly consider both subcarrier and power allocation problems and aim to maximize certain sum utility for scheduling in OFDMA networks [42–44]. Specifically, Jang *et al.* [42] proposed a greedy algorithm to assign subcarriers to STAs and a waterfilling power allocation scheme for subcarriers to maximize the sum rate in the downlink. For uplink OFDMA, Kim *et al.* [43] considered the joint problem of subcarrier and power

allocation and proposed a greedy algorithm to maximize the sum rate. Also, Ng and Sung [44], by taking into account the issue of fairness, proposed a fast algorithm for utility maximization of UL OFDMA.
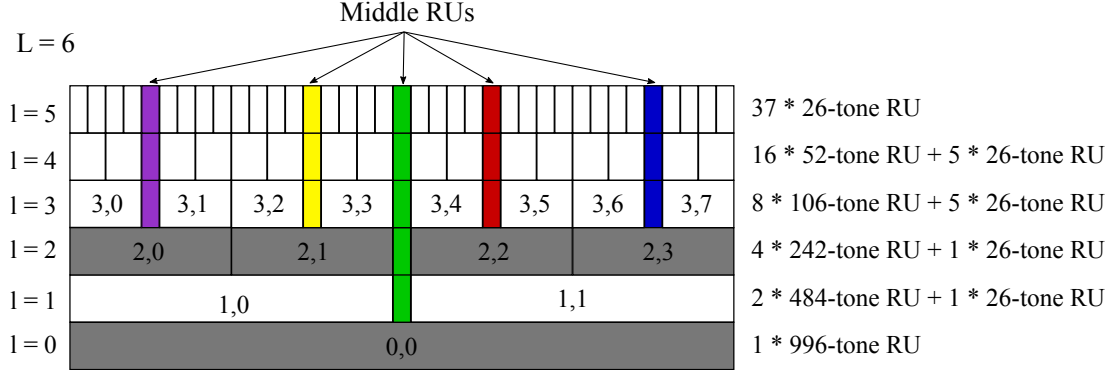
Figure 4.2: RU structure in 80 MHz bandwidth (L=6) with 5 mid-RU RUs shown with different colors. Only at certain levels can the RU(s) be split into 3 RUs (in this figure, levels 0 and 2).

For 802.11ax, compared to the classical OFDMA problems, there are two major differences: 1) Only one RU can be assigned to an STA; 2) the partition of channel bandwidth into RUs is fixed, so any random split of the OFDMA subcarriers is not allowed. For DL, owing to the similarity of RU partitions to a binary tree, Wang *et al.* [45] applied a divide-and-conquer method and proposed a binary recursive algorithm to maximize the sum-rate of a 802.11ax wireless network over two cases: only OFDMA and both MU-MIMO and OFDMA. For UL, Bankov *et al.* [46] assumed random generation of data flows by STAs and the UORA mechanism to transfer buffer status reports (BSRs) to AP. The authors formulated the allocation of RUs to STAs as an assignment problem and proposed "MUTAX" scheduler which minimizes the upload time by giving priority to the STAs with the shortest remaining time. However, the proposed scheduler might cause larger delays for STAs with more traffic. Since the RU assignment to STAs is represented as a matrix, in a later study [47], Bankov *et al.* used an extension of the Munkres algorithm, the Hungarian algorithm, to solve the assignment problem. They

further adapted some classic scheduling algorithms to resource allocation in 802.11ax. Dovelos *et al.* [48] proposed a scheduling algorithm to maximize the utility of average user rates in peak and average power constraints.

The majority of the proposed scheduling mechanisms for 802.11ax, only consider a single traffic type. Moreover, the access mechanism is either based on an oracle of knowing which STAs have traffic, the UORA mechanism, or traffic is saturated (queues having frames at all times). In this paper, we compare the merit of these studies and propose a multi-class, delay-based method for STA selection and a near optimal multi-class OFDMA scheduling scheme for IEEE 802.11ax networks.

4.3 Resource Units in 802.11ax

In this section, we describe the RU structure, present formulas to compute the number of RUs and present a recursive formula to compute all the valid partitions of a given bandwidth. In 802.11ax, the RU structure is fixed and an STA is not allowed to be allocated more than one RU. Fig. 4.2 illustrates the structure of RUs for the case of 80 MHz bandwidth. Like OFDM, the entire bandwidth (here, 80 MHz) can be perceived as one RU and be allocated to one STA. Also, the bandwidth can be divided into two equally-sized (here $\approx$ 40 MHz) subchannels (i.e., 2 RUs) and be allocated to two different STAs; each of the RUs can be further split into 2 RUs until reaching 26-tone RUs which are the smallest resource units. The RUs created from the splits of higher-level RUs are called regular or binary RUs. In certain levels (here, levels 0 and 2), one RU can be split into two equally-sized RUs plus one extra 26-tone RU. The extra RU(s) in the middle of RU(s) of these levels are then referred to as mid-RU RU(s).

Notation-wise, RUs are denoted by a pair (l, i), where l and i denote the level of split from the root RU, $RU(0, 0)$, and the index of the RU at that level, respectively.

The maximum level of RUs in a given bandwidth is denoted by L, where L can be either 4, 5, 6, or 7 corresponding to 20, 40, 80, or 160 MHz bandwidth, respectively. Regular RUs of level $(l < L - 1)$ can be split into two RUs, $RU(l+1, 2i)$ and $RU(l+1, 2i+1)$. Identifying the set of levels containing mid-RU RUs depends on L and can be derived by set $\alpha = \{L - 4, (L - 4)\%2\}$, where $|\alpha|$ indicates the cardinality of α. Once the set of mid-RU level(s) is computed, the number of RUs at each level can be computed. There are 2^l regular RUs at each level, and if $L \geq 4$, there exists mid-RU level(s) and hence mid-RU RU(s). In general, the total number of RUs in a level is computed by adding regular RUs of that level plus the mid-RU RU(s) if existent:

$$RU_l = 2^l + \sum_{i=1}^{|\alpha|} 2^{\alpha(i)} 1_{\{l > \alpha(i)\}}, \tag{4.1}$$

where $1_{\{l > \alpha(i)\}}$ is an indicator function; it is 1 when the condition $l > \alpha(i)$ is valid, and 0, otherwise. As an example, in Fig. 4.2 for 80 MHz bandwidth $(L = 6)$, the set of mid-RU level(s) is computed as $\alpha = \{0, 2\}$. Therefore, the total number of RUs in level 1 is $RU_1 = 2^1 + 2^0 = 3$ and in level 3 is $RU_3 = 2^3 + 2^0 + 2^2 = 13$. Note that for 80 MHz bandwidth, the number of mid-RU RUs in levels 1 and 2 is 1 and in level 3 to 5 is 5. For the sake of simplicity, we show the index of RUs in each level in the range $[0, 2^l - 1]$ for regular RUs and $[2^l, RU_l - 1]$ for the mid-RU RUs if they exist. For instance, in level 3 of Fig. 4.2, regular RUs are shown from $(3, 0)$ to $(3, 7)$, and mid-RU RUs are therefore shown from $(3, 8)$ to $(3, 12)$. The maximum number of 26-tone RUs in a bandwidth, $\mathcal{N}_{\mathrm{RU}}$, is computed based on L as shown in Eq. (4.2[4]). For instance, in 80 MHz, there are 6 levels of RUs with the total of 37 (26-tone) RUs. Table 4.1 presents the number of different RU types with data and pilot subcarriers in different

---

[4] IEEE 802.11ax only uses $4 \leq L \leq 7$. However, other IEEE standards such as IEEE 802.11p might use $L \leq 4$.

channel bandwidths of 802.11ax.

$$
\mathcal{N}_{\text{RU}} = \begin{cases} 2^{L-1} & L < 4 \\ 2^{L-1} + 2^{L-4} & L \leq 4 < 6 \\ 2^{L-1} + 2^{L-4} + 2^{L-6} & L \geq 6 \end{cases} \tag{4.2}
$$

Table 4.1: Number of 802.11ax RUs per bandwidth

Bandwidth (MHz) RU Type (Data, Pilot)	20	40	80	80+80/160
26-tone (24, 2)	8+1	16+2	32+5	64+11
52-tone (48, 4)	4	8	16	32
106-tone (102, 4)	2	4	8	16
242-tone (234, 8)	1	2	4	8
484-tone (468, 16)	-	1	2	4
996-tone (980, 16)	-	-	1	2
2×996-tone (1960, 34)	-	-	-	1

So far, we can compute the number of binary RUs at each level and the maximum number of RUs in a given bandwidth. To maximize the channel efficiency and satisfy the QoS requirements of each STA, allocation of RUs should be based on each STA's instantaneous condition and requirements such as channel quality over different RUs, type of service, delay requirements, and buffer length. Following the rules of 802.11ax, a valid RU partition in 802.11ax is a partition comprising identical or different RU sizes. If there is only one 26-tone RU, there is only one way to allocate it. If there are two 26-tone RUs, there are 2 ways to allocate them: (1) each one is allocated to one STA, and (2) both are merged and allocated to one STA. In general, for the number of 26-tone RUs that can be merged to create bigger RUs (m), the number of valid RU

partitions (P_m) can be computed recursively by:

$$P_m = \begin{cases} (P_{m/2})^2 + 1 & m \in \{2, 4, 8, 16, 32, 64\} \\ 1 & m = 1 \end{cases} \qquad (4.3)$$

For example, in 20 MHz bandwidth, there are eight 26-tone RUs that can merge in different ways (mid-RU RUs are unable to merge with each other or with regular RUs). The number of valid partitions created from these eight RUs depends on the number of valid partitions from 4 RUs and so forth. Thus, $P_8 = (P_4)^2 + 1 = \cdots = ((1^2+1)^2+1)^2+1 = 26$. With doubling of the bandwidth (and the number of mergeable 26-tone RUs), the number of valid RU partitions grows exponentially, e.g., for 80 MHz, $P_{32} = 458,330$. To find the optimal allocation of RUs to STAs to maximize a utility (e.g., sum-rate), any exhaustive search requires a matrix of the number of STAs by their rates over each of these valid partitions, which is too time consuming to compute for each TXOP. Other optimizations related to STA selection and RU allocation include, but are not limited to, maximizing queue serving, minimizing delay and minimizing the RU wastage. Therefore, new innovations are required to select the proper set of STAs to be scheduled and scheduling algorithms by pruning the search space efficiently. To cope with the complexity of the optimization, the metrics for STA selection and RU allocation are broken down into two layers. In the first layer, a subset of STAs are selected based on some metrics such as delay, and in the second layer, the selected STAs or a subset of them are allocated an RU based on other metrics such as channel quality over different RUs.

4.4 STA Selection Mechanism

In previous EDCA-based WLAN standards, upon receiving frame(s) in the MAC queues of an STA, the STA would choose a random backoff based on EDCA parameters

and count down by following CSMA/CA rules to transmit these frames. In 802.11ax, the AP needs the queue information of STAs in order to allocate RU resources to them. This information can be obtained by (1) AP polling STAs to learn their queue status (solicited BSR), (2) STAs piggy-backing their BSRs to their HE TB PPDU or ACK frames after successfully receiving DL PPDUs (unsolicited BSR), or (3) STAs announcing their requirements via the UORA mechanism. Although UORA allows STAs to announce their requests to the AP in a relatively short time, the MAC-layer efficiency is bounded by $1/e \approx 37\%$ in dense networks [37]. Naik *et al.* [38] showed that there is a trade-off between the achievable throughput and the delivery rate of buffer status report. On the other hand, if UORA is not used, a question arises as to how the STAs should be served not only to decrease their queuing delay but also to prioritize delay-sensitive traffic.

In the TRS access mechanism, the simplest approach to obtaining BSRs of the STAs is by using a round-robin (RR) algorithm. The AP transmits a BSRP to a subset of STAs based on a RR fashion and then, allocates one RU to each STA who has pending frames for the AP. Due to hardware limitations, the maximum number of STAs to be scheduled for simultaneous UL transmissions cannot exceed a limit $\mathcal{S}$ which is 16 in our study[5]. Also, note that sometimes the maximum number of associated STAs to an AP, $\mathcal{N}_\mathrm{S}$, is less than the maximum number of RUs in a given bandwidth. Since the BSRs of some STAs may be known (by unsolicited BSRs or former solicited BSRs), the set of STAs to be solicited for their BSRs, $\mathcal{N}_\mathrm{BSR}$, is computed based on the following inequality:

$$\mathcal{N}_\mathrm{BSR} \leq \min\left(\mathcal{N}_\mathrm{RU}, \mathcal{N}_\mathrm{S}, \mathcal{S}\right) \tag{4.4}$$

---

[5] This limitation only affects the bandwidths larger than 20 MHz since the maximum number of RUs, $\mathcal{N}_\mathrm{RU}$, in 20 MHz is 9.

When STAs report their BSRs, the number of STAs with pending frames for the AP (N_{UL}) can be 0 or less than $\mathcal{N}_{\text{RU}}$. Depending on N_{UL} and their queue(s), AP may solicit BSRs of more STAs in a MU cascading sequence. Therefore, possible enhancements to RR can be: (1) not to solicit BSRs of STAs that were unable to flush their queue(s) with one HE TB PPDU, and (2) to solicit multiple rounds of BSRs if more N_{UL} can be supported for a simultaneous UL HE PPDU. However, in dense scenarios where the number of STAs is large, RR is not efficient to satisfy the QoS requirements of delay-sensitive STAs.

In this section, based on the ability of the MAC layer to impose intervals on transmission of different traffic types, we propose a mechanism in which AP can learn the transmission intervals of high priority traffic and serve the STAs when they actually have traffic and within their QoS delay requirements. This scheme eliminates the need to solicit BSR of STAs when they have no frames to transmit.

4.4.1 Learning the intervals

When an STA with high priority traffic transmits its uplink frame for the first time, the scheduler on the AP records the transmission time. The scheduler then tries to find the frame interval by serving the STA with the minimum time between two consecutive scheduling of that same STA with RR scheduling until the interval is measured. Unlike the queue of voice traffic that gets flushed with each transmission, video frames, owing to their amount, might require multiple UL HE PPDUs to be transmitted. In this situation, learning the interval does not help to reduce the delay of video traffic as some frames remain in the queue. Therefore, not only is the interval of video traffic important, but also is the delay of the head-of-line (HOL) frame. Since HE STAs are able to piggy-back their buffer status reports with the transmitted HE TB PPDU, if a queue of video frames is not flushed during a TXOP, the scheduler records

the estimated delay of the HOL frame to be served within its QoS limits. Learning the traffic intervals and keeping the HOL delay of delay-sensitive traffics liberate the AP from frequently exchanging control frames (e.g., BSR) and use the channel time for the actual data transmissions.
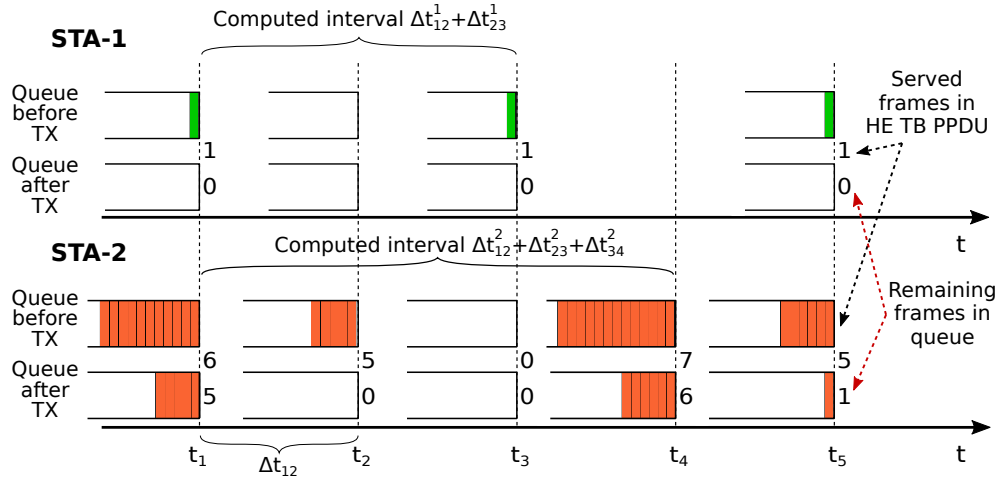
Figure 4.3: Finding and tuning the traffic intervals. Keeping the estimated delay of the HOL frame in the case the queue is not flushed.

Fig. 4.3 illustrates this learning process with two STAs with delay-sensitive applications. $\Delta t_{i,i+1}^{j}$ denotes the time between two consecutive serving of STA j in RR algorithm. At time t_1, with an HE TB PPDU, both STAs transmit their frames (STA-1 has only one voice frame while STA-2 can aggregate 6 frames into an A-MPDU). At time t_2, STA-1 is solicited for its BSR which returns to be none. However, since the queue of STA-2 did not flush, in the next TF, the scheduler allocates another RU for it. At time t_3, STA-1 is again fetched for its buffer status and since it has a frame to transmit, the interval of STA-1 is measured to be $\Delta t_{12} + \Delta t_{23}$. This interval is measured for STA-2 at time t_4 to be $\Delta t_{12} + \Delta t_{23} + \Delta t_{34}$. Since the queue of STA-2 is not flushed at times t_1, t_4, and t_5, the HOL frame delay is estimated for them to be served again in the following TXOP. With constant learning, the scheduler converges to the actual interval imposed on the traffic by the STA's MAC layer.

With the knowledge of frame intervals and HOL frame delays, the scheduler can estimate at any point in time, the STAs with pending UL frames. Applications are prioritized based on their access categories. However, some high priority access categories can tolerate larger delay within their threshold levels, and thus, are not necessary to be scheduled as soon as an STA receives such frames in its MAC queues. Therefore, we propose a threshold-based algorithm to serve the high priority access categories based on two thresholds (soft and hard). If few number of STAs have delay-sensitive traffic, STAs are served within their soft threshold. However, with the increase in the number of STAs with delay-sensitive applications or interference from neighboring APs working on the same channel, the AP might decide to increase the soft threshold of STAs up to the point where their hard threshold is reached. With efficient tuning of soft and hard thresholds, not only delay-sensitive access categories will be served within their delay requirements, but also higher amount of best effort traffic will be served.

Algorithm 3 Adaptive STA Selection based on HOL frame delay

Require: Traffic Interval of STAs with delay-sensitive traffic

    ▷ Compute number of active STAs

1: $A = |\mathcal{X}(\mathcal{D}^i > \gamma_{min}^i)| \qquad \forall i \in \mathcal{X}$

    ▷ Update the serving threshold

2: $\gamma_S^i = \gamma_{min}^i + (A \times \frac{\gamma_{max}^i - \gamma_{min}^i}{|\mathcal{X}_{max}|})$

    ▷ Minimize HE TB PPDU by serving only voice

3: **if** $|\mathcal{D}^j > \gamma_S^j)| > 0 \quad \forall j \in \mathcal{X}_{vo}$ **then**

4:      $\mathcal{L} = \mathcal{X}_{vo}(\mathcal{D}^j > \gamma_S^j)$

5:      $\mathcal{L} = \{\mathcal{L}, \min(\mathcal{N}_{RU} - |\mathcal{L}|, |\mathcal{X}_{vo}(\mathcal{D}^j > \gamma_{min}^j)|\}$

6:      **return** $\mathcal{L}$

7: **else**

8:      $\mathcal{L} = \mathcal{X}_{vi}(\mathcal{D}^k > \gamma_S^k) \quad \forall k \in \mathcal{X}_{vi}$

9:      $\mathcal{L} = \{\mathcal{L}, \mathcal{X}_{be}\}$

10:      **return** $\mathcal{L}$

11: **end if**

Among the set of active STAs associated with an AP, let $\mathcal{X}_{vo}$, $\mathcal{X}_{vi}$, and $\mathcal{X}_{be}$ be the

set of STAs with voice, video and best effort traffic, respectively. The scheduler keeps the HOL frame delay of voice and video STAs denoted as $\mathcal{D}_{vo}$ and $\mathcal{D}_{vi}$, respectively. Also, γ_S and γ_H denote the set of soft and hard thresholds for each delay-sensitive applications, respectively[6]. Since voice has the highest priority and voice frames are comprised of small frames, to shorten the length of UL TB PPDU, the scheduler first checks if there are enough voice STAs to serve them together (add them to $\mathcal{L}$). If there are not enough voice STAs, then STAs whose HOL delay has exceeded their hard threshold are chosen . If there are still available RUs for the UL HE PPDU, the scheduler chooses from the STAs whose soft threshold is reached. After selecting delay-sensitive STAs, if there are still some RUs left, they are allocated to data stations based on RR or proportional fairness algorithm [49].

Algorithm 3 shows the pseudocode of the framework for selecting STAs based on their HOL frame delay. In this algorithm, the number of scheduled STAs in each TXOP is computed based on Eq. 4.4 which brings down the computation of second layer. It is also possible to send all STAs to the second layer for resource allocation albeit with the price of over-prioritizing some access categories [50] and more computations. Two-layer schedulers show promising results; for instance, in [51], a two-layer scheduler for LTE systems is proposed to enhance the overall throughput of the network. In this algorithm, first, delay-sensitive applications are chosen whose HOL frame delay exceeds their hard threshold, (γ_H).

4.5 UL Scheduling in 802.11ax

Once the list is filled, it will be sent for scheduling. The scheduling is based on a modified version of [45] in which traffic differentiation and QoS are realized. Thus,

---

[6] Note that these thresholds might be different for different traffic types and different codecs.
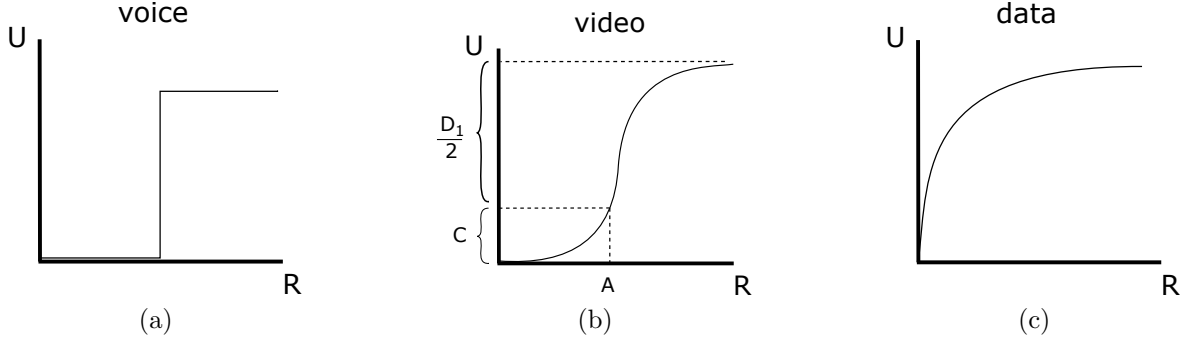
Figure 4.4: Utility functions: a) hard real-time utility for voice b) delay-adaptive utility for video (combination of two logistic functions) and c) Elastic utility for data.

instead of maximizing the sum-rate, we maximize the sum utility which is a function of rate and type of service.

4.5.1 Utility Functions

Since in practical scenarios, there are different traffic types, and the date rate of each STA varies over different RUs, we need utility functions that can prioritize traffic types and the STAs with the same traffic type. For voice, the utility can be a binary function; 0, if the rate is smaller than a threshold, and 1 if the rate is larger than a threshold. Equation (4.5) shows the utility of voice as the function of rate. Since voice frames are small, a 26-tone RU is enough for them, which is achieved by giving voice a flat utility.

$$U_{voice}(R) = \begin{cases} 10 & R > \Gamma_{voice} \\ 0 & R < \Gamma_{voice} \end{cases} \tag{4.5}$$

For video, we modified the utility function proposed in [52]. Since we would like to limit the video to higher rates, this can be realized with a logistic function before the threshold point (A) combined with another logistic function to achieve a sharp

increase before the flat point as illustrated in Fig. 4.4. Note that when the rate is zero the utility is also computed as zero. Eq. (4.6) represents this function.

$$U_{video}(R) = \begin{cases} \dfrac{D_2}{1 + e^{-B_2(R-A)}} - \dfrac{D_2}{2} + C & R > A \\ \dfrac{D_1}{1 + e^{-B_1(R-A)}} - \dfrac{D_1}{2} + C & R \leq A \end{cases} \tag{4.6}$$

where D_1 and D_2 are the maximum value of the utility before and after A. B_1 and B_2 are the slopes of the sigmoidal curves at the turning points and C is a constant to make sure that utility is zero when R is zero. For data, it should be a concave and monotonically increasing function [44,53]. This can be shown as a log function as shown in Eq. (4.7).

$$U_{data}(R) = \log_{10}(1 + \frac{R}{10}) \tag{4.7}$$

Since the priority is voice > video > data, the utility function of voice and video should have larger values. The final optimization function then becomes:

$$\max \sum_{i=1}^{N} \sum_{j=1}^{M} U_{voice} + U_{video} + U_{data} \tag{4.8}$$

4.5.1.1 Joint Scheduling and power allocation

To find an optimal user schedule, one way is to exhaust all the search space which is very time consuming and hence, impractical in Wi-Fi networks where the AP should decide the user schedule in each TXOP. Because of the binary-tree-like structure of RUs in the channel bandwidth, it is possible to use divide and conquer algorithm to assign RUs to different STAs based on their channel and bandwidth requirements; using the acquired information about each STA's queues and channel, AP tries to maximize the instantaneous utility by allocating the optimal RU to each STA and assigning the power to the RU by water-filling algorithm.
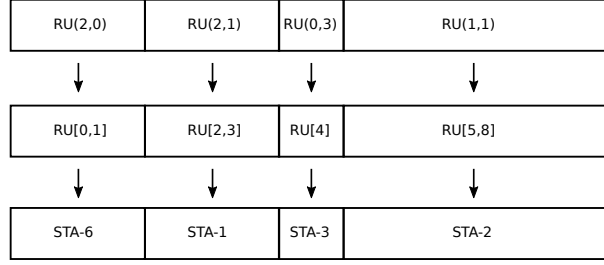
Figure 4.5: A sample valid partition of a 20 MHz bandwidth, mapping to last level $(l = L - 1)$ and allocation of STAs to the RUs.

Once the STAs to be served in the UL TXOP are selected, they are passed to the recursive scheduling algorithm, Algorithm. 4. In 802.11ax, the entire bandwidth can be divided into multiple RUs of different levels, each assigned to a single STA. For simplicity, we can represent each $RU(l, i)$ by mapping it to the highest level of the tree and showing the index of its start (s_n) and finish (f_n). For instance, $RU(1, 0)$ in 20 MHz is a 106-tone RU (the aggregation of four 26-tone RUs) and can be shown as $RU[0, 3]$. Let $p_i = \{RU[s_{i1}, f_{i1}], RU[s_{i2}, f_{i2}], \cdots, RU[s_{in}, f_{in}]\}$ be a valid partition of a bandwidth and $U = \{u_1, u_2, \cdots, u_n\}$ be the set of selected STAs to be scheduled. $\mathbb{S} = \{p_i, u_j\}$ denotes the one-to-one allocation of this valid partition to a set of n STAs. Figure. 4.5 illustrates a sample mapping and user allocation in a 20 MHz bandwidth.

Algorithm 4 RU allocation to chosen STAs
___
Require: The CSI of the selected STAs
 1: $\alpha \leftarrow \{L-4, (L-4)\%2\};$ ▷ levels with mid-RU RUs
 2: $ll \leftarrow 2i; r \leftarrow 2i+1;$
 3: $m \leftarrow \{\}; i \leftarrow 0; l \leftarrow 0;$
 4: **function** RECSCHED(U,l,i)
 5:     **if** $l < L-1$ **and** $i < 2^l$ **then**
 6:         **if** $l \in \alpha$ **then**
 7:             $\mathcal{I} \leftarrow 6; m \leftarrow 2^{l+1}+i;$
 8:         **else**
 9:             $\mathcal{I} \leftarrow 2; m \leftarrow \{\};$
10:         **end if**
11:         **for** $index \leftarrow 1$ **to** $\mathcal{I}$ **do**
12:             **switch** $index$ **do**
13:                 **case** 1
14:                     $a \leftarrow ll; b \leftarrow m; c \leftarrow r;$
15:                 **case** 2
16:                     $a \leftarrow r; b \leftarrow ll; c \leftarrow m;$
17:                 **case** 3
18:                     $a \leftarrow m; b \leftarrow ll; c \leftarrow r;$
19:                 **case** 4
20:                     $a \leftarrow m; b \leftarrow r; c \leftarrow ll;$
21:                 **case** 5
22:                     $a \leftarrow r; b \leftarrow m; c \leftarrow ll;$
23:                 **case** 6
24:                     $a \leftarrow ll; b \leftarrow r; c \leftarrow m;$
25:             $\mathbb{S}_{opt}(l+1,a) \leftarrow$ RECSCHED$(U, l+1, a);$
26:             $U_r \leftarrow U - \{u|u \in \mathbb{S}_{opt}(l+1,a)\};$
27:             **if** $b \neq \{\}$ **then**
28:                 $\mathbb{S}_{opt}(l+1,b) \leftarrow$ RECSCHED$(U_r, l+1, b);$
29:                 $U_r \leftarrow U_r - \{u|u \in \mathbb{S}_{opt}(l+1,b)\};$
30:             **end if**
31:             **if** $c \neq \{\}$ **then**
32:                 $\mathbb{S}_{opt}(l+1,c) \leftarrow$ RECSCHED$(U_r, l+1, c);$
33:                 $U_r \leftarrow U_r - \{u|u \in \mathbb{S}_{opt}(l+1,c)\};$
34:             **end if**
35:             $\mathbb{S}_{index}(l,i) \leftarrow$ MERGE$(\mathbb{S}_{opt}(l+1,a), \mathbb{S}_{opt}(l+1,b), \mathbb{S}_{opt}(l+1,c));$
36:             // Give entire RU to STA with highest utility
37:             $\mathbb{S}_{opt}(l,i) \leftarrow \underset{u \in U}{\operatorname{argmax}}(\text{UTILITY}(u))\};$
38:             // update
39:             $G \leftarrow \{\mathbb{S}_{opt}(l,i), \mathbb{S}_{index}(l,i)\};$
40:             $\mathbb{S}_{opt}(l,i) \leftarrow \underset{g \in G}{\operatorname{argmax}}(\text{UTILITY}(g));$
41:         **end for**
42:     **else**
43:         $\mathbb{S}_{opt}(l,i) \leftarrow \underset{u \in U}{\operatorname{argmax}}(\text{UTILITY}(u));$
44:     **end if**
45:     **return** $\mathbb{S}_{opt}(l,i);$
46: **end function**
___

In Algorithm 4, first, the mid-RU levels are computed based on the bandwidth (line 1). Left split (ll), right split (r) and the center split (m) are initialized. The reason that middle split is initialized to $\{\}$ is because splitting RUs into three RUs depends on the operation level. However, as we can see in line 6, if an RU can be split into three RUs, m will receive the index of the middle RU which is numbered $2^{l+1} + i$. In this case, there are $3! = 6$ permutations of user selection with a total of 18 recursive calls (shown in the switch/case statement). Therefore, the number of loops ($\mathcal{I}$) should be 6. Also, since "case 1" and "case 2" run for each loop iteration and the variable a is either assigned to ll or r, there is no need to check for not being null when calling the function recursively (line 25). However, this may not be true for variables b and c, and hence, should be checked. Eventually, the optimal user selections for the $\mathcal{I}$ cases should be merged and compared with assigning all the RUs to one user (lines 35-40). Note that the "else" part of the algorithm (line 42) is to return the optimal user selection when either the level of RUs is L-1 or a mid-RU RU is reached.

In Algorithm 4, user selection is the basic operation of the recursive method. The complexity of the algorithm depends on the bandwidth and the number of mid-RU levels. For each RU, there are either 2 splits with 2! permutations or 3 splits with 3! permutations. Therefore, there are either 4 recursive calls for the 2 splits or 18 recursive calls for the 3 splits. However, in the 3-split-case, 12 of the 18 calls will result in binary splits and 6 of them result in user selection. Therefore, at each level, there are one user selection for allocating the entire RU to a single user and one user selection at level L-1. If there are mid-RU levels, 6 user selections are required at each mid-RU levels. So, the number of user selections can be represented by the following

recursive equation:

$$\phi(l) = \begin{cases} 12\phi(l+1) + 7 & l = L - 4 \text{ or } l = L - 6 \\ 4\phi(l+1) + 1 & l \neq L - 4 \text{ or } l \neq L - 6 \\ 1 & l = L - 1 \end{cases} \qquad (4.9)$$

The amount of user selections for 802.11ax based on the above recursive formula is between 259 and 49805 user selections for 20 MHz and 160 MHz bandwidth, respectively.

4.6 Simulation Scenarios, Settings and results

4.6.1 Simulation Scenarios and Settings

We developed a simulator in Matlab with major MAC and PHY features of IEEE 802.11ax. STAs are random uniformly placed around the AP and the AP-STA distance is less than 6 m. In general, control frames are sent with the lowest data rate (MCS 0). The AP-initiated control frames (e.g., TF and MU-ACK) are sent over the entire primary bandwidth while the STA-initiated control frames (e.g., BSR) are sent over the individual 26-tone RUs. The MCS and data rate for the UL data transmissions are computed based on the receive sensitivity requirements outlined in [54]. In our simulations, we take into account the path loss (PL) and shadowing loss (SL); SL is based on the log normal distribution with standard deviation of 5 dB and The PL is computed based on WINNER II for indoor environment [55] with the following equation:

$$PL = 20 \times \log_{10}(d) + 46.4 + 20 \times \log_{10}(f_c/f_b), \qquad (4.10)$$

where d is the distance between transmitter and receiver; $f_c = 5.180$ GHz is the center frequency, $f_b = 5$ GHz is the base frequency.

We first simulate 802.11ax in UL direction with single access category (i.e., best effort AC[BE]). We present the results of different station selection algorithms, scheduling mechanisms and utility computations for saturated and non-saturated scenarios. Packet generation is based on Poisson distribution with $\lambda = 50$ and $\lambda = 4000$ for non-saturated and saturated scenarios, respectively. The MSDU arrival times are based on exponential distribution with $\mu = 1/\lambda$ and MSDU sizes are chosen randomly between 500 and 2304 Bytes.

Then, for traffic differentiation, we present a wireless network that consists of 20% VOIP users (AC[VO]), 20% Video users (AC[VI]), and the 60% data users (AC[BE]). For instance, if there are 5 STAs in the network, there are 1 VOIP STA, 1 video STA and 3 data STAs. AC[VO] is chosen based on the iLBC with 20 ms packet intervals and 38 Bytes packet sizes[7] [56]. Traffic for Video STAs is also interval-based; the interval is based on frame per second (FPS) and the frame size is based on target bitrate (TBR) of 2 Mbps. For instance, for 60 FPS, the video interval is $1/60 \approx 17$ ms with 4 MSDUs each 2304 Bytes. Traffic for data station are based on Poisson distribution with $\lambda = 200$ for stations. Other simulation parameters are based on the IEEE 802.11ax standards, as illustrated in Table 4.2.

4.6.2 Results and Evaluation

As mentioned earlier, we first examine different station selection mechanisms, scheduling techniques and popular utilities used in the literature in the context of one AP with a varying number of STA associated with it. Metrics of throughput, delay, and jitter are used to compare different techniques. We also introduce three new metrics that are important in achieving higher efficiency in practical scenarios: the number of TXOPs, RU efficiency (RUE), and In-RU efficiency (In-RUE). For a simulation, if the

---

[7] Note that voice MSDUs have 12 Bytes RTP, 8 Bytes UDP, and 20 Bytes IP headers. Therefore, voice MSDUs are 78 Bytes.

Table 4.2: Other parameters for the simulations

Parameter	Value
Channel Bandwidth	20 MHz
Channel number	36
Empty slot	9 μs
DIFS	34 μs
SIFS	16 μs
MU PPDU preamble duration	228 μs
UL TB PPDU preamble duration	168 μs
MAC queue size (Bytes)	80k
Simulation Runs	10
Frame Aggregation Type	only A-MPDU
Number of Aggregated Frames	up to 256
TXOP duration	5.484 ms

number of TXOP that is used to complete the simulation is smaller, it means that in multi-AP scenarios where interference from other APs operating on the same channel affect the results, the AP requires less contention to obtain a TXOP and serve their associated STAs. Let T be the number of TXOPs used in a simulation and $\mathbb{U}_{RU}$ be the number of RUs used in each TXOP[8]. $\mathbb{U}_{RU}$ indicates the number of 26-tone RUs used. From earlier, we know that $\mathcal{N}_{RU}$ is the maximum number of RUs in a BSS. Therefore RUE will be computed by:

$$\text{RUE} = \frac{\sum_{i=1}^{T} \mathbb{U}_{RU}}{T * \mathcal{N}_{RU}} \tag{4.11}$$

It is often the case that the traffic in a wireless network is not saturated. However, saturated scenarios are required to measure the maximum capacity of a wireless network. With a network comprising stations of having only best effort access category, saturated scenarios are possible (i.e., STAs are either constantly uploading or constantly downloading big files). However, in traffic differentiation, each access category

---

[8] Note that only one RU can be assigned to each STA, but that RU is either a 26-tone RU or is a binary combination of 26-tone RUs with some peculiarities discussed in Section 4.3.

has its own traffic characteristics. With the 802.11ax rule that all STAs should transmit for the entire PPDU duration, some waste in spectrum and energy consumption of STAs are unavoidable. To combat these waste, Multi-TID aggregation is proposed which is not achievable all the times. Therefore, another metric we define is In-RUE as the portion of the RU which is used as:

$$\text{In-RUE} = \frac{\sum\limits_{i=1}^{T} \left(\mathbb{U}_{RU} - \mathcal{W}_{RU} \right)}{T * \mathcal{N}_{RU}} \tag{4.12}$$

4.6.2.1 Single Access Category Scenario

As mentioned earlier, the problem of assigning one RU to each STA can be turned into assignment problem and solved using Munkres or Hungarian algorithms. However, since Munkres algorithm is slow and the number of computations increases exponentially with larger-than-20 MHz bandwidths, the inclusion of Munkres is to show the upperbound for our proposed scheduling algorithm. 4.6 presents the results of RR algorithm for station selection, different scheduling algorithms and proportional fairness (PF) as the utility function in saturated scenario.

It can be seen that our recursive algorithm (Rec-Opt), can achieve the same results as Munkres algorithm. The blue curves show the results on not taking into account the mid-RU RUs which is only one in 20 MHz. Since the scenario is single access category and saturated, the fairness results, RUE, and In-RUE are almost 1.

Now that we see our scheduling mechanism reaches near optimal results, we present the results of different station selection and utility computations. Fig. 4.7 illustrates the results of RR and Oracle-based station selection mechanisms with PF and max-rate utilities.

One of the well-known utilities is "max-rate" for which the goal is to maximize the rate. Therefore, at each round of scheduling only one STA gets selected that has
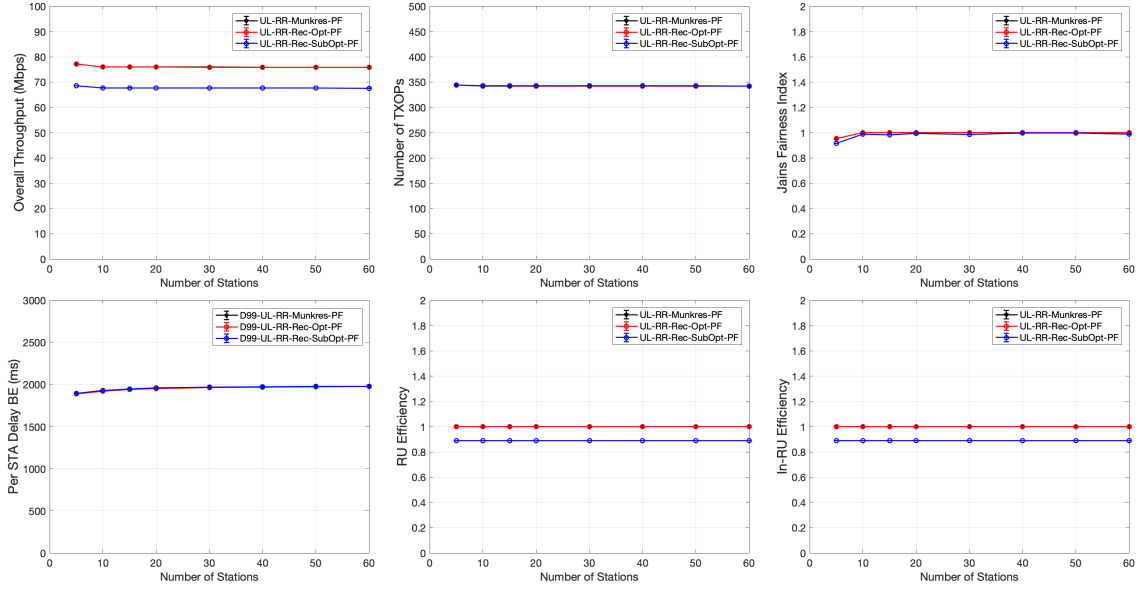
Figure 4.6:   The difference between scheduling techniques in saturated scenario: Recursive Binary scheduling achieves the same results as Munkres algorithm.
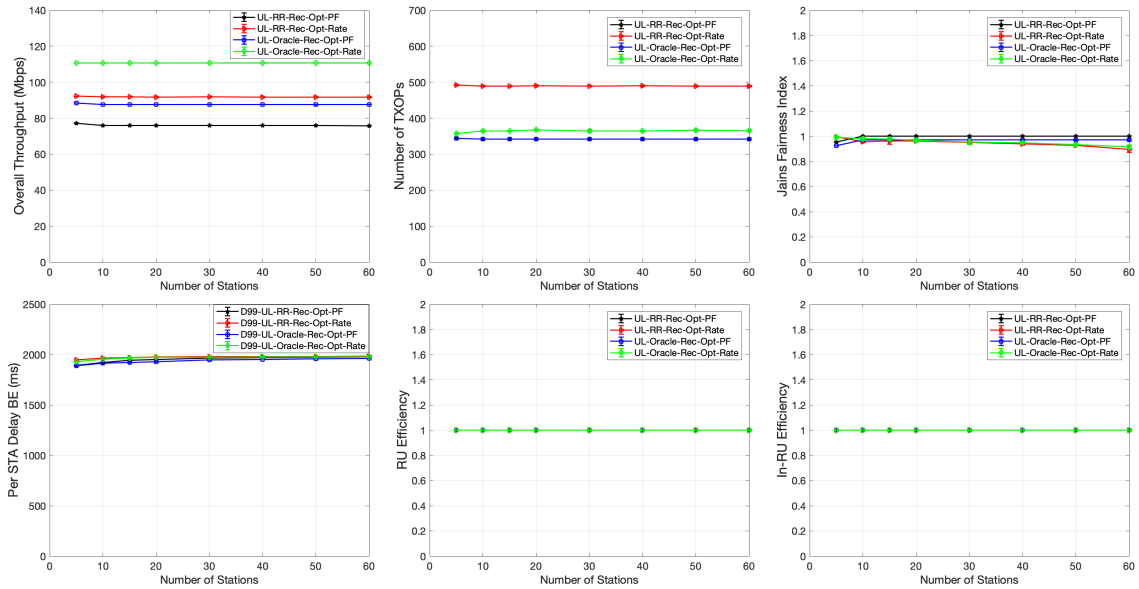
Figure 4.7:   The difference between station selection techniques and utility computations in saturated scenario: max-rate achieves highest throughput at the cost of lower fairness.

the highest rate based on its channel quality. Since the traffic is saturated, "max-rate" can achieve highest throughput. However, the number of used TXOPs is higher and

fairness among the stations are lower than PF. It should be also noted that oracle-based station selection mechanism achieves higher throughput than RR as the scheduler can decide among more stations as to pick the best possible subset.
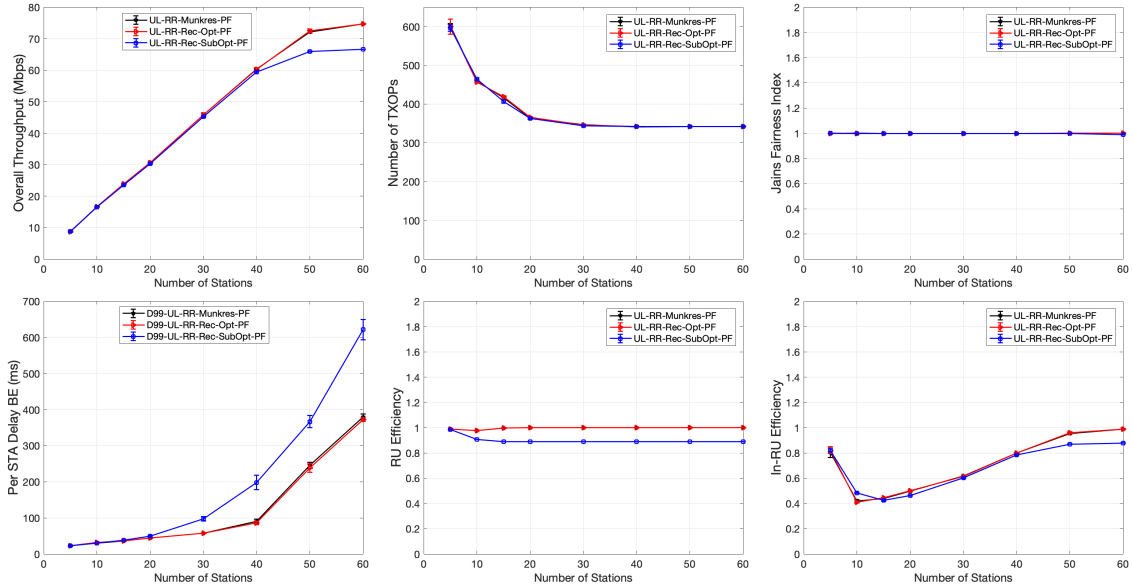
Figure 4.8:   The difference between Scheduling mechanisms in unsaturated scenario: Recursive optimal scheduling reaches almost the same results as Munkres.

Unsaturated single access category scenario reveals more information about what to consider when designing a proper utility function. As illustrated by Fig. 4.8, again, the throughput of our scheduling method matches the optimal throughput obtained by Munkres. However, the difference between the number of TXOP in 5-20 stations is significant. That calls for the ability to change UL/DL direction within a TXOP to reduce the number of contentions among the APs and legacy STAs. Also, note that the In-RU efficiency is below one up to 50 STAs when the network reaches the point where all the stations have enough frames in the queue to transmit for the entire PPDU duration advertised by the AP.

The results of unsaturated scenario comparing station selection mechanisms and utility computations are illustrated in Fig. 4.9. Again "max-rate" algorithm reaches
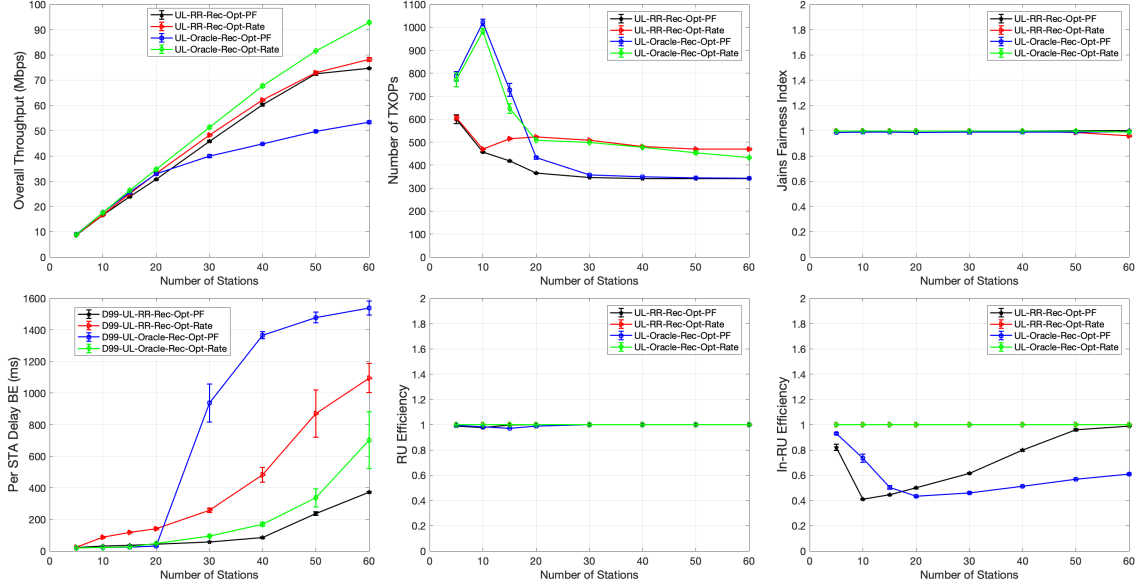
Figure 4.9: The difference between station selection techniques and utility computations in unsaturated scenario: max-rate achieves highest throughput at the cost of higher number of used TXOP.

the highest throughput which is expected as "max-rate" assigns the whole bandwidth to one STA and the UL TB PPDU duration is the PPDU duration of that STA. In this manner, the queue depth of that STA is taken into account. However, since PF chooses more than one STA, some of the UL TB PPDU duration is wasted for padding of STAs with durations shorter than the advertised duration.

From single access category simulations in saturated and unsaturated scenarios we can conclude that "max-rate" algorithm achieves the highest throughput because of assigning the entire bandwidth to the STA with best channel conditions . However, in traffic differentiation, the priority of STAs matters; scheduler should prioritize some access categories over the other although they may not have a better channel conditions.

4.6.2.2 Multiple Access Category Scenario

From Section 4.6.2.1, we see that oracle-based station selection (i.e., sending all the stations with pending frames to the scheduler) is better than RR as the scheduler

72
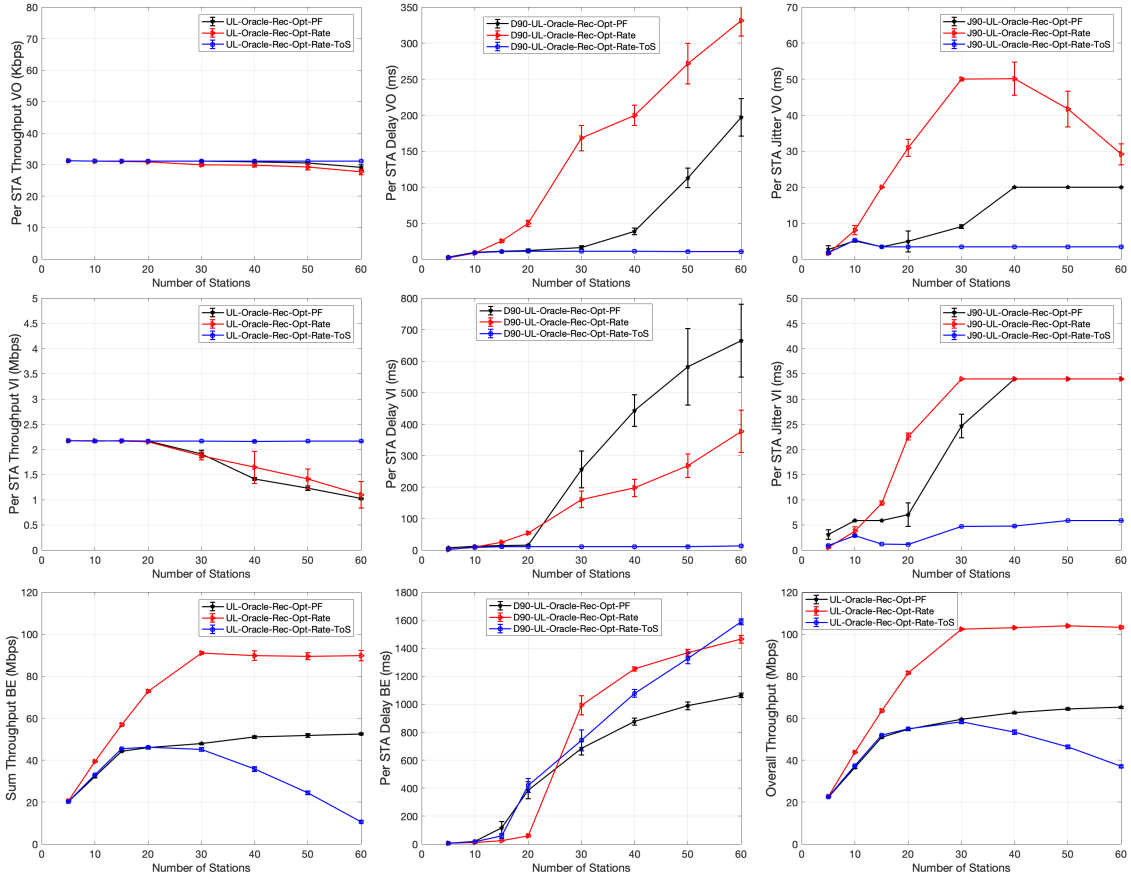
Figure 4.10: The difference between different utilities in traffic differentiation. Voice results are on the first row, video results on the second row and best effort and overall throughput on the third row. Throughput for voice and video access categories are per station but for best effort is sum of all stations.

Figure 4.11: Other simulation results pertaining to multi-class simulation with various utilities.

has more stations to choose a subset from them. We also noticed that the semi-binary recursive algorithm reaches the same results as Munkres algorithm, consumes all the RUs[9] at each round of scheduling and "max-rate" achieves the highest throughput. In this Section, we present the results of multiple access category with different utility functions and compare the results with our utility functions. Then, we present the results of oracle-based station selection compared to our smart station selection mechanism.

Fig. 4.10 illustrate the detailed results of oracle-based station selection, recursive scheduling, and max-rate, PF and rate-ToS utility functions. Since neither max-rate nor PF consider ToS when scheduling, the results of voice and video are adversely affected. With the increasing number of stations, to keep the QoS requirements of voice and video access categories, the scheduler does not starves the best effort access category.

Fig. 4.11 illustrates the other important metrics about the results. Fairness degrades with increasing number of stations. Also, the results of In-RU efficiency of our utility computations is worst among the three utilities. This is because the best effort access category becomes saturated, however, video traffic frames will be served before they can pile up in the queue resulting in an uneven PPDU duration and more padding.

The last sets of results of this Section are the combination of all designed parts: the smart uplink framework (i.e., learning the intervals with its load and delay-based threshold mechanism, semi-binary recursive scheduling and two PPDU duration mechanism) for the scheduling and resource allocation in next generation Wi-Fi standard.

---

[9] Note that the binary recursive algorithm which is depicted sub optimal (SubOpt) in the results does not consume all the RUs.
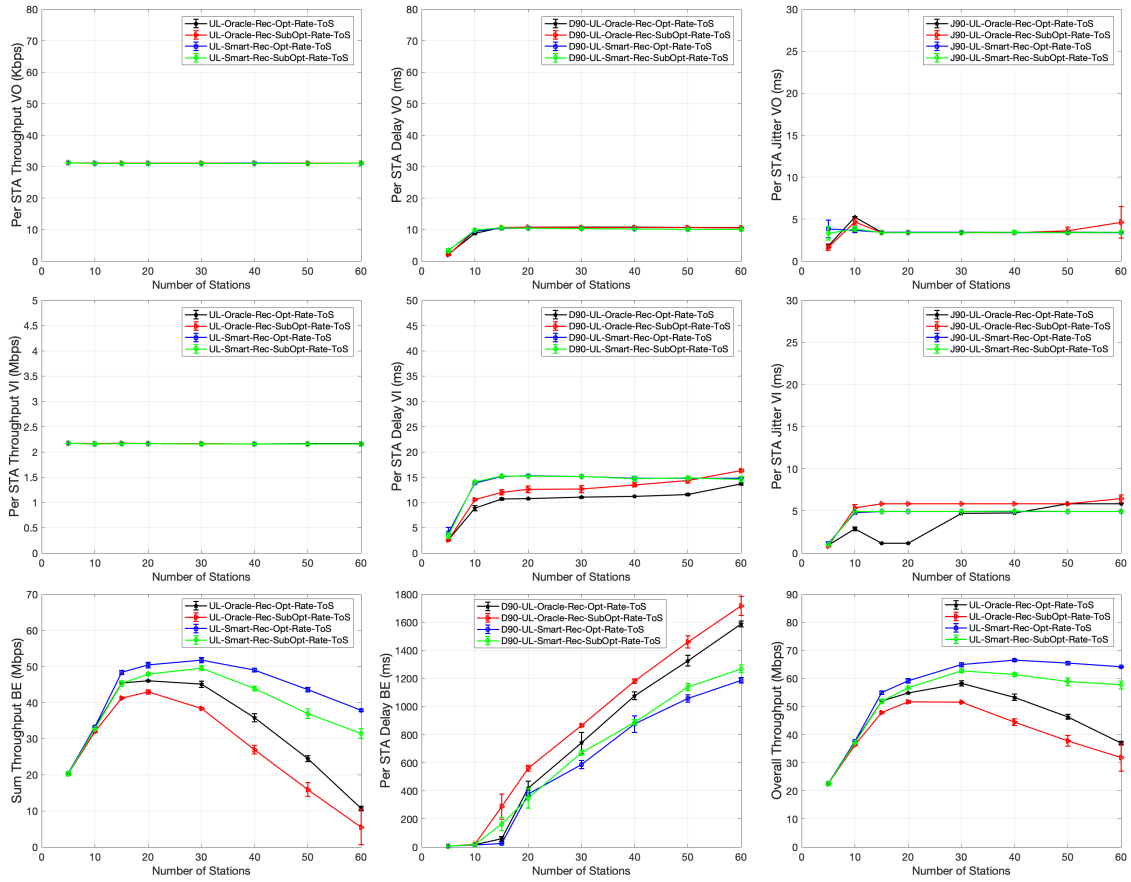
Figure 4.12: The comparison of Smart uplink framework with oracle-based station selection and sub-optimal binary recursive algorithm. Voice results are on the first row, video results on the second row and best effort and overall throughput on the third row. Throughput for voice and video access categories are per station but for best effort is sum of all stations.
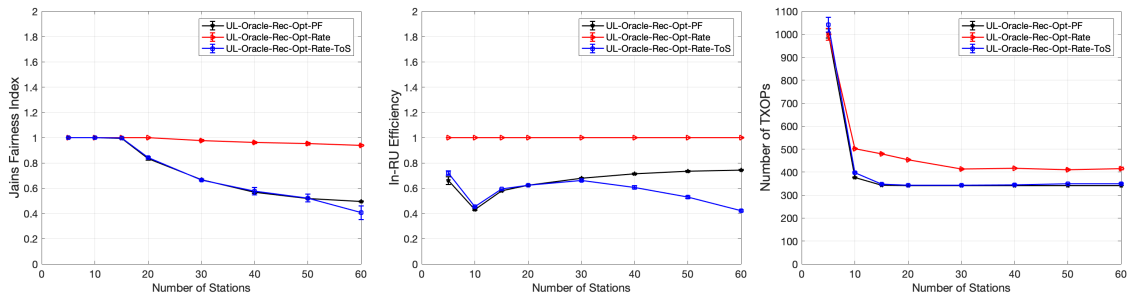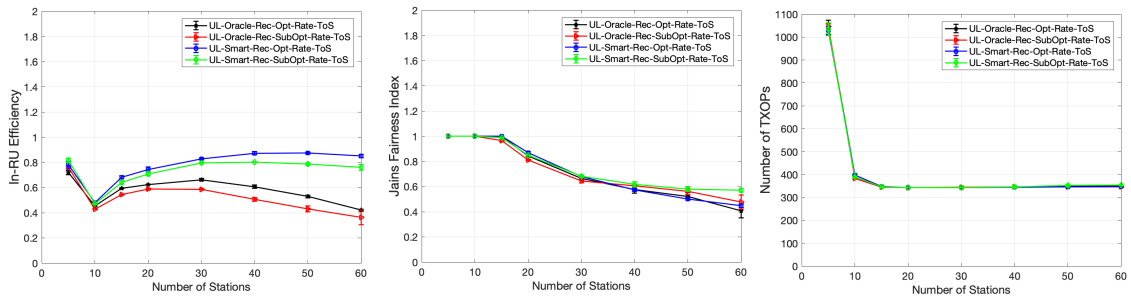

Figure 4.13: Other simulation results pertaining to multi-class simulation of Smart uplink framework in comparison to oracle-based and sub-optimal binary recursive algorithm.

We compare the results of this station selection and scheduling with oracle-based station selection and binary recursive algorithm.

From Fig. 4.12, we can see that the Smart framework achieves almost same results for voice and video access categories and higher throughput for best effort access category. Since the semi-binary recursive algorithm consumes all the RUs, it achieves higher throughput than the binary recursive algorithm. Also, because of different optimizations in learning the intervals and selecting stations based on load and double PPDU duration mechanism, its performace is superior to the performance of oracle-based station selection mechanism.

4.7 Chapter Summary

To combat the frequency selectivity nature of wireless communications and overcome the inefficiency of contention-based protocols, new Wi-Fi standard (IEEE 802.11ax or Wi-Fi 6) has major enhancements. Wi-Fi 6 employs the OFDMA technology where multiple STAs can simultaneously transmit or receive information on different chunks of the channel bandwidth (i.e., RUs). Moreover, the access point is given more authority to schedule the transmission of different stations. However, due to rules associated with sub-channel assignments in Wi-Fi 6, new scheduling mechanisms are required to use the full potential of this standard.

In this research, we divide the issue of resource allocation in IEEE 802.11ax into: (1) selection of STAs for scheduling, (2) optimal RU allocation to the selected STAs, and (3) PPDU duration for the scheduled stations. By using this division and based on the ability of the MAC layer to impose intervals on the transmission of different access categories, we design an interval learning mechanism at the access point coupled with a station selection mechanism based on application delay constraints and network load. We also design a semi-binary recursive scheduling algorithm that optimally allocates

the RUs to the selected stations, and a PPDU duration computation technique that reduces padding and channel overhead. We simulate a next generation Wi-Fi network operating with the Smart framework and compare the results to other state-of-the-art proposed mechanisms. We measure the performance using popular network metrics of throughput, delay and jitter, and introduced three new parameters: number of used TXOPs, RU, and In-RU efficiency.in a 802.11ax network. Simulation results demonstrate higher efficiency of the proposed framework.

Chapter 5

EXTENDING CHANNEL/QOS-AWARE SCHEDULER TO SUPPORT VR TRAFFIC

5.1 Introduction

Augmented reality (AR) and virtual reality (VR), together termed mixed reality (MR) are technologies of broad societal impacts. Through immersive experiences, these technologies will bring a new paradigm for how we can interact with the world, offering unprecedented experiences and unlimited possibilities that will enhance our work and lives in many ways. For instance, for enterprise users and vertical markets such as manufacturing and design, health care, transportation, and retail, MR is expected to raise productivity, allowing workers to visually interact with one another and with data to perform remote collaboration, diagnosis, and maintenance. For consumers, MR will provide personalized content and make everyday experiences more realistic, engaging, and satisfying.

MR applications delivered over mobile wireless networks have attracted huge interest in recent years from both academia and industry [57–59]. In particular, MR has been identified as the first wave of killer apps of the 5G ecosystem [60]. However, a truly immersive MR experience is yet to come due to many technical challenges. Among them, being able to deliver MR over mobile wireless networks is most challenging. Today, MR services are mainly consumed locally and statically, where most head mounted displays (HMDs), such as HTC Vive and Oculus Rift, are wired[1] to high-end

---

[1] Microsoft's Hololens is a pair of mixed reality glasses that connects to backend servers or Cloud via IEEE 802.11ac wirelessly.
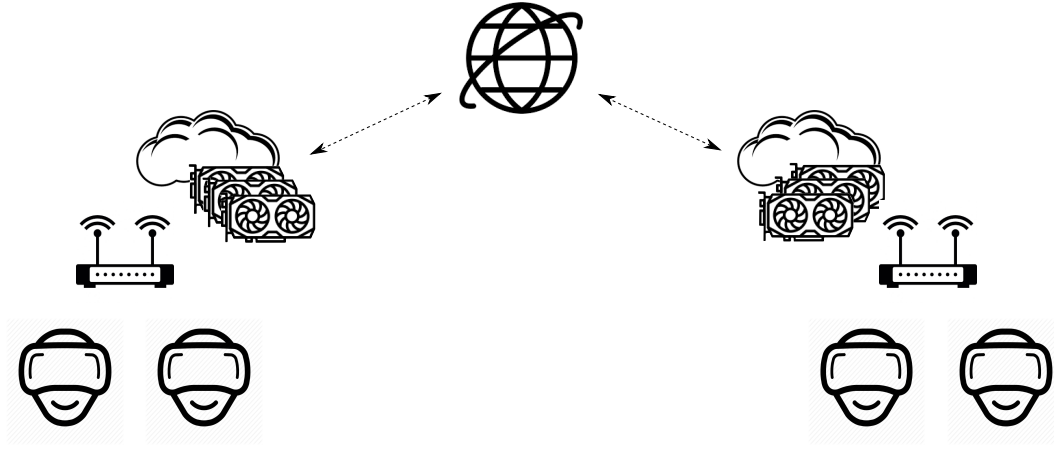
Figure 5.1: Edge computing enabled 802.11ax architecture to support Virtual Reality.

computers equipped with GPUs. We envision that the current localized and individualized MR capabilities will be moved to the **Fog**[2] and/or the Cloud to facilitate **social MR** applications where multiple geographically separated people can communicate and interact as if they were face to face in the same location.

By wearing a pair of MR glasses (such as Microsoft's HoloLens) and employing a video camera, you may participate in video conferencing and communicate face-to-face with remote colleagues in real-time as if we were all in the same room. As another example, imagine being at the Super Bowl and trying to live stream the kickoff (along with 50,000 other fans) using a 360° camera or the multiple cameras in your smartphone. Friends and families at home using MR will be able to enjoy the same experience in real time and feel like they are at the game (as long as the network is not bogged down).

However, to scale social MR over the number of participants and large geographical areas, 5G alone is not sufficient, and demands an end-to-end network architecture

---

[2] In this dissertation, Fog, also termed Edge, refers to base stations and access points that are within the radio access networks and in close proximity to customers, and to provide computing and storage capabilities.
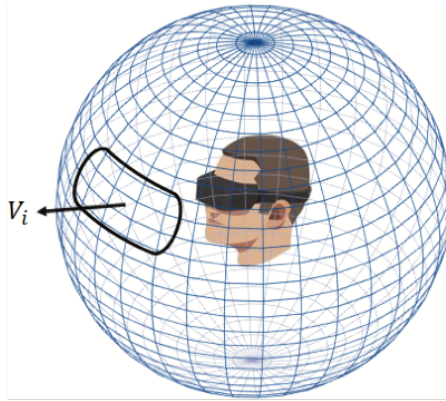
Figure 5.2: 360°-navigable 3D immersion [1]

to realize the envisioned immersive experiences. In this dissertation, we take a holistic view of the network architecture and social VR application depicted in Fig. 5.1 to articulate our efforts.

One of the biggest challenges for VR is the amount of time between a user's movement and the screen being updated, which is known as *motion to photon* (MTP) latency. The total MTP must be less than 20 milliseconds (ms) for a reasonable immersive experience in VR. To put this challenge in perspective, a display running at 60 Hz is updated every 17 ms, and a display running at 90 Hz is updated every 11 ms. In addition, there are many processing activities required before updating the scene in HMD, which include sensors sensing user's movement, fusion of sensor information, viewpoint generation, rendering, decoding, scene correction, and finally updating the scene in HMD.

In contrast to off-line settings, where 360°-navigable 3D scenes are rendered for a user from the high-end computer to which her HMD is attached, on-line delivery of 360°-navigable videos to MR users over wireless networks has attracted much attention. In such an on-demand setting, an MR video is to be delivered to a user in a streaming session, which is presently emerging as a 360°-video-on-demand service provided by

companies like Facebook and YouTube. One naive implementation of such 360°-video-on-demand service is to download the entire 360° video file locally.

More advanced approach allows an MR 360°-navigable 3D video to present the user with an *interactive* immersive visual representation of the remote scene of interest that the user can navigate from any possible 3D viewpoint. As depicted in Fig. 5.2, the present *viewpoint* of the user is denoted as V_i, and the horizontal and vertical fields of view of the MR HMD determine the surface area of the spherical video content surrounding V_i rendered on the display. By constantly uploading the current viewpoint V_i into a Cloud or Fog MR service, rendering can be done adaptively in real-time in the Cloud/Fog and the corresponding spherical video content surrounding V_i is streaming back to user's HMD. This allows immersive experience with live events.

To support VR usage wirelessly, the literature advocates the use of either mmWave [58, 61, 62] or cellular networks [1, 63, 64]. However, mmWave requires line of sight (LoS) communications and deployment of APs capable of mmWave communications. Cellular networks (e.g., 5G) suffer from scarce deployment and are not free. Therefore, in this dissertation, we investigate the possibility of supporting VR applications with Wi-Fi 6. In [65], authors proposed "Chord," a cross-layer (Application and Network layers) optimizer to enable VR applications over Wi-Fi. Aside from optimizations in the application layer (e.g., predicting which viewing tile to fetch and render, special codecs to decrease the communication overhead, etc), we investigate how many HMDs with a target bitrate of 8 Mbps and 60 FPS can be supported using 802.11ax APs.

The rest of this chapter is organized as follows. Section 5.2 introduces the 802.11ax TDD mode where both UL and DL can happen in one TXOP. Section 5.3 describes the enhancements to the Channel- and QoS-aware scheduler proposed in Chapter 4 to facilitate VR within the context of 802.11ax. Section 5.4 describes the
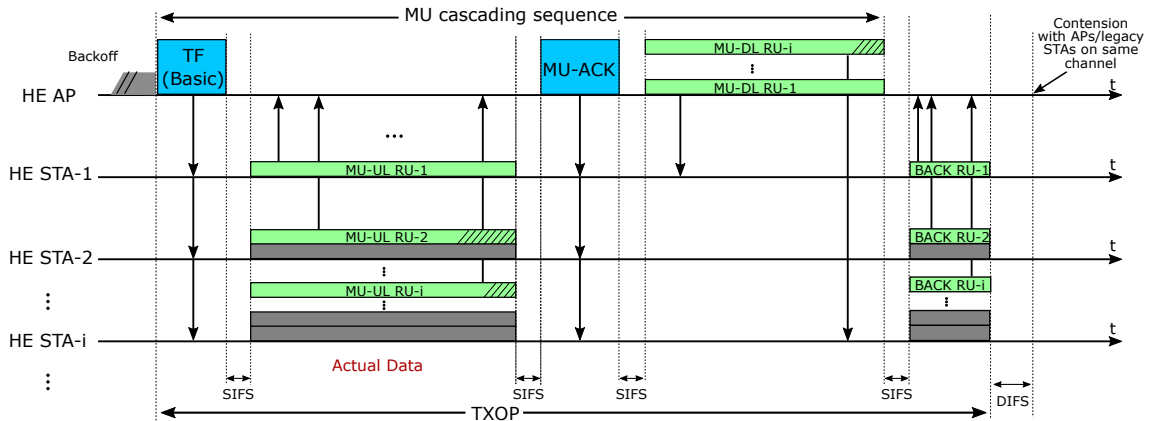
Figure 5.3: Wi-Fi in TDD mode: with realization of MU Cascading Sequence, 802.11ax AP can switch between UL/DL directions.

simulation settings, results and discusses the results of supporting VR with 802.11ax. Finally, Section 5.5 concludes this Chapter with future research directions.

5.2 IEEE 802.11ax in TDD mode

As mentioned in Chapter 4, unlike the previous generations of 802.11 where AP and STAs would contend for channel access, in 802.11ax, AP is given more authority over the network – AP decides which STAs can transmit their frames. However, there is still contention among the APs operating on the same channel and APs with legacy STAs. If we assume a network of only 802.11ax-capable devices, AP can devote some TXOPs to "fetch" UL traffic and some TXOPs to transmit DL traffic to STAs. Also, since one TXOP can be as long as 4.484 ms, it is conceivable that AP can switch transmission direction within a TXOP. This will enable AP to use the obtained TXOP efficiently (1) if there is not enough traffic in one direction, and (2) if there is high priority traffic in the other direction that should be served within their delay constraints. Figure 5.3 illustrates the new Wi-Fi standard operating in the TDD mode; after a multi-user block acknowledgement (MU-BA) is sent to the polled STAs, AP transmits

a MU-PPDU to some STAs[3]. Note that if the recipients of DL MU-PPDU frame is exactly like the UL TB PPDUs with the same RU sizes, the BA can be aggregated into the same MU-PPDU.

With the 802.11ax standard, although new STAs may join the network, AP serves the STAs based on the priority of their application traffic. Therefore, some of the STAs carrying application traffic of lower priority might not get served if there are other STAs that have higher priority application traffic. With this new access mechanism, 802.11ax is capable of serving high priority applications within their QoS constraints.

5.2.1 How to change the direction?

To answer the question of how to switch the UL and DL directions, we need to know how the traffic is generated in both UL and DL directions. For instance, the amount of UL and DL traffic for voice application is almost the same. Depending on the video application the amount of UL and DL can be different, and for the best-effort traffic, the amount of DL traffic is usually higher than that of UL traffic. However, that is not all; the number of antennas, the transmit power and the access mechanism for UL/DL are also different. An efficient direction switching algorithm would take into account all the aforementioned factors.

Although there is no standard mechanism to measure the amount of UL/DL traffic rather than polling STAs to obtain their queue status, the Smart STA selection mechanism introduced in Chapter 4 can help in measuring the amount of traffic for each STA in the UL direction. Therefore, we can assign a weight to each traffic priority, and predict their next transmissions. For I STAs associated with the AP, the weight of the UL direction (W_{UL}) can be computed by a weighted sum of STAs' applications

---

[3] Note that HE MU-PPDU in 802.11 is used for transmission to one or more users that is not a response of a Trigger frame

if the STA has pending frames, plus the δ_{UL} computed based on differences in UL and DL.

$$W_{UL} = \sum_{i=1}^{I} W_i \times X_i + \delta_{UL} \qquad (5.1)$$

where w_i is the weight of an application, X_i is the decision variable which is 1 if an STA has traffic of a particular application and 0 otherwise. δ_{UL} takes into account the differences between UL and DL for the number of antennas, amount of best-effort traffic, and the UL extra overhead. This is the same for DL direction as depicted in Eq. 5.2.

$$W_{DL} = \sum_{i=1}^{I} W_i \times X_i + \delta_{DL} \qquad (5.2)$$

Comparing the weights for UL and DL directions, AP can decide when to switch directions to bound the delay of high priority applications. Note that AP can also add the queuing delay to the weighting formula so as not to starve other access categories. This is important not to over-prioritize the access categories that have certain delay budget.

5.3 VR with IEEE 802.11ax

As mentioned in Section 5.1, the MTP latency of VR systems should be less than 20 ms for a satisfying immersive experience. This latency includes the computation delay (video rendering), communication delay and delay in the HMD. If we take 6 ms for the other delays, the radio access delay (addition of UL and DL) should be within 14 ms [62].

In this section, we explain the enhancements added to the SCQ scheduler to be able to support VR traffic. These enhancements fall into three categories, queue considerations, split access categories, and PPDU duration.

5.3.1 Queue Considerations

The SCQ scheduler presented in Chapter 4 considers the data rate and type of service (ToS) of STAs. However, it is important to also consider the queue length when scheduling STAs. This will ensure the STAs with longer queue to get bigger chunks of the channel. Since queue consideration should be added to the recursive function, we implemented a penalty function that penalizes the generated utility when the entire queue cannot be sent with the considered RU size. Thus, the changes to the utility computations of the video traffic is as follows.

$$U_{video} = \begin{cases} U_{video} & d_{S_i}^A + O^{tr} \geq d_p \\ U_{video}/2 & d_{S_i}^A + O^{tr} < d_p \end{cases} \tag{5.3a}$$

where $d_{S_i}^A$ depicts the AMPDU duration, O^{tr} is transmission overhead, and d_p depicts the PPDU duration.

Utility for voice is still the same as voice frames are small and a flat utility gives them the smallest RU size (26-tone). Note that these utility computations are in favor of STAs with smaller queue sizes because STAs with larger queue sizes might be penalized for all RU sizes. However, since the STA selection algorithm tracks[4] how much traffic from each STA is served, STAs with larger queues get selected again to transmit.

5.3.2 Split traffic types

With traffic differentiation, in each round of scheduling, there might be multiple STAs with different access categories. The recursive algorithm first sends all the STAs to left branch of the RU tree, and compute the utility of the scheduled STAs. It then

---

[4] Since delay of best-effort access category is not tracked by the scheduler, applying the penalty function will result in overall lower throughput for the best-effort traffic.

sends the remaining STAs to the right branch and computes the utility of the scheduled STAs. The addition of these utilities are compared against a scenario in which first the STAs are sent to the right branch and the remaining to the left and the higher utility is the final scheduling of the STAs. However, there might be two mis-scheduling:

1. If the number of STAs are smaller than half of the number of 26-tone RUs, all the STAs might be scheduled at one direction leaving the other direction empty.

2. If all high priority access categories are sent to one direction, the scheduling will not be as intended; they will all be scheduled to maximize the utility, therefore, STAs with lower priority will be scheduled in the other branch.

If we split STAs of each category into both branches, we achieve better results in terms of delay and throughput for STAs with VR traffic. However, the overall throughput obtained is lower than no splitting. Therefore, the combination of the two techniques seems promising; if there is no VR STAs, splitting is not required. However, if there are STAs with VR traffic splitting results in higher performance of VR STAs because they are allocated larger RU chunks in both branches of the RU tree.

5.3.3   PPDU duration based on VR traffic

In Chapter 4, we proposed a linear optimization technique to minimize the number of UL transmissions and paddings. This technique can also be applied to DL in order to choose the optimal MU-PPDU duration. However, since the most important traffic to handle is the VR traffic, if the VR traffic is present we can choose the PPDU duration to be as long as the VR PPDU duration. In the absence of VR traffic, we can still use the optimization.

Since the scheduler can measure the next interval of VR STAs, it is also possible to include the VR delay prediction into the PPDU duration time. From Chapter 4, the

scheduler keeps the HOL frame delay to track the delay of each STAs. If all the frames in the queue of an STA are served with the UL PPDU, the HOL frame delay becomes the next learned interval of that STA. Otherwise, it becomes the queuing delay of the last served frame. With this information, the scheduler computes the minimum time to another video arrival by $d'_p = \min(t - \mathcal{D}^i_{vi}) \forall i \in S$ and the maximum of d_p might get updated as follows.

$$d_p = \begin{cases} d'_p & d'_p < d_{rem} \\ d_p & \text{otherwise} \end{cases} \tag{5.4}$$

5.4 Evaluation

5.4.1 Topology and Simulation Settings

The network topology and simulation settings are as follows. The STAs are random uniformly placed in an $8m \times 8m$ area with AP at the center. The channel model is based on WINNER II [55], with path loss:

$$PL = 20 \times \log_{10}(d) + 46.4 + 20 \times \log_{10}(f_c/f_b) + L_w \times W, \tag{5.5}$$

where d is the distance between transmitter and receiver; $f_c = 5.180$ GHz is the center frequency, $f_b = 5$ GHz is the base frequency; L_w is wall loss and W is the number of Walls between transmitter and receiver.

To be close to a practical scenario, 20% of STAs are voice, 20% video (VR), and the rest having best effort access category. As mentioned earlier, the video traffic generated in this study roughly resembles the 8K video traffic with TBR = 8 Mbps in both DL and UL directions. Therefore, the application packets are about 18 kB and are generated every 17 ms to account for 60 FPS. In general, frame aggregation can happen for both MSDUs and MPDUs. Although MPDU aggregation incurs more overhead to the network, it is advantageous in scenarios with higher interference. As

our future research is to measure the performance of VR support by 802.11ax in OBSS where interference from other BSSs operating on the same channel affects the results, we only simulated MPDU aggregation.

Table 5.1: Other parameters for the simulations

Parameter	Value
Channel Bandwidth	80 MHz
Empty slot	9 μs
DIFS	34 μs
SIFS	16 μs
Packet size AC[VO] (Bytes)	38
Packet size AC[VI] (Bytes)	$\approx$18 kB
Packet size AC[BE] (Bytes)	500-2300
Simulation Runs	10
Frame Aggregation Type	only A-MPDU
Number of Aggregated Frames	up to 256
TXOP duration	5.484 ms

Since VR traffic should be transmitted as soon as it arrives to the queue of an STA, the soft threshold (γ_S) and hard threshold (γ_H) of VR traffic should be very small[5]. Other simulation parameters are outlined in Table 5.1.

5.4.2 Results and discussion

In Section 4.6.2.2, we see that the results of UL Smart framework is superior to even oracle-based station selection. We also noticed that with traffic differentiation, it is necessary to take into account the STA's type of service when scheduling. We further noticed that considering the mid-RU RU in 20 MHz does not have noticeable impact on the results of voice and video access categories and only benefits best effort access category.

---

[5] $\gamma_S = 0$ and $\gamma_H = 100\mu s$, respectively and the serving threshold based on load is chosen in this range.
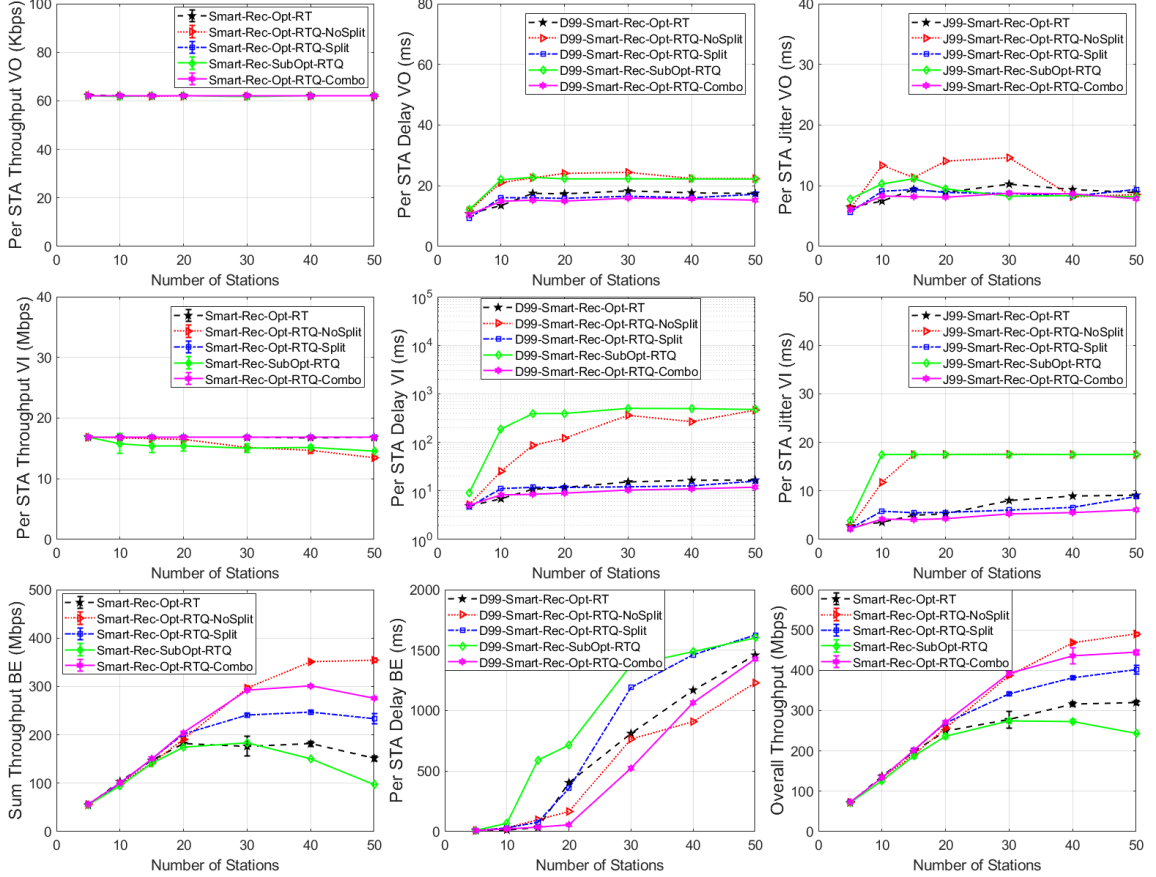
Figure 5.4: The comparative results of enhancements added to the semi-binary recursive scheduler. Voice results are on the first row, video results on the second row and best effort and overall throughput on the third row. Throughput for voice and video access categories are per station but for best effort is sum of all stations.

In this Section, we present the results of station splitting and the new "rate-to-queue" utility with its penalty function. Since the bandwidth used in these simulations is 80 MHz and the number of mid-RU RUs are 5 in 80 MHz, we also present the results of binary recursive scheduling (i.e. SubOpt) to measure whether the added computations are worthwhile in semi-binary recursive scheduling. Fig. 5.4 illustrates the comparative results. With heavy VR traffic, if we do not split the stations to both sides of the binary tree, when computations, stations with high priority access category traffic are selected at one side giving the other side to best effort access category. Moreover, if we always

split the STAs, the throughput gap between the splitting and no splitting is large. Therefore, the combination of these two mechanisms, "RTQ-Combo", can close this throughput gap. Lastly, the impact of not considering the mid-RU RUs are more visible in these results. If the assigned RUs to the selected stations are all smaller than 242-tone RUs, then only 5 RUs are wasted in 80 MHz bandwidth. However, since voice stations should get one of the binary RUs, these RUs cannot be merged and be allocated to other stations which results in significantly lower performance for the binary recursive scheduler.

Smart scheduling technique with Rate-ToS-Queue (RTQ) utility and combo-splitting can support VR application with its stringent QoS requirements (the addition of delay and jitter of VR traffic should not exceed 14 ms) up to 50 stations, 10 of which are VR stations. Although Smart technique with splitting and Rate-ToS (RT) utility can also support up to 40 stations (8 VR HMDs), its overall throughput is up to 40% less than that of RTQ utility.
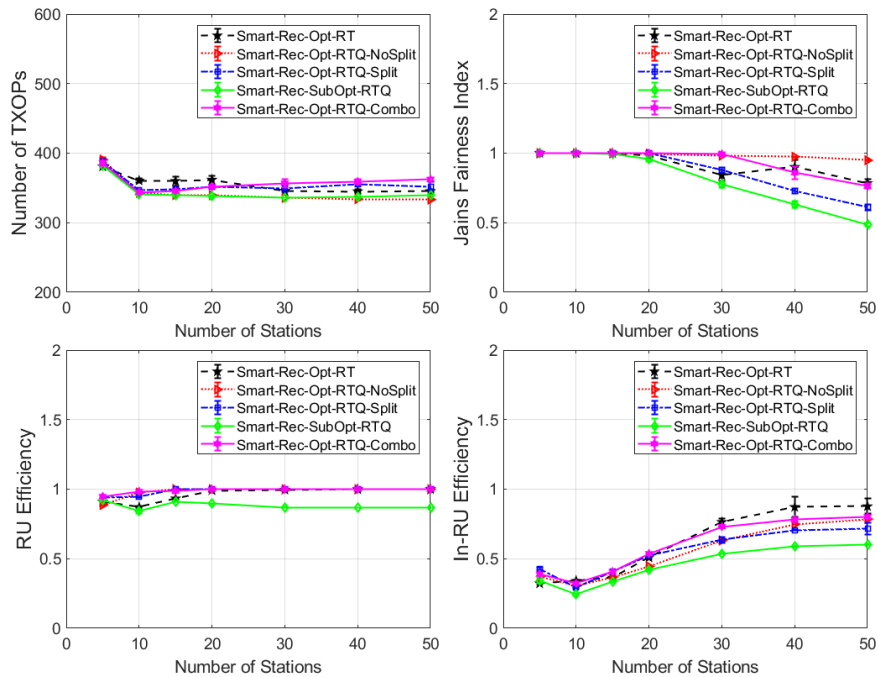
Figure 5.5: Other simulation results related to multi-class simulation with VR traffic.

Fig. 5.5 shows the other results related to handling VR traffic among other traffic classes with Wi-Fi 6. Although "RTQ-NoSplit" utility is the most fair among the utilities and achieves the highest throughput, it can only support 1 VR HMD. From the RU efficiency subplot, we can see that in few number of stations (less than 10), sometimes, the scheduler cannot allocate all the RUs. For instance, if there are only 2 stations with traffic, the AP gives each one a 484-tone RU ($\approx$40 MHz) and one RU is wasted. Also, note that for binary recursive scheduler (i.e., SubOpt), if any of the assigned RUs are greater than or equal to 242-tone RU, then not all 5 extra 26-tones RUs of the 80 MHz bandwidth is wasted. This is especially important in large bandwidths and few number of STAs to be scheduled [6].

5.5   Chapter Summary

Owing to the wide range of VR applications in military, healthcare, education, business, entertainment, engineering, etc., and their stringent QoS requirements, VR HMDs are usually wire-connected to the computers to which the video rendering is delegated. As wire connection limits user mobility, research in academia and industry is focused to handle VR traffic with a wireless technology. With the current contention-based Wi-Fi technology, protocol optimizations across all the layers of the network stack can only support a few VR devices in low interference situations. Therefore, other communication technologies, such as mmWave (WiGig and 5G New Radio), have become the options to support VR. However, they both require their specific base stations. Moreover, 5G is not free.

As the new generation of the Wi-Fi technology, IEEE 802.11ax, has employed OFDMA and new access mechanisms to overcome the inefficiency of former Wi-Fi standards. In this research, we enhanced our proposed UL framework to support VR

---

[6] IEEE 802.11be is considering not to use the mid-RU RUs due to the added complexity.

traffic with its stringent QoS requirements among other access categories. In particular, we added DL traffic and the mechanism to switch between UL/DL directions within each TXOP. We also enhanced the scheduling mechanism to split STAs on both side of the bandwidth tree. We further enhanced our utility computation with a penalty function to take into account the queue length of STAs when scheduling. Simulation results indicate that the with the new enhancements a network comprising of 50 stations with a traffic mix of 20% voice, 20% VR (8 Mbps target bitrate and 60 frame per second resolution) and 60 % best-effort can be supported.

Chapter 6

HYBRID INFRASTRUCTURE FOR AUV OPERATIONS

6.1 Introduction

The oceans cover more than 70% of the surface of our planet, forming one of the most critical physical systems to life. To support ocean monitoring and exploration missions, the prevailing strategies have been to use either seafloor fiber-optic cables, e.g., ocean observatories around the globe [66–69], or satellite-linked stationary in-water moorings [70] as backbones for communications and networking. The sea-floor observatories often have enormous price tags for development and maintenance. Further, the seafloor infrastructures are inflexible to relocate or to accommodate evolving societal needs, although supporting invaluable long-term ocean observations. In addition, although a dense array of satellite-linked stationary moorings may cover a relatively large area, this static solution results in high costs as well as operational difficulties for deployment and recovery.

In recent decades, autonomous underwater vehicles (AUVs) (including underwater gliders) have emerged as effective and versatile tools to respond to vital needs in the oceans, lakes, and estuaries [71]. Successful applications enabled by AUVs include, just to name a few, adaptive environmental monitoring, geological surveys, ocean observations, and national defense. In these applications, AUVs may gather orders of magnitude more measurements than the traditional ship-based surveys, at much lower cost and/or in hazardous conditions (e.g., underwater during hurricanes). In addition, the ability to retrieve imagery and scientific data from AUVs via a communication

network will greatly enhance human-vehicle interactions and real-time decision making [72], thus supporting critical real-time underwater missions, *e.g.*, disaster responses.

Fleets of coordinated AUVs operating together facilitate applications of distributed sampling and exploration [73], including 1) tracking marine life to understand the life cycles of sharks, jellyfish, lobsters, etc. [74]; 2) monitoring and tracking fast-evolving plumes, algae, or other fast-evolving features [75]; 3) mine detection and other national defense applications [76]. In addition, several trends have driven the needs to establish motion coordination and team behaviors [77, 78]. For instance, distributed real-time measurements are critical to sparse sampling in vast oceans or Great Lakes. Coordinated AUV-fleets are poised to perform sophisticated missions in highly dynamic oceans, and AUV-fleets can greatly reduce the sensory and capability requirements on individual members, thus reducing the overall mission cost.

These applications all demand reliable communication and networking among the participating AUVs, and between AUVs and their external monitoring, control, and human decision making. However, it is well known that wireless communications in the underwater realm is an intractable challenge. In field operations, scientists have been adopting the concepts of delay-tolerant networking to cope with intermittent underwater communications [79]. In such context, *encounters* are used as the main opportunities to communicate.

When considering underwater wireless communications over ranges beyond tens of meters, acoustic communications should be used, because both electro-magnetic and optical waves suffer strong attenuation in the aquatic environment. At the same time, the unique characteristics of acoustics further challenge underwater communications. The fundamental difficulty lies in the limited bandwidth, with a maximum of only tens of kilohertz. In addition, due to the highly dynamic ocean environment, the acoustic communication channel suffers large dispersion in both time and frequency domains
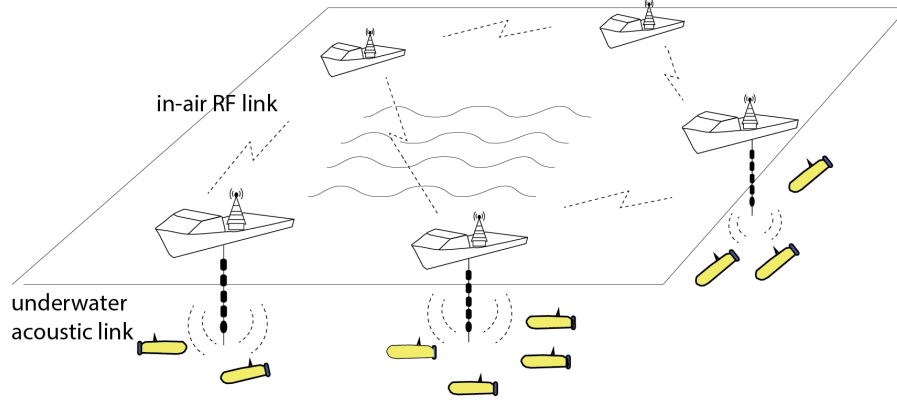
Figure 6.1: Scenario of hybrid RF-acoustic networking and ASV navigation.

(i.e., time-varying multipath), constraining spectral efficiency. Further, underwater sound speed, 1500 m/s, is five orders of magnitude slower than that of electromagnetic waves in air. The resulting long propagation delay introduces spatio-temporal uncertainty [80], which seriously limits the efficiency of networking protocols.

The mobility of AUV-fleets introduces additional challenges. First, AUVs often experience high uncertainties in localization and time synchronization, due to the lack of GPS signals underwater. Second, AUVs may be sparsely deployed over a large aquatic region, so that network connectivity becomes intermittent. Third, the network topology of a fleet of AUVs is in constant change, leading to variable and long propagation delay. Mobility also creates variation on data rates in different geographical locations of the network, as the achievable data rate decreases with the increase of communication range.

We propose to use low-cost autonomous surface vehicles (ASVs) equipped with both acoustic and RF modems to support underwater missions, as depicted in Fig. 6.1. The ASVs form a connected and adaptive backbone via RF links above the water surface while connecting AUVs via underwater acoustic links. The connected backbone is maintained by a swarming-based ASV navigation strategy for enhanced data rates and much reduced end-to-end latency.

Fig. 6.2 illustrates the functional architecture of the proposed mission-defined hybrid infrastructure, which 1) directly addresses the communication and network challenges and 2) allows seamless integration with autonomy and control. The hybrid infrastructure complements existing AUV autonomy middleware and behavior architecture, such as MOOS-IvP [81], and tri-level hybrid control architecture of mission planning and executive [82], as an efficient and reliable communication infrastructure among AUVs. Using the defined mission from mission planning as inputs, the ASV-based hybrid RF-acoustic infrastructure facilitates networking among AUVs and to the outside world by *optimizing* the navigation of ASVs to *jointly* (1) trail respective AUVs to maintain short range and close to 'vertical' acoustic links for improved data rates, reduced propagation delay, and enhanced reliability, and (2) form an adaptive and connected RF 'backbone' above water surface to support high data rate and reliable communications. The hybrid short range underwater acoustic links and low-latency in-air RF links create much improved network throughput, efficiency, and reliability. To sustain a connected ASV backbone, AUVs may be instructed not to move away from associated ASVs so as to be connected with other AUVs within the same mission.

Such a hybrid networking infrastructure represents a new network, where two communication constituents differ greatly in their data rates, link performance dynamics, power efficiency, and network coverage. Further, the five order of magnitude difference in wave propagation speed leads to large disparity in network latency between subsurface and in-air sub-networks. One critical issue is to guarantee reliable connectivity among AUVs through navigation of ASVs, in the presence of aquatic dynamics (ocean currents, surface waves) and location uncertainty of AUVs.
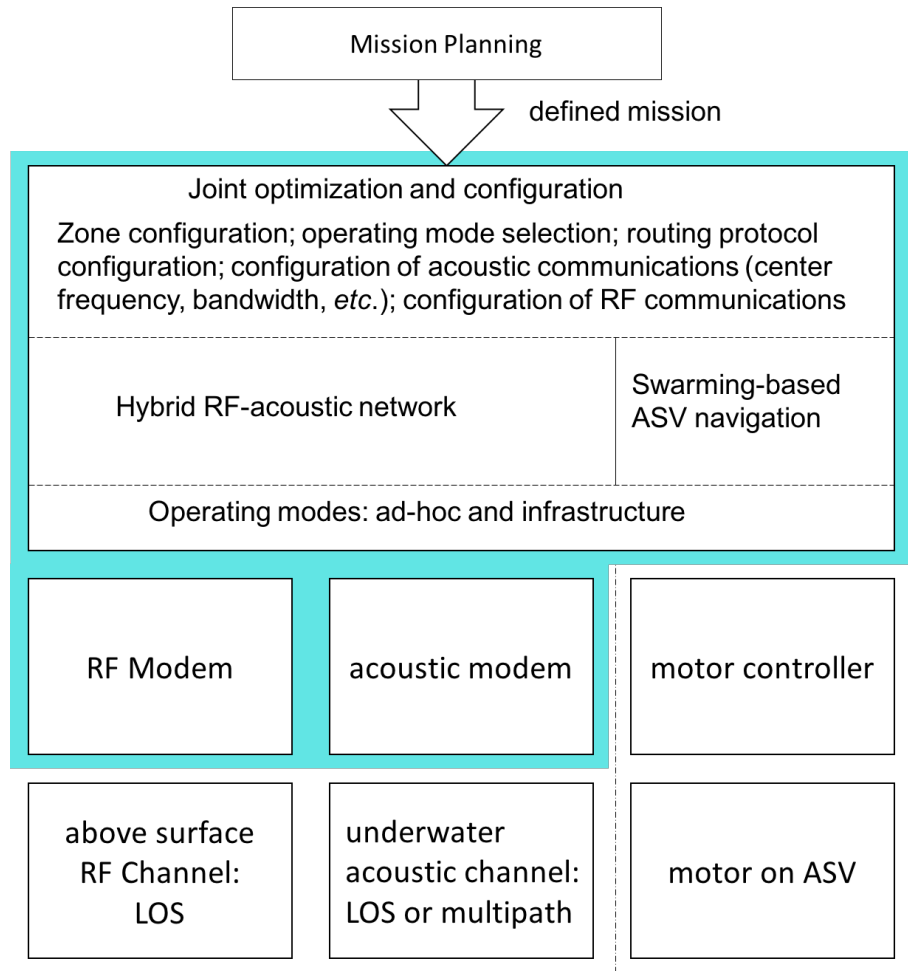
Figure 6.2: Functional architecture of hybrid infrastructure.

The chapter proceeds to review related work in Section 6.2. Hybrid RF-acoustic networking among AUVs via ASVs is introduced in Section 6.3. Swarming-based ASV Navigation is briefly described in Section 6.4. Parameters used for the simulation along with Simulation results of hybrid RF-acoustic communications between AUVs are presented in Section 6.5. Section 6.6 summarizes this chapter with future research directions.

6.2   Related Work

It is well recognized that acoustic communications alone can not meet the needs of data telemetry in underwater missions. To address the issues, a number of hybrid schemes have been proposed: acoustics combined with fiber-optic cabled sea-floor stations (OOI projects), acoustics with satellite links, and RF-acoustic method that is used in a centralized network to collect sensory information of underwater nodes and to control them.

Mobility of AUVs has been used to assist routing among drifting sensors [83–85] or in data muling and encounter-based connectivity [86, 87]. Some of these schemes used only acoustic communications [88], while others used a combination of optical and acoustic methods for communications [89].

ASVs are low-cost, easy-to-operate, and versatile platforms [90–92]. Being on the surface, ASVs have several advantages: 1) access to GPS and RF communications [91], 2) more cargo space and possible long endurance in the ocean, 3) access to solar energy [93] and different propulsion solutions. In addition, ASVs can continuously provide GPS information to assist AUVs with more accurate and precise localization [94–96].

The use of ASVs has also been reported in various scientific field experiment efforts since 2000, for example in cooperative marine autonomy [97], ocean remote sensing [98], and hydrographic survey. [99]. As reported in [100–102], *individual* ASVs were used as communication gateways for underwater platforms. A single semi-submersible ASV was used to support AUV communication and positioning [103]. Large scale experiments in [104, 105] also reported the use of individual ASVs as communication gateways to control centers or satellites. *To our best knowledge, there are no reported efforts on using multiple ASVs to form a hybrid network or even an RF network above the sea surface.*

As a communication platform, although ASVs face several challenges, solutions exist. First, the stability of these ASVs are subject to the dynamics of surface waves. Therefore, they are more suitable to operate in relatively calm sea water surfaces. One solution is to use semi-submersibles. Second, close to the surface, the acoustic receiving array may not have good reception when the ocean is downward-refracting for acoustic waves. One solution is to use relatively long cables for reception as well as transmission. Third, the RF modems above the water surface often rely on line-of-sight (LOS) for reliable communications. To cover large areas, ASVs need to install elevated RF antennas which can be accomplished with bigger vessels.

6.3 Hybrid RF-Acoustic Networking among AUVs via ASVs

The proposed hybrid infrastructure consists of two complementary components: hybrid RF-acoustic networking of ASVs and AUVs and swarming-based ASV navigation. The benefits of hybrid RF-acoustic networking can be illustrated by the simple scenario depicted in Fig. 6.3, where two AUVs, separated by some distance apart, navigate collaboratively to sample the ocean. Using conventional schemes, the two AUVs communicate via the direct acoustic link over a *horizontal* channel. Due to the slow underwater sound speed, the communication latency is high. In addition, due to the long distance between the two AUVs, the acoustic link can only support lower data rates with limited reliability subject to multipath and ocean fluctuations.
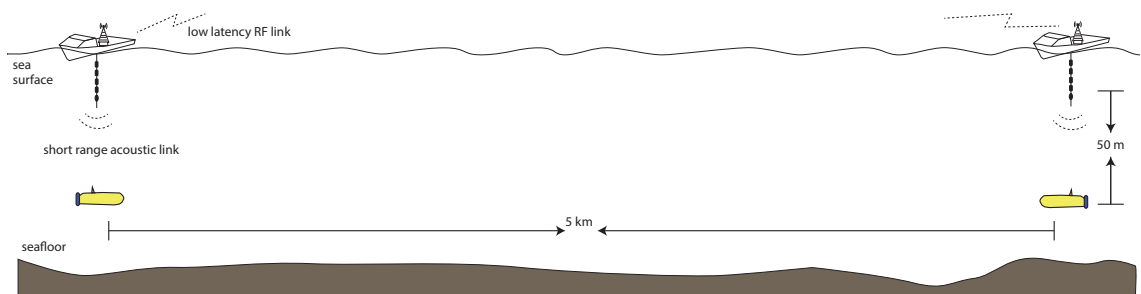
Figure 6.3: Simple scenario of hybrid RF-acoustic networking.

In contrast to a single long delay, unreliable acoustic link, the central idea of hybrid RF-acoustic networking is to use ASVs to *trail* AUVs by a short distance so as to bridge the two short range underwater acoustic communications (between two pairs of AUV and ASV) with high speed, low latency RF communications (between the two ASVs above the sea surface). Having short range underwater acoustic communications between a pair of AUV and ASV not only reduces the latency of acoustic communications, but also makes the acoustic communications closer to *vertical* to mitigate refraction[1] and multipath. Overall, end-to-end communications between two AUVs over a hybrid RF-acoustic network achieve lower latency, higher bandwidth, and improved reliability.
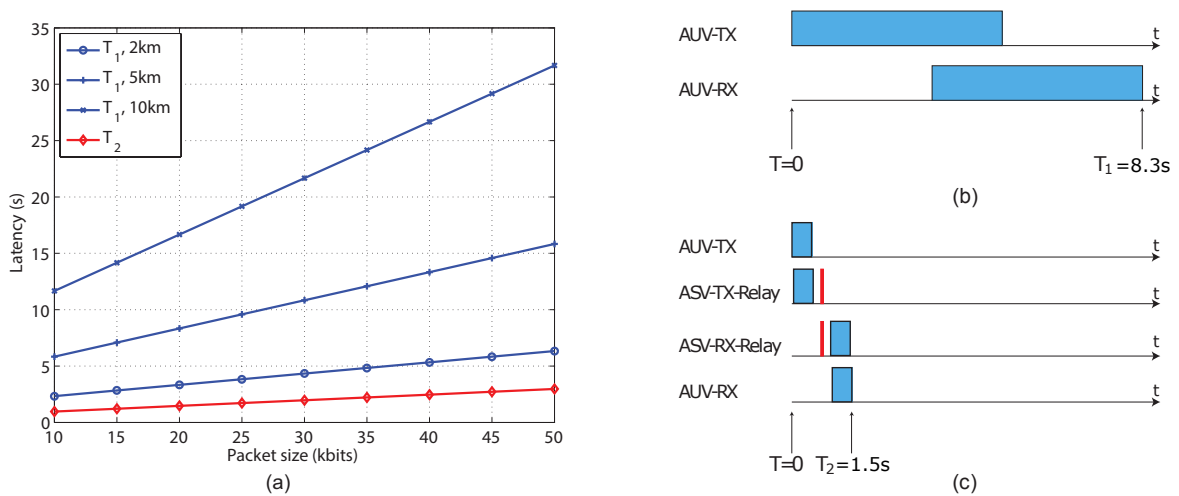
Figure 6.4: (a) Comparison of packet delivery latency between the traditional and proposed schemes for different AUV-AUV ranges. Timing diagram comparison between the traditional scheme, shown in (b), and our hybrid scheme, shown in (c), for $W = 20$ kilobits and $D_{HA} = 5$ km. In (b), $T_1 = 8.3$ sec while $T_2 = 1.5$ sec in (c).

Fig. 6.4 compares the latency of transmitting one data packet between the two AUVs in Fig. 6.3. In this illustrative comparison, the data packet has W kbits. The two AUVs are separated by distance D_{HA} ranging from 2 km to 10 km. Distance D_{VA}

---

[1] Because water is much more stratified in the vertical than the horizontal.

between an AUV and its trailing ASV is 50 m. Underwater sound speed c_A is 1500 m/s. It is commonly believed that the achievable data rate R_{HA} over a horizontal acoustic channel decreases with the increase of communication distance, so that the achievable *rate-range product* is a constant, say K kbps $\times$ km (*i.e.*, $R_{HA} \cdot D_{HA} = K$). Over the vertical acoustic channel, the data rate is largely limited by the available bandwidth. Based on these two principles, we assume that the rate-range product $R_{HA} \cdot D_{HA}$ is 20 kbps $\times$ km for the direct horizontal acoustic link between the two AUVs. We assume that the vertical acoustic channel supports data rate R_{VA} of 40 kbps. These data rates are realistic and have been demonstrated via different commercial products. Using the traditional schemes, the latency associated with packet delivery is $T_1 \simeq \frac{W}{R_{HA}} + \frac{D_{HA}}{c_A}$.

Using the hybrid scheme, the same data packet traverses two (short-range) acoustic links and one (long-range) RF link, and ASVs need to translate the data packet between the acoustic and RF links. We assume there is a delay, T_δ, associated with such translations. We assign $T_\delta = 0.2$ sec to allow the conversion between acoustic and RF signals and the forwarding decisions for data packets across the two constituent networks. The RF link, with a propagation speed of $c_{EM} = 3 \cdot 10^8$ m/s, can support much higher data rates than the acoustic links, for example 500 to 800 kbps. Therefore, not only is RF link's propagation latency negligible when compared with that of acoustic links, but RF link's packet transmission latency is also very small (T_ϵ). Therefore, the packet delivery latency in the hybrid scheme is $T_2 \simeq 2 \left(\frac{W}{R_{VA}} + \frac{D_{VA}}{c_A} + T_\delta \right) + T_\epsilon$.

For different communication ranges (i.e., is the AUV-to-AUV distance), latency does not vary in the hybrid scheme, where the RF link is used to address the range above the surface. In the traditional pure acoustic solution, the communication range matters in two ways. First, it increases the acoustic propagation delay. Second, the range reduces the allowable acoustic data rates. At a 2 km range, the traditional scheme uses 50 to 100 percent of extra time to deliver the same packet, compared

with the proposed scheme. When the range increases to 5 or 10 km, the advantage of hybrid scheme becomes significant. The traditional scheme uses about 5.8 and 11.6 sec to deliver a 10 kilobit packet at 5 and 10 km, which are 3.7 and 7.4 folds of the latency in the hybrid scheme, respectively. Timing diagrams for transmission of a data packet of $W = 20$ kilobits are shown in Figs. 6.4(b) and (c) for direct and hybrid schemes, respectively. The latency values in the direct AUV-AUV link and the hybrid network are $T_1 = 8.3$ and $T_2 = 1.5$ sec, respectively.

When the packet size increases, the traditional scheme lags even more behind than the hybrid scheme. We neglect the PHY receiver decoding delay, which is often small compared with packet duration. If we take into account the link reliability, we will see further advantage of the hybrid scheme. The short-range acoustic links are much more reliable than the long-range horizontal acoustic link, especially in the dynamic ocean environment. Often in the traditional scheme, high packet loss in the long horizontal channels leads to excessive re-transmission and even network failure. Furthermore, in the hybrid scheme, there are two segments of short-range acoustic links in the end-to-end path between two AUVs, which may be far apart to form two different contention domains so that respective acoustic transmissions do not interfere with each other. This allows concurrent acoustic transmissions to further reduce packet delivery latency.

6.4 Swarming-based ASV Navigation

Given a defined mission for AUVs (such as waypoints, destination, etc.), the hybrid infrastructure is to navigate ASVs by jointly (1) trailing respective AUVs to maintain local acoustic links, and (2) forming a connected and adaptive RF backbone to support inter-AUV communications. However, given the dynamic nature of the aquatic environment (current, wind, etc.), a fully decentralized scheme is deemed necessary to

'coordinate' the navigation of ASVs so that all the AUVs move toward the common goal to complete the defined mission, stay connected during the mission, and avoid potential collision. To accomplish this objective, we propose *swarming-based ASV navigation* based on the three-zone swarming model [106].
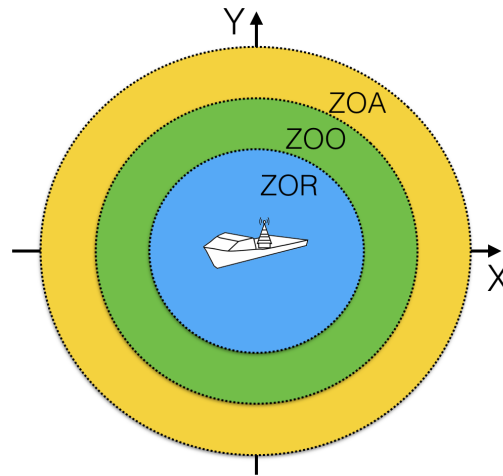

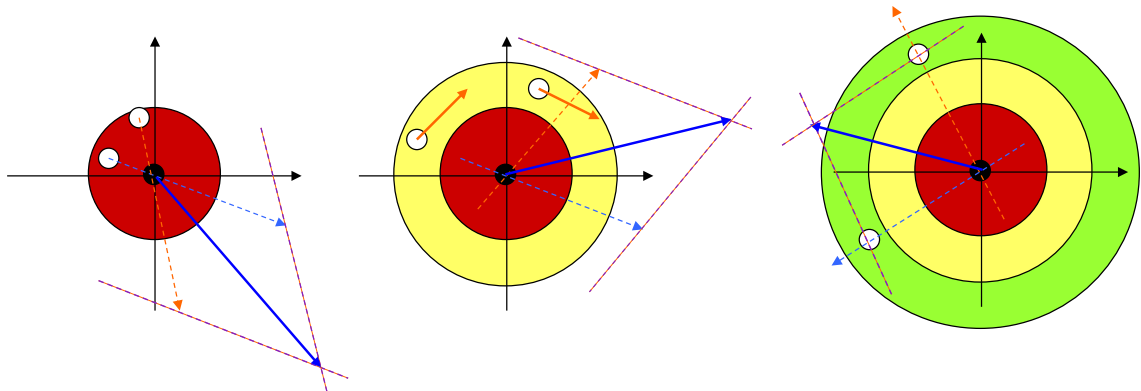Figure 6.5: Three-zone ASV swarming model

Figure 6.6: Move away, move along, and move towards

In general, swarming is a collective behavior exhibited by entities, particularly animals, of similar size which aggregate together, perhaps milling about the same spot or perhaps moving *en masse* or migrating in some direction. Swarming is typically

defined by a set of rules which a group of nodes follow to interact *locally* with other proximal nodes without any centralized control.

In ASV swarming, the perceptual field of each ASV, as defined by its RF communication range, is divided into zone of repulsion (ZOR), zone of orientation (ZOO) and zone of attraction (ZOA), as depicted in Fig. 6.5. Given a distribution of N ASVs, to coordinate with neighboring ASVs in different zones, an ASV will move *away* from its neighboring ASVs in ZOR or move *along* with its neighboring ASVs in ZOO while moving *towards* its neighboring ASVs in ZOA, as depicted in Fig. 6.6.

Let ASV i be located at position vector P_i and pointing in direction D_i. We define three decision vectors,

$$DR_i = \sum_{j \in S_{ZOR}} \frac{R_{ij}}{|R_{ij}|} \qquad DO_i = \sum_{j \in S_{ZOO}} \frac{D_j}{|D_j|} \qquad DA_i = \sum_{j \in S_{ZOA}} \frac{R_{ji}}{|R_{ji}|} \qquad (6.1)$$

where $R_{ij} = P_i - P_j$ is a displacement vector between ASV i and ASV j, and S_{ZOR}, S_{ZOO} and S_{ZOA} are the sets of indices of ASVs in the zones of repulsion, orientation and attraction, respectively.

Let $|S_Z|$ denote the number of ASVs in zone Z. Assuming that decision vectors are normalized as unit vectors, a generic ASV swarming algorithm can be summarized as follows.

1. If $|S_{ZOR}| \neq 0$ then $V_i = DR_i$, Break;

2. If $|S_{ZOO}| \neq 0$ and $|S_{ZOA}| = 0$ then $V_i = DO_i/|DO_i|$, Break;

3. If $|S_{ZOO}| = 0$ and $|S_{ZOA}| \neq 0$ then $V_i = DA_i/|DA_i|$, Break;

4. If $|S_{ZOO}| \neq 0$ and $|S_{ZOA}| \neq 0$ then $V_i = \alpha \times DO_i/|DO_i| + (1-\alpha) \times DA_i/|DA_i|$,

where α is an optimization variable between 0 and 1. Changing the relative sizes of the zones in this model resulted in different swarming behavior [107], e.g., milling or

migrating in some direction. In the context of swarming-based ASV navigation, defined mission, such as desired destination, represents extra information. In this case, let $F_i = P_d - P_i$ point to the desired destination, where P_d is the position vector of the desired destination. Each ASV i then sets its new orientation to be $D_i = \beta \times V_i + (1 - \beta) \times F_i$, where β is another optimization variable between 0 and 1.

6.5 Evaluation of Hybrid AUV-AUV Communications
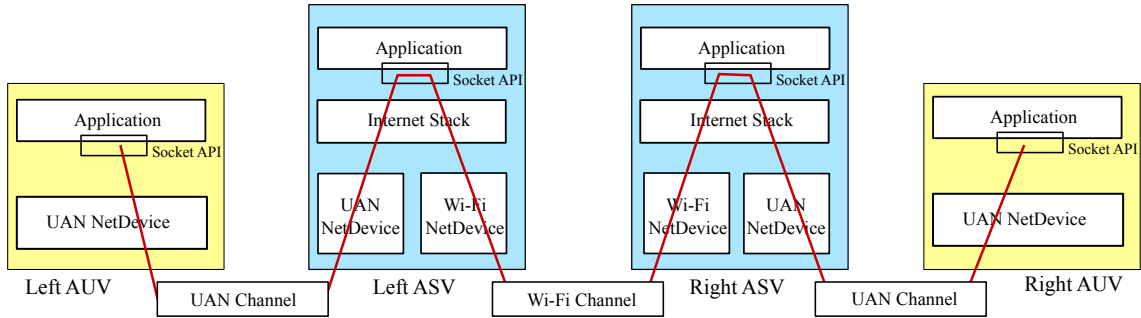
Figure 6.7: Simulation model of Fig. 6.3 in ns-3

We simulate different scenarios in the ns-3 simulator, where underwater acoustic network modules are available. To create hybrid network simulations, we integrate multiple components of acoustic and RF networks (PHY and MAC layers, Channel models, and Net Devices) on ns-3 node objects. On the ASV nodes, we install the Internet stack that is used by both acoustic and RF networks. The detailed hybrid network structure in ns-3 is depicted in Fig. 6.7. In the hybrid method, application packets of source AUV are encapsulated in the UDP protocol, sent to its associated ASV, routed to the destination AUV's associated ASV and finally received by the destination AUV. Since each source ASV knows the IP address of destination ASV in order to successfully route the packets, we use a mapping class at each ASV to transform the IP address of destination AUV to its associated ASV, and vice versa.

Table 6.1: Parameters for the simulations

Parameter	Direct AUV-AUV	Hybrid AUV-AUV
PHY Rate (sps)	4000	40000
Data Rate (kbps)	range-rate product(20 $km \times kbps$)	40, 800
Packet Size (Bytes)	500, 1000, 1500, 2000	500,1000,1500,2000
Center Frequency(kHz)	12	200
TX Power(dB re 1 muPa)	187	177
Acoustic Model	Thorp	Thorp
Simulation Stop Time (s)	400	400

Parameters used for simulations are depicted in Table 6.1. In all simulations, since the traffic load of RF links is less than that of acoustic links, we use the RTS/CTS mechanism to reserve the channel. In the hybrid scheme, the data rate is 40 kbps for the acoustic link and 800 kbps for the RF link [108], the AUV transmission power level is 177 dB re 1 muPa, the acoustic carrier frequency is 200 kHz, and the symbol rate is 40 kHz. In direct acoustic AUV-AUV communications, the AUV transmission power level is 187 dB re 1 muPa, the acoustic carrier frequency is 12 kHz, and the symbol rate is 4 kHz. In both schemes for the acoustic links, BPSK modulation is used. An acoustic attenuation model, the Thorp approximation in ns-3, is used [109] to characterize the pathloss. Therefore, multipath is not simulated for either of the schemes. We simulated four packet sizes varying between 500 and 2000 bytes. We assume an oracle to compute optimal intervals for traffic generations. Packet generation rate has an inverse relationship with the next packet transmission (Next TX) time. In other words, a higher packet generation rate leads to a shorter transmission interval, which is computed by the following formula:

$$\text{Next TX} = \text{PacketSize}(bit)/\text{PacketGenerationRate} \qquad (6.2)$$

Throughput is computed as total received bits divided by the time it takes from transmission of the first packet (by a sending AUV) to reception of the last packet (by a

receiving AUV). Simulations are chosen to assess the maximum achievable throughput (at the application layer) for a single AUV per each AUV-ASV pair in the hybrid Acoustic-RF and cross layer MAC-Routing protocols. Hence, to build a collision-free schedule, the Aloha MAC protocol is used in the simulations. Our simulation results show that higher throughputs are achieved with the hybrid method, which also remain intact even with increasing distance. As an example, for two AUVs located 5 km apart, and transmitting packet sizes of 2 kB, direct acoustic link achieves a maximum one-way throughput of 3960.6 bps. In contrast, the hybrid network achieves a maximum of 39847.5 bps, ten folds of the direct acoustic link's maximum throughput. Further, the end-to-end delay between two AUVs (5 km away from each other) is 0.1 second in the ns-3 simulations for the hybrid network. The delay includes both propagation delay and PHY/MAC algorithm processing delay (T_δ is not added). In comparison, the delay is 3.53 seconds in direct acoustic AUV-AUV communications.
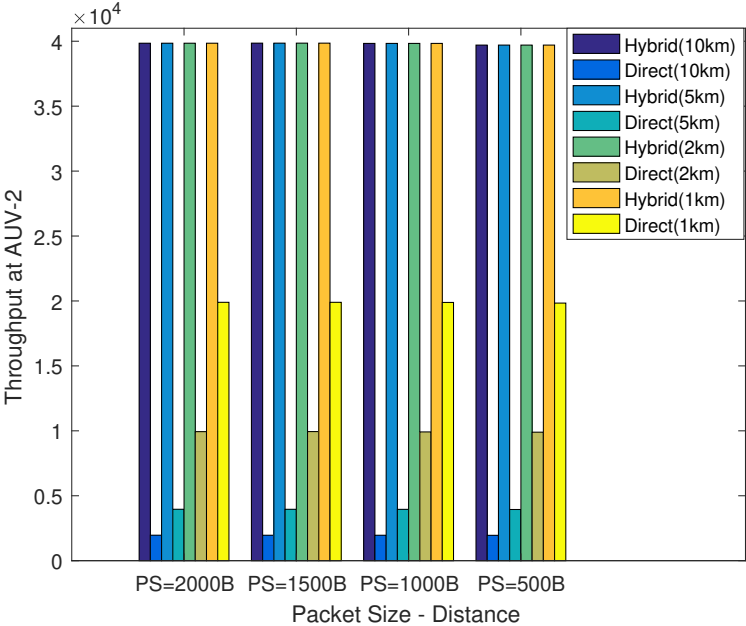

Figure 6.8: Packet Size (PS) *vs.* Throughput for one-way flow from AUV-1 to AUV-2 using hybrid RF-acoustic and direct method (only acoustic). Throughput is computed at AUV-2

We choose three scenarios to simulate in ns-3 with variable AUV-AUV distances of 1, 2, 5 and 10 km. The first scenario simulates one-way and two-way (bidirectional) communications among two AUVs. The second scenario simulates a network of four AUV nodes with four application flows running on them. The third scenario simulates underwater infrastructure-based networks. Each scenario compares the achieved throughputs between the hybrid and direct methods. Variable packet sizes and different distances are examined.

6.5.1 First Scenario: One-way and bidirectional AUV-AUV communications

The deployment scenario is shown in Fig. 6.3. Results for one-way application from AUV-1 (left) to AUV-2 (right) are shown in Fig. 6.8, where four clusters of bars denoting throughput for different packet sizes (PS). Each cluster has eight thin bars for four different distances of the hybrid and direct schemes. In the hybrid scheme, with 40 kbps AUV-ASV link data rate, the throughput obtained is not affected by the packet size or AUV-AUV distance, because of contention-free in the acoustic and RF domains. Thus we observe a throughput of 40 kbps. In the direct scheme, the acoustic link data rate is computed from the range-rate product of 20 $kbps \times km$, $that\ is$ 20 kbps at 1km distance. Thus, this results in higher data rate (hence throughput) for closer AUVs. The throughput for the direct one-way application flow from AUV-1 to AUV-2 is also unaffected by the packet size in the direct scheme.

Throughput results in bidirectional hybrid/direct AUV-AUV communications for variable distances/packet sizes are shown in Fig. 6.9. In the direct scheme, if the application start times for both AUV1 and AUV2 are the same, the packet size of 2 kB cannot be used. This is due to TX-RX interference since in half-duplex communications, a node cannot send and receive at the same time using the same frequency. When
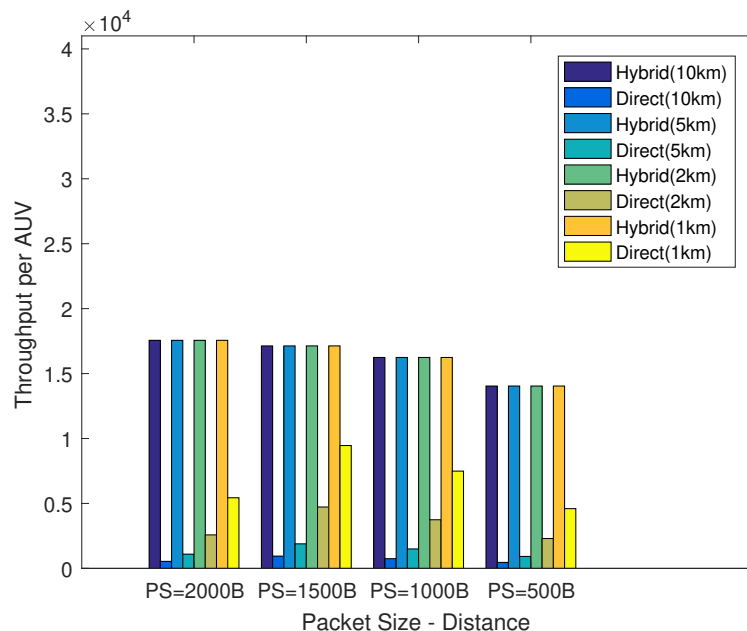
Figure 6.9: Packet Size vs. bidirectional throughput for two application flows between the two AUVs in the hybrid and direct scheme.

the data rate is 2 kbps (in the case of 10 km AUV-AUV distance), 8-second packet transmission delay and 6.6-second propagation delay cause a collision and packet loss. To transmit packets of a 2 kB size, packet scheduling is used in which an AUV transmits right after reception of a packet. For other packet sizes, no scheduling is used.

We notice from Fig. 6.9 that the aggregated throughput of the network is on average 10% lower than one-way results for packet size of 2 kB and 30% for packet size of 500 B. Since we use no pipelining and packet generation is interval-based, larger packets are preferred. For example, PS=1500 B reaches throughput of 10 kbps per AUV. If we use pipelining and scheduling for other packet sizes (not presented in this chapter), the attainable throughput reaches half of the acoustic link data rate for each AUV. In the hybrid method, with the increase in the number of packets when smaller packet sizes are used, collision probability of RF transmissions also increases. This is due to more transmissions of control packets to reserve the channel, and, hence, larger
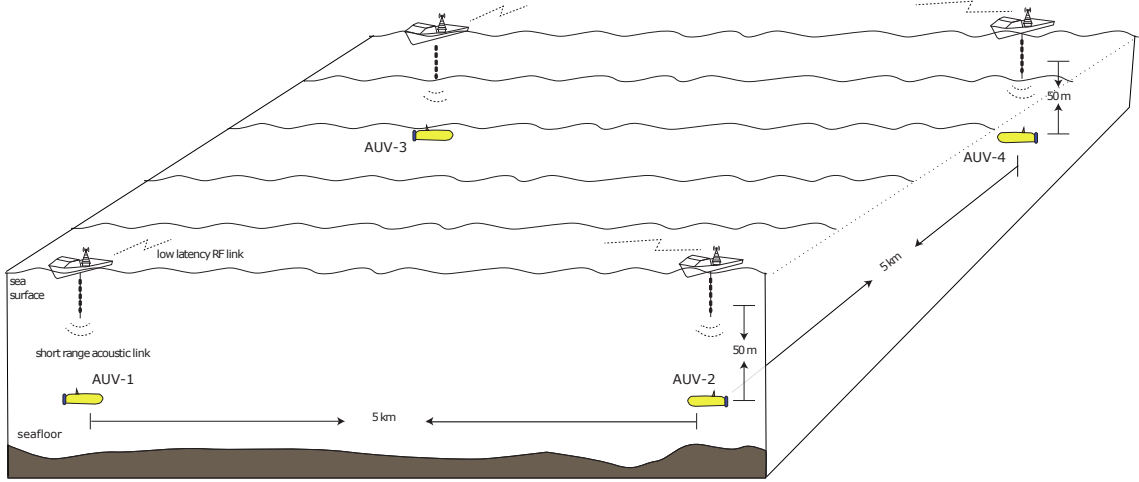
Figure 6.10: Network of four AUVs.

packet sizes are preferred.

In the simulations of direct scheme and bidirectional communications, except for the packet size of 2 kB, no scheduling is used. Further, in the RF domain, both ASVs send and receive packets, which limits the achievable throughput. In the second scenario, we relax this constraint by four one-way flows in a network of 4 AUVs along with an optimal scheduler [110].

6.5.2 Second Scenario: Network of four nodes with four application flows

This scenario has four ASV-AUV pairs located at the edges of D_{HA} by D_{HA} grid as shown in Fig. 6.10. There are two flows from AUV-1 to AUV-2 and from AUV-3 to AUV-4 on the sides of the grid. There are two diagonal flows from AUV-1 to AUV-4 and AUV-3 to AUV-2. In direct AUV-AUV communications, packets of the diagonal flows traverse longer distance $\sqrt{2} \cdot D_{HA}$, and, therefore, have a slightly lower data rate, as we assumed a constant rate-range product of 20 $kbps \times km$.

In the direct method, if applications start at the same time, we experience high collision rate. To deal with this issue, we use scheduling in the direct scheme where application start times have a lag to avoid collisions. As shown in Fig. 6.11, the

110
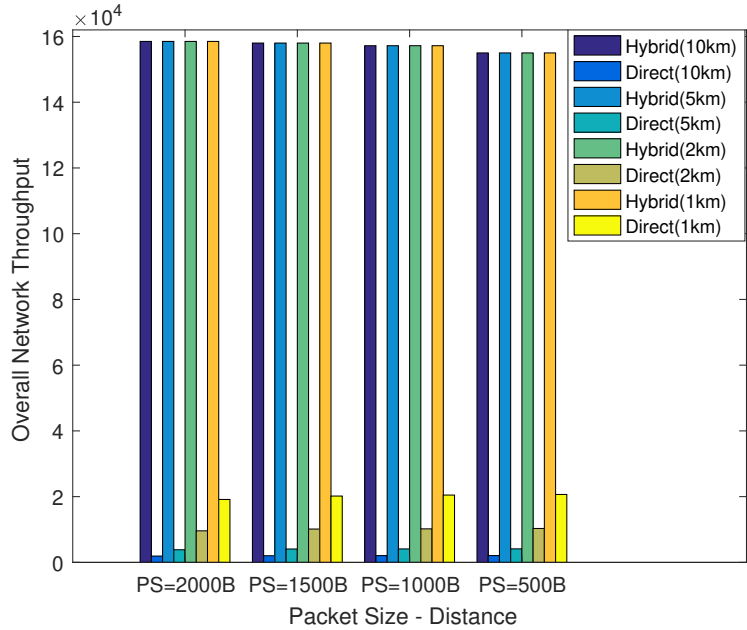
Figure 6.11: Throughput results of four AUVs

aggregate throughput of the direct scheme is far less than that of the hybrid scheme. This is due to lower acoustic link rates in the direct scheme, which cause higher packet transmission delays. In the hybrid scheme, using the RTS/CTS mechanism for the RF links does not affect the network efficiency because of the higher data rates of the RF links.

This simulation highlights the difference between the hybrid and direct AUV-AUV communications in a network of four AUVs. As mentioned earlier, since the traffic load of RF links is far less than that of the acoustic links, the RTS/CTS mechanism is suitable for hybrid networks.

6.5.3 Third Scenario: Infrastructure-based networks

Underwater networks are often constructed with a centralized (infrastructure-based) structure, where all the nodes transmit their sensory information to a centralized entity, or an Access Point (AP). An AP will have another antenna to communicate

with a sink node by using RF link. This scenario simulates either two or four AUVs communicating with one AP using the hybrid or the direct scheme. The AP is located equidistant from the AUVs. In the hybrid method, ASVs transfer the information collected from the AUVs to the AP using RF links. Fig. 6.12 illustrates two AUVs 5 km apart from each other. The AP is located half-way between the two AUVs at water surface and AUVs navigate at depth of 50m similar to previous scenarios.
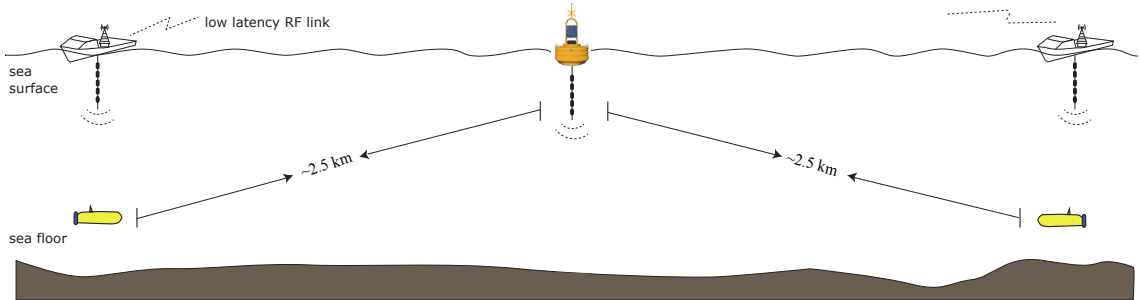
Figure 6.12: Infrastructure mode.

The result of aggregate network throughput for two and four nodes are presented in Fig. 6.13. In the direct scheme, we use optimal packet scheduling (pipelining), where the AP is always receiving packets and an AUV transmits a packet with a lag. The lag is referred to as the packet transmission delay plus inter-frame space (IFS), which is 0.01 s in our simulations. For instance, if two AUVs are 2 km apart and the packet size is 2 kB, packet transmission delay (PTD) is 0.8 s. If the first AUV transmits at time $T = 0s$, the second AUV transmits at time $T = PTD + IFS = 0.81$ s, the third AUV at time $T = 2 * (PTD + IFS) = 0.162s$, and so on. The acoustic link data rate is also computed based on the same rate-range product as before, 20 $kbps \times km$. In case of two AUVs separated by 2 km, the acoustic link data rate is 20 kbps for the AUV-AP link.

In the hybrid scheme, higher throughputs are achieved for larger packet sizes owing to smaller amount of control packets (RTS/CTS). Advantages of the hybrid scheme are more remarkable with increase in the network size or AUV-AUV distance.

112
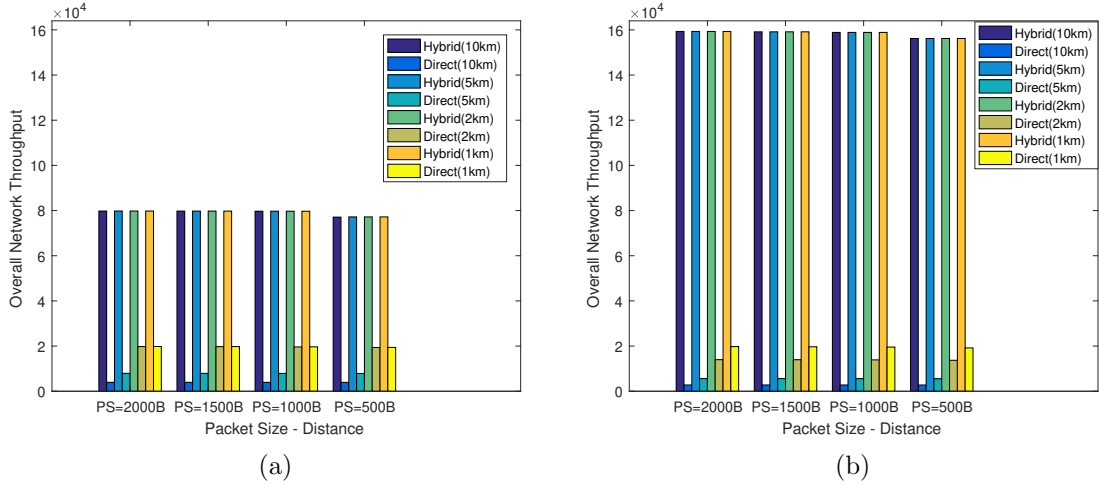
Figure 6.13: Aggregate throughput of variable packet sizes for (a) two and (b) four AUVs communicating with an AP equidistant from the AUVs.

6.6   Chapter Summary

With wide range of underwater applications, underwater acoustic sensor networks (UASNs) have recently gained more attention. The low bandwidth and long propagation delay of acoustic networks call for efficient MAC protocols and new architectures. By using ASVs at the sea surface, we designed a functional architecture for autonomous underwater operations with swarming-based ASV navigation and hybrid RF-Acoustic communications as its constituents. The connected RF backbone is maintained by a swarm of ASVs for enhanced data rates and much reduced end-to-end latency for AUV-AUV communications. We evaluated, via ns-3 simulations, the performance of hybrid RF-acoustic communications in comparison to direct underwater AUV-AUV acoustic communications.

Chapter 7

A MAC PROTOCOL FOR UNDERWATER ACOUSTIC FULL-DUPLEX COMMUNICATIONS

7.1 introduction

Recently, Underwater Acoustic Sensor Networks (UASNs) have attracted an increasing attention owing to numerous applications in industry, military, and academia. The applications span from oceanography, marine biology, deep-sea archaeology, seismic and tsunami predictions, pollution detection in long-term aquatic monitoring to natural resource discovery, hurricane disaster recovery, anti-submarine military mission etc. in short-term usages [111]. Unlike terrestrial communications, in underwater wireless communications, water is the medium for signal propagation. Even though Radio Frequency (RF) and Optical waves are successfully tested, RF signals undergo significant attenuation and optical waves are absorbed by the water. Thus, they can only be used for short range communications. However, Acoustic waves can propagate in longer distances (up to 4 km) which is more than an order of magnitude longer than RF modems (i.e., around 150 m) [112].

The propagation speed of sound in the water (i.e., 1500 m/s) is almost five orders of magnitude less than RF frequency over the air (i.e., 3×10^8 m/s). Thus, although acoustic waves can traverse long distances in the water, they are restricted by long propagation delay. Moreover, the available bandwidth and hence the data rate of acoustic waves are limited and are highly dependent on the frequency and transmission

range. So, to compute the data rate for a communication range, the notion of range-rate product is used (i.e., between 10-70 km * kbps) [111]. Since the nodes in UASNs are battery-powered, the power saving is another important issue in these networks.

The propagation delay for over-the-air communications is near-zero and hence negligible in protocol designs. Thus, adopting RF domain MAC protocols directly to underwater domain results in lower efficiency. In this chapter, we first survey some of the important MAC protocols proposed for UASNs communications. Second, we describe challenges for designing an in-band full-duplex (IBFD) MAC for UASNs and highlight key points that should be taken into account when designing an IBFD MAC for UASNs. Then, we propose a novel technique to reduce power consumption in UASNs. Finally, a half-duplex and an in-band full-duplex MAC protocol based on this technique are proposed. To the best of our knowledge this is the first study to reduce the power consumption of UASNs by targeting multiple nodes simultaneously.

The remainder of this Chapter is organized as follows. Section 7.2 describes the issue caused by large propagation delay in UASNs. In Section 7.3, we survey the MAC protocols proposed to address spatio-temporal uncertainty and increase the communication efficiency in the UASNs. Section 7.4 explains the challenges in designing MAC protocols for UASNs. In Section 7.5, we explain our proposed technique to reduce power consumption and propose a full-duplex MAC for UASNs. Finally Section 7.8 concludes this chapter with future research directions.

7.2 Spatio-temporal uncertainty

Since the propagation speed of electromagnetic wave is close to the speed of light, we can ignore the propagation time in RF networks, and as a result, packet transmission time is the only significant delay between the transmitter and the receiver. Nevertheless, in acoustic underwater communications, propagation delay can also be
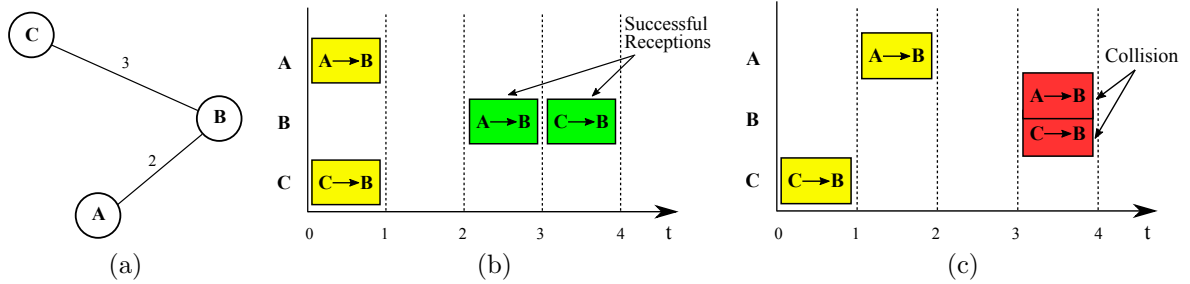
Figure 7.1: Spatio-temporal uncertainty a) Example topology b) Collision-free simultaneous transmissions and c) Collision due to different propagation delays.

significant which will impact the protocol design. In wireless networks, *transmission collision* occurs when two or more data frames arrive at a receiving node simultaneously. Since in half-duplex RF networks, simultaneous transmissions will result in a collision at the receiving node, only one node is permitted to transmit at a time. However, in UASNs, because of the long propagation delay, simultaneous transmissions might be successful; also, transmissions at different times might lead to transmission collisions. Therefore, not only the success of a transmission depends on transmission time but it also depends on the transmission distance (i.e., spatio-temporal uncertainty).

Figure 7.1 illustrates the impact of spatio-temporal uncertainty on acoustic underwater communications. Imagine the example topology of Fig. 7.1a with propagation delay (t_{pd}) between nodes as the labeled numbers. Fig. 7.1b illustrates two transmissions starting at time 0 and successfully received by their associated receivers. Moreover, two other transmissions that resulted in a collision and not started at the same time are shown in Fig. 7.1c. Therefore, assuming frame delays of one time-slot (T_s), if node A transmits to node B at time $T_1 = 0$, B receives the complete frame at time $T_1 + t_{pd,A \to B} + T_s$, and if node C wants to have a collision-free transmission to node B, its transmission start time can be computed as $T_c = T_1 + t_{pd,A \to B} + T_s - t_{pd,C \to B}$. Here, assuming the slot time to be 1 s, T_c is computed as 0.

7.3 Related Literature

In RF domain, the problem of power consumption in wireless devices is different from underwater devices. In RF-devices, batteries can be easily recharged (handheld devices) or replaced (WSNs). However, the process of recharging or replacing underwater sensor nodes can be expensive. Thus, efficiency in using power is also an integral part of performance measurement besides throughput and delay. The proposed UASNs MAC protocols can be classified into three main categories: (1) Contention-free MAC protocols, (2) Contention-based MAC protocols, and (3) hybrid MAC protocols. We compare the most notable MAC protocols for half-duplex UASNs based on their architecture, synchronization requirement, advantages and disadvantages in Table 7.1.

7.3.1 Contention-Free MAC Protocols

The protocols of this section assign to each node either different frequency sub-channels (FDMA), different time slots (TDMA), or different coding schemes (CDMA). Since power consumption of underwater sensor nodes is relatively high, power inefficiency occurs with higher number of transmission collisions. Since in contention-free protocols, transmission collisions are fewer than contention-based MAC protocols, contention-free MAC protocols are considered power-efficient.

7.3.1.1 FDMA

In these protocols, the entire spectrum is divided into several sub-channels and is assigned to different nodes to simultaneously communicate with each other. However, due to very low bandwidth available in UASNs and the additional guard bands needed to prevent interband interference these protocols are not efficient for UASNs communications.

7.3.1.2   CDMA

CDMA method uses spread spectrum techniques and special coding scheme so that each node in the network can modulate its signal using an assigned unique code and simultaneously communicate to other nodes. If the cross-correlation of nodes are low, CDMA technique results in long codes that are not efficient in UASNs. Also, the inherent CDMA near-far problem that is aggravated in underwater communications due to long-range communications and long distances made CDMA not a very suitable approach for UASNs [112]. In UW-MAC [113], authors propose a distributed protocol that sets the optimal transmit power and code length to minimize the near-far effect. It achieves its objectives in deep-water communications because of low multipath effect. However, in shallow waters, due to heavier multipath effect, the performance of the protocol degrades notably. Another CDMA-based MAC protocol is POCA-CDMA-MAC [114] proposed for multi-hop networks. In [114], each path is given a unique code and simultaneous packet transmission is based on round robin manner. Since the transmission of each intermediate node depends on the transmission of head-of-path node, the protocol is not scalable and has high overhead.

7.3.1.3   TDMA

In TDMA method, the entire channel bandwidth is allocated to a node but for a limited time. TDMA-based protocols have attracted a lot of attentions because of the special characteristics of underwater communications. Although in infrastructure-based networks, the AP can allocate the channel time to different nodes in a contention-free manner, in distributed TDMA protocols, achieving collision-free schedule is hard provided the random arrival of frames to the MAC queue of the nodes.

In ECS [115], authors propose a centralized one-slot TDMA-based protocol with sender oriented conflict model based on continuous time allocation. Nodes will compute

their priority based on some heuristics and synchronize with local neighbors for collision avoidance. ECS assumes identical nodes, clock synchronization and nodes' ability to calculate their positions. [116] proposes a multi-slot TDMA centralized algorithm that tries to use smaller frame size for higher efficiency. ST-MAC creates a weighted, directed conflict graph for the transmission scheduling problem. Scheduler assigns colors to transmissions (edges). However, the difference of colors between adjacent vertices should be greater than the weight of the edge connecting them which makes it hard to apply conventional heuristics. Moreover, when the number of nodes becomes large the algorithm becomes inefficient. [110] is a centralized TDMA-based MAC protocol that formulates transmissions as constraints to be satisfied by the scheduler in order to avoid collisions. It assumes slot times to be the same as transmission time of a node. It uses proper guard times obtained by simulations to overcome variations in delay, water salinity etc. to avoid collisions. However, it does not explain how transmission requests are gathered at the centralized controller. Authors in [117] have proposed two algorithms to compute schedules by taking into account all scheduled transmissions. One of the algorithms is for fixed order of transmissions and the other can compute the best order to schedule algorithms.

7.3.2 Reservation-based MAC protocols

These protocols rely on random channel access and usually add enhancement to ALOHA or CSMA protocol [112]. Thus, there is no prior allocation of the channel to any node and if collision happens, they employ some recovery methods or retransmission techniques. To reduce the number of collisions, they employ a reservation mechanism prior to the actual data transmission [118–120].

T-Lohi [118] is the first proposed reservation-based MAC protocol. It employs short contention-based tones to reserve the channel. It is not power efficient as it

requires a node to be idle and listening to the channel in contention periods to compete for the channel. Also a node should listen at least the maximum single-trip propagation time plus the time needed to detect contention tone. Its maximum throughput as a result is limited to 66 percent of channel capacity. R-MAC [119] is also a reservation-based protocol that adjusts the timing between control packet exchanges to reduce the long propagation delay in UASNs as well as to notify neighbors of forthcoming communications. It also transmits burst of packets with delayed ACKs that would improve channel throughput. UW-FLASHR [120] is a distributed protocol that does not need propagation delay estimation or synchronizations. It works in cycles which are divided into experimental and established portions. To receive a time slot to transmit data, a node should send request at random times in experimental portion of several consecutive cycles to reserve the channel. This randomness in requesting slot time builds a loose distributed transmission schedule resulting in waste of the channel time.

7.3.3 Hybrid MAC protocols

These protocol try to collect advantages of both contention-free and reservation-based MAC protocols when there is a need. HR-MAC [121] is a sender initiated distributed protocol that employs a 4-way handshake ordered-CDMA to avoid collisions; nodes should first reserve the channel and then transmit their information in a given order. However, the more control packet exchange the lower the performance due to high propagation delay of underwater. Also "notice" is based on spreading sequence that could limit number of associated nodes in a cluster.

7.4 Challenges in Designing MAC protocols of UASNs

There are some limitations in underwater communications such as long and variable propagation delays, low data rate, noise and high Bit Error Rates (BER), and high power consumption by nodes. These limitations should be taken into account when

Table 7.1: Classification and Comparison of Half-Duplex MAC Protocols for UASNs

Domain		Protocol	Architecture	Synchronization	Advantage(s)	Disadvantage(s)
Contention-Free	TDMA	ECS [115]	Distributed Multi-hop	Yes	Continuous time scheduling	Not suitable for mobile networks
		High Throughput [110]	Centralized Multi-hop	Yes	Prioritizes (1) Earliest deadline first (2) Longest distance	Best start requires heavy computations
		ST-MAC [116]	Centralized Multi-hop	Yes	Prioritizes (1) Load (2) Max. conflicting node	Breaks frames into pieces, suboptimal
		SetOfSimple [117]	Centralized Multi-hop	Yes	Takes into account former scheduled transmissions	No heuristics is used
	CDMA	UW-MAC [113]	Distributed	Yes	Optimal transmit power and code length	Requires information of all nodes, not suitable for shallow waters
		POCA-CDMA-MAC [114]	Multi-hop	Yes	Simultaneous packet transmission using round robin	Not scalable High overhead
Reservation-Based		UW-FLASHR [120]	Distributed	No	Does not require (1) Synchronization (2) Propagation Delay	Gradual creation of gaps between transmissions
		T-Lohi [118]	Distributed	No	Short wake-up tones Data reservation	Requires idle and listening-to-the-channel nodes
		R-MAC [119]	Multi-hop	No	Packet bursts, Scheduled transmission at both transmitter and receiver	Scalability issues
Hybrid		HR-MAC [121]	Multi-hop	Yes	CDMA to get order TDMA to transmit	Not scalable

designing a new MAC protocol for UASNs. Depending on the scenario, architecture and the use case of the UASN, different metrics might have higher preference in the design of an efficient MAC protocol. For instance, power consumption is less important in a temporary UASN compared to a long-term UASN.

7.4.1 Synchronization

In UASNs, synchronization is a critical challenge owing to cyclic working periods. Without synchronization, the collision rate would be extremely high due to long propagation delays. Although synchronization is out of scope of this research, the avid reader can refer to [122] and [123] and references therein.

7.4.2 Network Topology and Deployment

To communicate more efficiently, some of the proposed protocols try to build the network topology. Size of the network and density of the node deployments are two important factors that impact the design and performance of UASNs. An efficient MAC protocol should take into account these factors for higher efficiency.

7.4.3 Mobility

Nodes in large UASNs usually have mobility with the water current about 3 to 6 km/h [111]. This has impact on the protocols that build the network topology and adjust the transmission power.

7.4.4 Suboptimal Handshake Mechanism

Channel reservation via control frame exchange in RF networks (i.e., RTS/CTS) would help to reduce hidden and exposed terminal problems. It should be noted that the RTS/CTS mechanism should be activated for large frames, otherwise, it will incur an extra overhead to the network and will degrade the performance. Likewise, in underwater communications, activating the channel reservation should be based on the network conditions such as traffic load, network architecture, etc.

7.5 Description of the Multi-Targeted Full-Duplex MAC

With acoustic IBFD communications, Fig. 7.2 depicts three concurrent transmission modes: (a) bidirectional FD (BFD) transmissions (between nodes A and B) with overlap, (b) source based FD (SBFD) transmissions, where primary transmitter node B, while transmitting a packet to primary receiver node C, can simultaneously receive a packet from secondary transmitter node A; and (c) destination based FD (DBFD) transmissions, where primary receiver node B, while receiving a packet from primary transmitter node A, can simultaneously transmit a packet to secondary receiver node C. Although RF full-duplex transmissions also exhibit similar concurrent transmission modes [23], the long and non-uniform propagation delays between nodes in UASNs make the task of scheduling much harder, as 'control' information sent between acoustic nodes may experience different propagation delays.

Our MAC designs are motivated by the following observations: collision in underwater networks is very expensive in terms of energy and channel utilization [124];
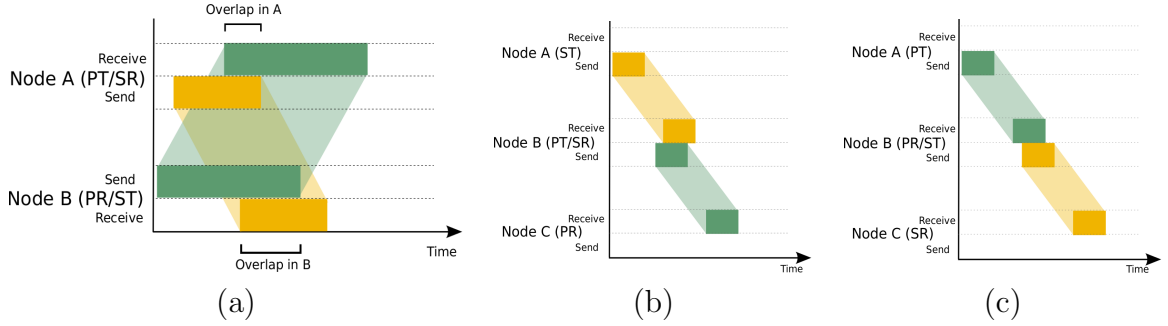
Figure 7.2: Acoustic IBFD transmission modes: (a) bidirectional FD transmission with overlap (BFD, mode=00), (b) source-based (SBFD, mode=01) , and (c) destination-based (DBFD, mode=10).

acoustic transmissions consume significantly more energy than reception (*e.g.*, ratio of 125:1) or staying idle [125]; although RTS/CTS takes up channel time, it helps avoid collisions due to hidden nodes [126]; and for collision avoidance in networks with random placement of nodes, the RTS wait time should be longer than the longest propagation delay and the CTS wait time should be longer than RTS transmission time plus two times the longest propagation delay [125, 127].

We propose a new class of collision avoidance protocols using "variable-length" control packets (RTS, CTS, or ACK) to facilitate concurrent transmissions with acoustic IBFD. A node, based on the available data to be transmitted in its buffer, dynamically adds 'control information' into a variable-length control packet so as to target different nodes that will either receive or overhear the packet. We add the '# of sub-headers' field to the common header of the variable-length control packet to indicate the number of sub-headers to examine and the two-bit 'Mode' field to indicate the mode of transmission in the decreasing priority of BFD > SBFD/DBFD > HD.

As an example, we use the network topology in Fig. 7.3(a), where both the distance between any two nearest nodes and the acoustic transmission range are 1500 m, so that it takes 1 second for a packet to reach the nearest neighboring node(s). Fig. 7.3(b) depicts sample operations of the network over time, where the transmissions of overheard packets are denoted via dashed arrows. When a node finds a
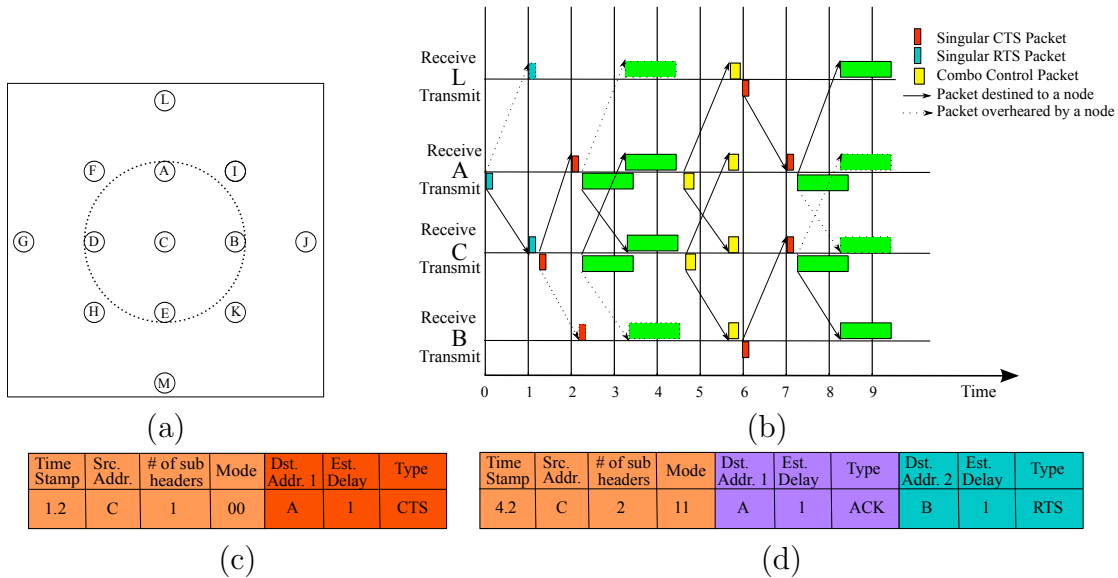
Figure 7.3: (a) Topology, (b) time-line, (c) singular CTS packet, and (d) combo control packet.

received/overheard control packet conflicting with its own schedule of transmission or reception, it will remain silent to not cause any collision. Node A transmits an RTS to node C (overheard by nodes L, F, and I to prevent them from transmitting) followed by a singular CTS packet with Mode "00" (Fig. 7.3(c)) to exploit BFD opportunities and to prevent node C's neighbors from sending RTS to node C. After successful BFD transmission/receptions between nodes A and C, both nodes transmit a 'combo' control packet, acknowledging the correct receipts of each other's packets and making another RTS request to their neighboring nodes L and B, respectively, for future transmissions. Fig. 7.3(d) depicts the combo control packet sent by node C to node B requesting an HD [Mode "11"] transmission. In general, prioritizing BFD opportunities over other modes of operations not only results in a smaller exclusive access area, but also eliminates the exposed node problem for the future transmissions of the involved nodes.

The benefit of this protocol is three-fold: (1) multi-targeted transmissions with embedded collision avoidance save the channel time, hence higher throughput and less

delay. The protocol also exploits all the benefits of IBFD; (2) battery life of the nodes is extended with fewer number of transmissions; and (3) nodes can learn each neighboring node's distance and transmission schedules by examining its received control packets.

7.6 Simulation Settings

In most of underwater applications, nodes collect data and transmit them to a sink at the sea surface. As the aim is to design a full-duplex protocol capable of activating all full-duplex modes, the sink also has data to transfer to the nodes. The nodes are random uniformly placed in an 5 km × 5 km area and in depth randomly selected between 100 and 300 m. In this research, we did not take into account the bit error rate (BER) and instead we assume that the rate-range product is 20 kbps × km for the acoustic link between the two nodes [128].

The common assumption in the literature for transmit power of underwater nodes is 188 dB re μPa. The energy (E) of an acoustic signal can be computed as the product of intensity (I) and time duration (T) of the signal, $E = I \times T$. On the other hand, sound pressure level (SPL) is related to rms pressure (P_{rms}) based on following formula [129]:

$$SPL(dB) = 20 \log \left(\frac{P_{rms}}{1\mu Pa} \right) \tag{7.1}$$

Also, we can compute I_{rms} based on the following formula:

$$I_{rms} = \frac{P_{rms}}{\rho c} \times 10^{-12}, \tag{7.2}$$

where P_{rms} is in units of μPa, ρ is the density of water (i.e., 1,060 kg/m³) and c is the sound velocity of water (1,500 m/s). Therefore, the emitted power from the source can be measured by the following formula at $r = 1$ m:

$$P_0 = 4\pi r^2 I_{rms} \tag{7.3}$$

In this research, we assumed that the noise power is the same at both transmitter and receiver and is 35 dB for the center frequency of 12 kHz. Therefore, when computing the transmission power, knowing the path loss, the transmitter transmits with a power that receives at the receiver dB above the noise floor. Other simulation parameters are outlined in Table 7.2.

Table 7.2: Other parameters for the simulations

Parameter	Value
IFS	$0.05s$
Center Frequency (kHz)	12
Data rate (rate-range product)	20 kbps $\times$ km
Packet size (Bytes)	1000
Frame arrival rate	$\lambda = 10$
Simulation Runs	10
Frame retransmission	3
Simulation time	1000 s

7.7   Results and discussion

In this Section, we present the results of a half-duplex network operating with the designed protocol. We compare the results of the half-duplex protocol with a network where only the sink is capable of full-duplex transmissions and a network that all nodes are capable of full-duplex transmissions. Fig. 7.4 presents the comparative results.

Enabling the sink with full-duplex ability does not bring much gain to the network because of the interference from other nodes in the network. However, if all nodes are capable of full-duplex transmissions, since (1) bi-directional full-duplex becomes possible, and (2) the inter-node interference is subsided, the overall throughput of the network becomes 2.5 times higher the half-duplex version. Also, we can see that full-duplex networks with optimized power significantly consume less energy than the
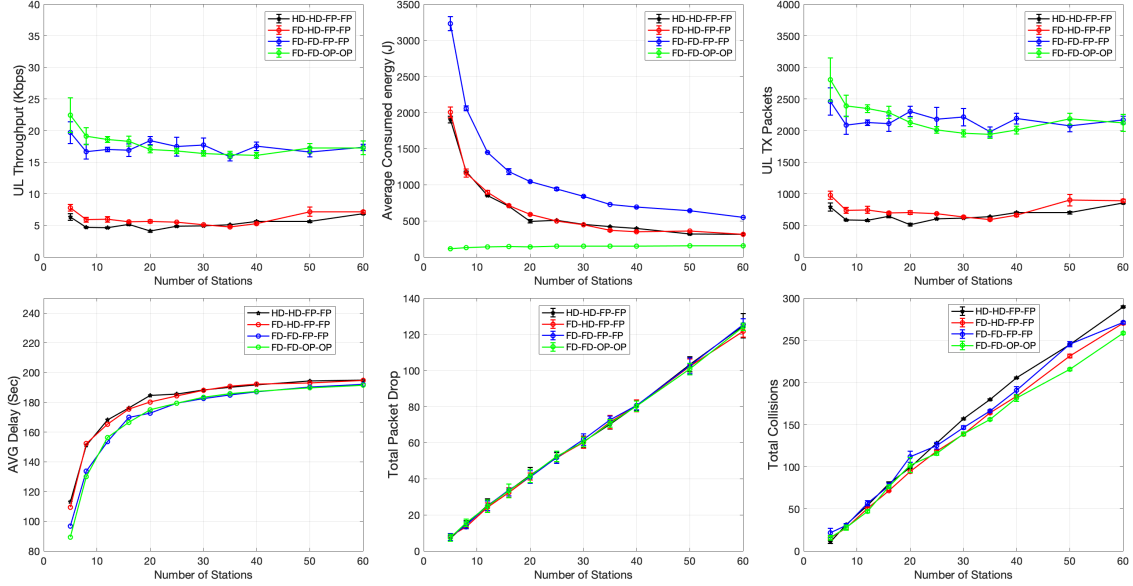
Figure 7.4: Comparative results between half-duplex network, full-duplex sink and half-duplex nodes, and full-duplex sink and nodes in full power (FP) and optimized power (OP) modes. Legends are in the form of A-B-C-D. A: sink operation mode, B: nodes operation mode, C: optimal control power, and D: optimal data power.

other networks while keeping the throughput almost intact; if the number of nodes are small (< 15), the optimal power adjustments is superior to the full-power transmissions.

7.8 Chapter Summary

Full-duplex communications can increase the capacity of wireless networks, and therefore, are especially suitable for underwater acoustic sensor networks (UASNs) where data rate is very limited. As the underwater applications are rising and there is no standardized MAC protocol for either half-duplex or full-duplex underwater communications, designing efficient MAC protocols for this domain is extremely important. In this research, we assume that full-duplex is possible in underwater acoustic communications which is still under study.

The goal of this research is to increase the performance of UASNs by designing

127

a power efficient full-duplex MAC protocol. Since acoustic transmission consumes significantly more energy than reception, collision in UASNs is very expensive in terms of energy consumption. Moreover, although RTS/CTS incurs overhead on the communications, it is important in reducing the collisions. We designed a multi-targeted MAC protocol capable of adjusting transmission power by taking into account the noise and distance between a pair of transmitter and receiver. Since nodes can target more than one destination with their frames, the amount of control frame transmissions also has been reduced. The protocol is able to achieve same throughput results as fixed power transmission mode albeit with noticeable reduced energy consumption.

Chapter 8

CONCLUSIONS AND FUTURE RESEARCH DIRECTIONS

Wireless technology has become one of the inseparable technologies in every day life for all of us. From laptops, phones and cellphones, to smart TVs and car navigation system, they all use wireless technology to transmit and/or receive data. Since the beginning of 2016, the amount of traffic carried over wireless networks has surpassed that of wired networks. However, wireless resources are scarce and expensive, and efficient usage of these resources is of utmost importance. With the ever increasing data demand comprising data hungry and delay-sensitive applications, the deployment of wireless base stations has been densified with small cells. Therefore, the inter-cell and intra-cell interference has been increased. Moreover, new technologies have been invented to increase the capacity of wireless networks. Thus, new MAC protocols are required to efficiently coordinate the transmission of different wireless stations not only to reduce the delay and frame collisions but to also increase the overall throughput of the network. In this dissertation, we studied the problem of efficient coordination among the stations in different wireless networks. We designed different access mechanisms, scheduling techniques and innovative architectures to increase efficiency.

Many of the terrestrial wireless technologies (e.g., Wi-Fi, Bluetooth, ZigBee) employ a contention-based MAC protocol called carrier sense multiple access with collision avoidance (CSMA/CA). With the shift in dense deployment of wireless base stations and traffic differentiation, CSMA/CA performance drops due to excessive number of

frame collisions which results in lower throughput and larger end-to-end delays. One of the alternative protocols proposed to replace CSMA/CA is CSMA/ECA in which a station selects a *deterministic backoff* value after a successful transmission. This deterministic backoff is computed based on the transmitting backoff stage and the access category of the transmitting stations. Therefore, if the transmitting station incorporates its transmitting backoff stage (a three-bit field) into its MAC frame, owing to the broadcast nature of wireless transmissions, the stations overhearing this transmission can compute the next transmission of the transmitting station (in terms of time slots) and refrain from a transmission that might cause a frame collision. This mechanism is called *distributed reservation*, in which stations collaborate to increase the efficiency of a wireless network. The results from both saturated and unsaturated scenarios demonstrate higher performance of this protocol.

Wireless communications are half duplex; a station cannot transmit and receive at the same time with the same frequency because of the interference that the transmission causes on its own reception (i.e., self interference). Recently, with cancelling the self interference, full-duplex (FD) wireless communications have become possible. FD communications can increase the capacity of wireless networks and are orthogonal to other technologies. Since FD transmissions can take place between three stations, new MAC protocols are required to utilize the full potential of this technology. However, the proposed MAC protocols need RTS/CTS to reserve the channel or else frequent frame collisions decrease the efficiency of these networks. We designed FD CSMA/ECA-DR, a protocol based on CSMA/ECA-DR, that achieves four times the throughput of CSMA/CA even in dense deployments.

The future research of this study can apply CSMA/ECA-DR and FD CSMA/ECA-DR in other communication types such as multi-hop wireless networks, LAA Wi-Fi co-existent networks [130], and other networks such as Bluetooth, ZigBee, etc. The idea

of collaboration (based on deterministic values rather than random values) to achieve higher performance can be applied to any network that nodes should contend to obtain the channel time.

To combat the inefficiency of contention-based wireless networks, the new Wi-Fi standard, IEEE 802.11ax, employed the technology of orthogonal frequency division multiple access (OFDMA). Moreover, access point is given more authority to schedule the uplink transmission of stations and assign them proper sub-channels sizes. Although OFDMA scheduling is not new, the intricacies associated with access and scheduling in 802.11ax require new scheduling and resource allocation mechanisms developed specifically for this standard. To be able to design a framework for UL scheduling in 802.11ax networks, we divided this problem into station selection, resource scheduling to the selected stations and transmission duration computations. Based on the ability of MAC layer to impose intervals on transmission of different access categories, we designed an interval learning mechanism for the access point coupled with a delay threshold mechanism that serves the stations when they actually have pending frames and within their delay threshold proportional to the network load. For the scheduling, we designed a semi-binary recursive function that assigns proper size sub-channels to the stations in a near-optimal fashion. For the transmission duration computation, we formulated an optimization function that minimizes the channel waste time (i.e., padding and transmission overhead).

Future studies for this research can be enhancing the scheduling framework even further. Although the proposed algorithm achieves higher performance compared to the baseline study and minimizes the spectrum waste, it is still important to devise novel mechanisms for the selection of STAs and Multi-TID aggregation mechanisms to further improve the In-RU efficiency of the 802.11ax. Furthermore, the proposed scheduler is biased toward STAs with better channel quality. As a future research,

we plan to employ different mechanisms to increase fairness among STAs of the same ToS. Other future studies include extending the Smart framework to work with LAA, UORA, and simulating Smart framework in OBSS where the contention among different BSSs can cause frame collisions. Although IEEE 802.11ax standardized BSS coloring and two different network allocation vectors (NAVs) to increase spatial reuse, further investigations are still required to measure how to best make use of each additions.

Wide range of virtual reality (VR) applications in military, healthcare, education, business, entertainment, engineering etc., have made this technology one of the top research fields in computer science. However, with stringent QoS requirements of VR applications, VR head mounted displays (HMDs) are usually wire-connected to the computers to which the video rendering is delegated. As wire connection limits the user mobility, research in academia and industry is focused to handle VR traffic with a wireless technology. With the current contention-based Wi-Fi technology, protocol optimizations across all the layers of the network stack can only support a few VR devices in low interference situations. Therefore, other communication technologies such as mmWave (WiGig and 5G New Radio) have become the options to support VR. However, they both require their specific base stations. Moreover, 5G is not free.

The new Wi-Fi standard, IEEE 802.11ax, has employed OFDMA and new access mechanisms to overcome the inefficiency of former Wi-Fi standards. In this research, we enhanced our proposed UL framework to support VR traffic with its stringent QoS requirements among other access categories. In particular, we added DL traffic, and the mechanism to switch between UL/DL directions. We also enhanced the scheduling mechanism to split the station on both sides of the bandwidth tree. We further enhanced our utility computation with a penalty function to take into account the queue

length of stations when scheduling. The results indicate that with the new enhancements, a network comprising of 50 stations 20% voice, 20% VR (8 Mbps target bitrate and 60 frame per second resolution) and 60 % best effort can be supported. A future research direction in this area is to consider the next arrival of VR traffic when computing the PPDU duration. Therefore, the scheduler can support more VR stations even with higher resolutions.

With wide range of underwater applications, underwater acoustic sensor networks (UASNs) have recently gained more attention. The low bandwidth and long propagation delay of acoustic networks call for efficient MAC protocols and new architectures. By using ASVs at the sea surface, we designed a functional architecture for autonomous underwater operations with swarming-based ASV navigation and hybrid RF-Acoustic communications as its constituents. The connected RF backbone is maintained by a swarm of ASVs for enhanced data rates and much reduced end-to-end latency for AUV-AUV communications. We evaluated, via ns-3 simulations, the performance of hybrid RF-acoustic communications in comparison to direct underwater AUV-AUV acoustic communications.

In the simulations we have one AUV associated with one ASV. In practice, there might be multiple AUVs or even hierarchical clusters of AUVs (at different depths) associated with one ASV, which demands effective MAC protocols to coordinate AUV and ASV transmissions. If the distance of two AUVs are less than the two acoustic links of the hybrid method, it might also be beneficial to activate horizontal acoustic communication. As future research, we intend to design protocols that activate hybrid or horizontal communications based on AUV-AUV distances and network load. Also, mission-defined joint optimization of ASV navigation and adaptive RF backbone will be of further interest.

We also developed a multi-targeted MAC protocol capable of adjusting transmission power based on the noise floor and distance between transmitter and receiver. Since acoustic transmissions consumes significantly more energy than reception, collision in UASNs is very expensive in terms of energy consumption. Moreover, although RTS/CTS incurs overhead on the communications, it is important in reducing the collisions. We designed a multi-targeted MAC protocol capable of adjusting transmission power by taking into account the noise and distance of the receiver. Since the nodes can target more than one destination with their frames, the amount of control frame transmissions also has been reduced. The protocol is able to achieve same throughput results as fixed power transmission mode albeit with noticeable reduced energy consumption.

The assumption in this research is that the transmitter is aware of the noise floor at the receiver. However, in practical scenario, the noise floor can be sent to the transmitter with a MAC header field. Moreover, as this protocol is not based on time slots, the future research for this study can be comparing this protocol with slotted protocols and measure what will be the best slot duration based on network load and the distance between a pair of transmitter and receiver.

BIBLIOGRAPHY

[1] J. Chakareski, "VR/AR Immersive Communication: Caching, Edge Computing, and Transmission Trade-Offs," in *Proceedings of the Workshop on Virtual Reality and Augmented Reality Network*, ser. VR/AR Network '17. New York, NY, USA: ACM, 2017, pp. 36–41. [Online]. Available: http://doi.acm.org/10.1145/3097895.3097902

[2] L. Sanabria-Russo, J. Barcelo, B. Bellalta, and F. Gringoli, "A High Efficiency MAC Protocol for WLANs: Providing Fairness in Dense Scenarios," *IEEE/ACM Transactions on Networking*, vol. 25, no. 1, pp. 492–505, 2017.

[3] "Cisco Visual Networking Index: Forecast and Methodology, 2016–2021," https://www.cisco.com/c/en/us/solutions/collateral/service-provider/visual-networking-index-vni/complete-white-paper-c11-481360.pdf, 2017, accessed: Sep 4, 2017.

[4] J. G. Andrews, S. Buzzi, W. Choi, S. V. Hanly, A. Lozano, A. C. Soong, and J. C. Zhang, "What Will 5G Be?" *IEEE Journal on selected areas in communications*, vol. 32, no. 6, pp. 1065–1082, 2014.

[5] "TGax Specification Framework," https://mentor.ieee.org/802.11/dcn/15/11-15-0132-17-00ax-spec-framework.docx, accessed: Sep 4, 2017.

[6] L. Sanabria-Russo and B. Bellalta, "Traffic Differentiation in Dense Collision-free WLANs using CSMA/ECA," *Ad Hoc Networks*, 2018.

[7] L. Sanabria-Russo, A. Faridi, B. Bellalta, J. Barcelo, and M. Oliver, "Future Evolution of CSMA Protocols for the IEEE 802.11 Standard," in *Communications Workshops (ICC), 2013 IEEE International Conference on*. IEEE, 2013, pp. 1274–1279.

[8] R. A. da Silva and M. Nogueira, "MAC Protocols for IEEE 802.11ax: Avoiding Collisions on Dense Networks," *arXiv preprint arXiv:1611.06609*, 2016.

[9] I. Syed, S.-h. Shin, B.-h. Roh, and M. Adnan, "Performance Improvement of QoS-Enabled WLANs Using Adaptive Contention Window Backoff Algorithm," *IEEE Systems Journal*, 2017.

[10] S. Chun, D. Xianhua, L. Pingyuan, and Z. Han, "Adaptive Access Mechanism with Optimal Contention Window Based on Node Number Estimation Using Multiple Thresholds," *IEEE Transactions on Wireless Communications*, vol. 11, no. 6, pp. 2046–2055, 2012.

[11] N. Xie, L. Zhang, J. Wu, and H. Wang, "An Adaptive Backoff Algorithm Based on Channel Utilization For IEEE 802.11," *Wireless Personal Communications*, vol. 83, no. 4, pp. 2965–2973, 2015.

[12] K. Hong, S. Lee, K. Kim, and Y. Kim, "Channel Condition Based Contention Window Adaptation in IEEE 802.11 WLANs," *IEEE Transactions on Communications*, vol. 60, no. 2, pp. 469–478, 2012.

[13] M. Khatua and S. Misra, "D2D: Delay-Aware Distributed Dynamic Adaptation of Contention Window in Wireless Networks," *IEEE Transactions on Mobile Computing*, vol. 15, no. 2, pp. 322–335, 2016.

[14] G. Bianchi and I. Tinnirello, "Kalman filter estimation of the number of competing terminals in an IEEE 802.11 network," in *INFOCOM 2003. Twenty-Second Annual Joint Conference of the IEEE Computer and Communications. IEEE Societies*, vol. 2. IEEE, 2003, pp. 844–852.

[15] J. Choi, J. Yoo, S. Choi, and C. Kim, "EBA: An Enhancement of the IEEE 802.11 DCF via Distributed Reservation," *IEEE Transactions on Mobile Computing*, vol. 4, no. 4, pp. 378–390, 2005.

[16] D.-J. Deng, C.-H. Ke, H.-H. Chen, Y.-M. Huang *et al.*, "Contention Window Optimization for IEEE 802.11 DCF Access Control," *IEEE Transactions on Wireless Communications*, vol. 7, no. 12, p. 5129, 2008.

[17] J. Barcelo, B. Bellalta, C. Cano, A. Sfairopoulou, M. Oliver, and J. Zuidweg, "Traffic Prioritization for Carrier Sense Multiple Access with Enhanced Collision Avoidance," in *Communications Workshops, 2009. ICC Workshops 2009. IEEE International Conference on*. IEEE, 2009, pp. 1–5.

[18] G. Chen and B. K. Szymanski, "Reusing Simulation Components: COST: A Component-Oriented Discrete Event Simulator," in *Proceedings of the 34th conference on Winter simulation: exploring new frontiers*. Winter Simulation Conference, 2002, pp. 776–782.

[19] J. Choi, J. Na, Y.-s. Lim, K. Park, and C.-k. Kim, "Collision-Aware Design of Rate Adaptation for Multi-Rate 802.11 WLANs," *IEEE Journal on Selected Areas in Communications*, vol. 26, no. 8, 2008.

[20] A. Sahai, G. Patel, and A. Sabharwal, "Pushing the limits of full-duplex: Design and real-time implementation," *arXiv preprint arXiv:1107.0607*, 2011.

[21] W. Cheng, X. Zhang, and H. Zhang, "Rts/fcts mechanism based full-duplex mac protocol for wireless networks," in *Globecom Workshops (GC Wkshps), 2013 IEEE*. IEEE, 2013, pp. 5017–5022.

[22] W. Zhou, K. Srinivasan, and P. Sinha, "RCTC: Rapid concurrent transmission coordination in full DuplexWireless networks," in *Network Protocols (ICNP), 2013 21st IEEE International Conference on*. IEEE, 2013, pp. 1–10.

[23] S. Goyal, P. Liu, O. Gurbuz, E. Erkip, and S. Panwar, "A distributed MAC protocol for full duplex radio," in *Signals, Systems and Computers, 2013 Asilomar Conference on*. IEEE, 2013, pp. 788–792.

[24] M. Jain, J. I. Choi, T. Kim, D. Bharadia, S. Seth, K. Srinivasan, P. Levis, S. Katti, and P. Sinha, "Practical, real-time, full duplex wireless," in *Proceedings of the 17th annual international conference on Mobile computing and networking*. ACM, 2011, pp. 301–312.

[25] K. M. Thilina, H. Tabassum, E. Hossain, and D. I. Kim, "Medium access control design for full duplex wireless systems: challenges and approaches," *IEEE Communications Magazine*, vol. 53, no. 5, pp. 112–120, 2015.

[26] Y. Zhang, L. Lazos, K. Chen, B. Hu, and S. Shivaramaiah, "FD-MMAC: Combating multi-channel hidden and exposed terminals using a single transceiver." Citeseer.

[27] B. Radunovic, D. Gunawardena, A. Proutiere, N. Singh, V. Balan, and P. Key, "Efficiency and fairness in distributed wireless networks through self-interference cancellation and scheduling," *Microsoft Research, Cambridge, UK, Technical Report MSR-TR-2009-27*, 2009.

[28] N. Singh, D. Gunawardena, A. Proutiere, B. Radunovi, H. V. Balan, and P. Key, "Efficient and fair MAC for wireless networks with self-interference cancellation," in *Modeling and Optimization in Mobile, Ad Hoc and Wireless Networks (WiOpt), 2011 International Symposium on*. IEEE, 2011, pp. 94–101.

[29] J. Y. Kim, O. Mashayekhi, H. Qu, M. Kazandjieva, and P. Levis, "Janus: A novel MAC protocol for full duplex radio."

[30] X. Wu, S. Tavildar, S. Shakkottai, T. Richardson, J. Li, R. Laroia, and A. Jovicic, "FlashLinQ: A synchronous distributed scheduler for peer-to-peer ad hoc networks," *IEEE/ACM Transactions on Networking (ToN)*, vol. 21, no. 4, pp. 1215–1228, 2013.

[31] S. Salehi, L. Li, C.-C. Shen, L. Cimini, and J. Graybeal, "Traffic Differentiation in Dense WLANs with CSMA/ECA-DR MAC Protocol," in *2018 IEEE 88th Vehicular Technology Conference (VTC-Fall)*. IEEE, 2018, pp. 1–5.

[32] J. L. Sobrinho, R. De Haan, and J. M. Brazio, "Why RTS-CTS is not your ideal wireless LAN multiple access protocol," in *IEEE Wireless Communications and Networking Conference, 2005*, vol. 1. IEEE, 2005, pp. 81–87.

[33] E. Khorov, A. Kiryanov, A. Lyakhov, and G. Bianchi, "A Tutorial on IEEE 802.11 ax High Efficiency WLANs," *IEEE Communications Surveys & Tutorials*, 2018.

[34] O. Sharon and Y. Alpert, "Scheduling strategies and throughput optimization for the Downlink for IEEE 802.11ax and IEEE 802.11ac based networks," *arXiv preprint arXiv:1709.04818*, 2017.

[35] G. Bianchi, "Performance analysis of the ieee 802.11 distributed coordination function," *IEEE Journal on selected areas in communications*, vol. 18, no. 3, pp. 535–547, 2000.

[36] B. Bellalta and K. Kosek-Szott, "AP-initiated Multi-User Transmissions in IEEE 802.11ax WLANs," *arXiv preprint arXiv:1702.05397*, 2017.

[37] L. Lanante, H. O. T. Uwai, Y. Nagao, M. Kurosaki, and C. Ghosh, "Performance analysis of the 802.11ax UL OFDMA random access protocol in dense networks," in *Communications (ICC), 2017 IEEE International Conference on.* IEEE, 2017, pp. 1–6.

[38] G. Naik, S. Bhattarai, and J.-M. J. Park, "Performance Analysis of Uplink Multi-User OFDMA in IEEE 802.11ax."

[39] O. Sharon and Y. Alpert, "Scheduling Strategies and Throughput Optimization for the Uplink for IEEE 802.11ax and IEEE 802.11ac Based Networks," *arXiv preprint arXiv:1803.10657*, 2018.

[40] E. Khorov, V. Loginov, and A. Lyakhov, "Several EDCA parameter sets for improving channel access in IEEE 802.11ax networks," in *Wireless Communication Systems (ISWCS), 2016 International Symposium on.* IEEE, 2016, pp. 419–423.

[41] M. Karaca, S. Bastani, B. E. Priyanto, M. Safavi, and B. Landfeldt, "Resource management for OFDMA based next generation 802.11 WLANs," in *Wireless and Mobile Networking Conference (WMNC), 2016 9th IFIP.* IEEE, 2016, pp. 57–64.

[42] J. Jang and K. B. Lee, "Transmit power adaptation for multiuser OFDM systems," *IEEE Journal on selected areas in communications*, vol. 21, no. 2, pp. 171–178, 2003.

[43] K. Kim, Y. Han, and S.-L. Kim, "Joint subcarrier and power allocation in uplink OFDMA systems," *IEEE Communications Letters*, vol. 9, no. 6, pp. 526–528, 2005.

[44] C. Y. Ng and C. W. Sung, "Low complexity subcarrier and power allocation for utility maximization in uplink OFDMA systems," *IEEE Transactions on Wireless Communications*, vol. 7, no. 5, 2008.

[45] K. Wang and K. Psounis, "Scheduling and Resource Allocation in 802.11ax," in *IEEE INFOCOM 2018-IEEE Conference on Computer Communications*. IEEE, 2018, pp. 279–287.

[46] D. Bankov, A. Didenko, E. Khorov, V. Loginov, and A. Lyakhov, "IEEE 802.11ax uplink scheduler to minimize, delay: A classic problem with new constraints," in *Personal, Indoor, and Mobile Radio Communications (PIMRC), 2017 IEEE 28th Annual International Symposium on*. IEEE, 2017, pp. 1–5.

[47] D. Bankov, A. Didenko, E. Khorov, and A. Lyakhov, "OFDMA Uplink Scheduling in IEEE 802.11ax Networks," in *2018 IEEE International Conference on Communications (ICC)*. IEEE, 2018, pp. 1–6.

[48] K. Dovelos and B. Bellalta, "Optimal Resource Allocation for Uplink OFDMA in 802.11ax Networks," *arXiv preprint arXiv:1811.00957*, 2018.

[49] G. Liu, L. Li, L. J. Cimini, and C.-C. Shen, "Extending proportional fair scheduling to buffer-aided relay access networks," *IEEE Transactions on Vehicular Technology*, vol. 68, no. 1, pp. 1041–1044, 2018.

[50] A. Esmailpour, S. Salehi, and N. Safavi, "Quality of service differentiation measurements in 4G networks," in *2013 Wireless Telecommunications Symposium (WTS)*. IEEE, 2013, pp. 1–5.

[51] S. Salehi, "Impact of a two-layer QoS-aware channel-aware packet scheduler on end-to-end delay and throughput of LTE," Master's thesis, University of New Haven, CT, USA, 2013.

[52] M. Hemmati, B. McCormick, and S. Shirmohammadi, "QoE-Aware Bandwidth Allocation for Video Traffic Using Sigmoidal Programming," *IEEE MultiMedia*, vol. 24, no. 4, pp. 80–90, 2017.

[53] S. Shenker, "Fundamental design issues for the future Internet," *IEEE Journal on selected areas in communications*, vol. 13, no. 7, pp. 1176–1188, 1995.

[54] Aruba, "802.11AX," https://www.arubanetworks.com/assets/wp/WP_802.11AX.pdf, date accessed: August, 2018.

[55] J. Meinilä, P. Kyösti, T. Jämsä, and L. Hentilä, "WINNER II channel models," *Radio Technologies and Concepts for IMT-Advanced*, pp. 39–92, 2009.

[56] S. Andersen, "Internet Low Bit Rate Codec (iLBC)," https://tools.ietf.org/html/rfc3951, date accessed: September, 2019, Tech. Rep.

[57] E. Bastug, M. Bennis, M. Médard, and M. Debbah, "Towards Interconnected Virtual Reality: Opportunities, Challenges and Enablers," *IEEE Communications Magazine*, vol. 55, no. 6, pp. 110–117, June 2017.

[58] O. Abari, D. Bharadia, A. Duffield, and D. Katabi, "Enabling High-Quality Untethered Virtual Reality," in *14th USENIX Symposium on Networked Systems Design and Implementation*, Boston, MA, March 27-29 2017.

[59] Qualcomm, "Making Immersive Virtual Reality Possible in Mobile," Tech. Rep., March 2016.

[60] ABI Research, "Augmented and Virtual Reality: the First Wave of 5G Killer Apps," Tech. Rep., February 2017.

[61] M. S. Elbamby, C. Perfecto, M. Bennis, and K. Doppler, "Toward low-latency and ultra-reliable virtual reality," *IEEE Network*, vol. 32, no. 2, pp. 78–84, 2018.

[62] C. Perfecto, M. S. ElBamby, J. Del Ser, and M. Bennis, "Taming the latency in multi-user VR 360°: A QoE-aware deep learning-aided multicast framework," *CoRR [Online]. Arxiv Prepr. abs/1811.07388*, 2018.

[63] J. Park and M. Bennis, "URLLC-eMBB slicing to support VR multimodal perceptions over wireless cellular systems," in *2018 IEEE Global Communications Conference (GLOBECOM)*. IEEE, 2018, pp. 1–7.

[64] Y. Sun, Z. Chen, M. Tao, and H. Liu, "Communications, caching and computing for mobile virtual reality: Modeling and tradeoff," *IEEE Transactions on Communications*, 2019.

[65] X. Liu, C. Vlachou, F. Qian, and K. H. Kim, "Supporting untethered multi-user VR over enterprise Wi-Fi," in *29th ACM SIGMM Workshop on Network and Operating Systems Support for Digital Audio and Video, NOSSDAV 2019*. Association for Computing Machinery, Inc, 2019, pp. 25–30.

[66] U. OOI, "US Ocean Observatories Initiative (OOI)," http://oceanobservatories.org/observatories/, 2017, accessed: Mar 4, 2017.

[67] MBARI, "Monterey accelerated research system (mars)," http://www.mbari.org/at-sea/cabled-observatory/, 2017, accessed: Mar 4, 2017.

[68] EMSO, "European-scale distributed research infrastructure of seafloor & water-column observatories (emso)," http://www.emso-eu.org/, 2017, accessed: Mar 4, 2017.

[69] Ocean Networks Canada, "Neptune," http://www.oceannetworks.ca/observatories/pacific, 2017, accessed: Mar 4, 2017.

[70] M. Chaffey, L. Bird, J. Erickson, J. Graybeal, A. Hamilton, K. Headley, M. Kelley, L. McBride, E. Mellinger, T. Meese, T. O'Reilly, W. Paul, M. Risi, and W. Radochonski, "MBARI's buoy based seafloor observatory design," in *OCEANS'04. MTTS/IEEE TECHNO-OCEAN'04*, vol. 4. IEEE, 2004, pp. 1975–1984.

[71] F. Zhang, G. Marani, R. N. Smith, and H. T. Choi, "Future trends in marine robotics," *IEEE Robotics & Automation Magazine*, vol. 22, no. 1, pp. 14–122, 2015.

[72] J. B. De Sousa and G. A. Gonçalves, "Unmanned vehicles for environmental data collection," *Clean Technologies and Environmental Policy*, vol. 13, no. 2, pp. 369–380, 2011.

[73] S. Redfield, "Cooperation between underwater vehicles," in *Marine Robot Autonomy*. Springer, 2013, pp. 257–286.

[74] B. Reed, J. Leighton, M. Stojanovic, and F. Hover, "Multi-vehicle dynamic pursuit using underwater acoustics," in *Robotics Research*. Springer, 2016, pp. 79–94.

[75] S. Petillo, A. Balasuriya, and H. Schmidt, "Autonomous adaptive environmental assessment and feature tracking via autonomous underwater vehicles," in *OCEANS 2010 IEEE-Sydney*. IEEE, 2010, pp. 1–9.

[76] F. Maurelli, P. Patrón, J. Cartwright, J. Sawas, Y. Petillot, and D. Lane, "Integrated MCM missions using heterogeneous fleets of AUVs," in *OCEANS, 2012-Yeosu*. IEEE, 2012, pp. 1–7.

[77] N. E. Leonard, "Cooperative vehicle environmental monitoring," in *Springer Handbook of Ocean Engineering*. Springer, 2016, pp. 441–458.

[78] P. F. Lermusiaux, T. Lolla, P. J. Haley Jr, K. Yigit, M. P. Ueckermann, T. Sondergaard, and W. G. Leslie, "Science of autonomy: time-optimal path planning and adaptive sampling for swarms of ocean vehicles," in *Springer Handbook of Ocean Engineering*. Springer, 2016, pp. 481–498.

[79] R. Rahman and M. Frater, "Delay-tolerant networks (dtns) for underwater communications," in *Advances in Delay-Tolerant Networks (DTNs)*. Elsevier, 2015, pp. 81–103.

[80] A. Syed, W. Ye, B. Krishnamachari, and J. Heidemann, "Understanding Spatio-Temporal Uncertainty in Medium Access with ALOHA Protocols," in *Proc. WUWNet*, 2007, pp. 41–48.

[81] MOOS-IvP, "Open source C++ modules for providing autonomy on robotic platforms, in particular autonomous marine vehicles," http://oceanai.mit.edu/moos-ivp/pmwiki/pmwiki.php, 2017, accessed: Mar 4, 2017.

[82] C. C. Sotzing and D. M. Lane, "Improving the coordination efficiency of limited-communication multi–autonomus underwater vehicle operations using a multia-gent architecture," *Journal of Field Robotics*, vol. 27, no. 4, pp. 412–429, 2010.

[83] Z. Guo, B. Wang, and J.-H. Cui, "Prediction Assisted Single-copy Routing in Underwater Delay Tolerant Networks," in *Global Telecommunications Conference (GLOBECOM 2010), 2010 IEEE*, Miami, Florida, USA, 2010.

[84] X. Hong, M. Kuai, and W. Hu, "Routing with Bridging Nodes for Drifting Mobility," in *WUWNet '12 Proceedings of the Seventh ACM International Conference on Underwater Networks and Systems*, Los Angeles, CA, USA, 2012.

[85] S. Yoon, A. K. Azad, H. Oh, and S. Kim, "AURP: An AUV-Aided Underwater Routing Protocol for Underwater Acoustic Sensor Networks," *Sensors*, vol. 12, no. 2, pp. 1827–1845, 2012.

[86] I. Katz, "A Delay-Tolerant Networking Framework for Mobile Underwater Acoustic Networks," 2007. [Online]. Available: http://www.cs.unh.edu/cnrg/publications/uust07-ikatz.pdf

[87] F. J. L. Ribeiro, A. C. P. Pedroza, and L. H. M. K. Costa, "Deepwater Monitoring System Using Logistic-Support Vessels in Underwater Sensor Networks," *IEEE Latin America Transactions*, vol. 10, no. 1, pp. 1324–1331, 2012.

[88] J.-H. Cui, J. Kong, M. Gerla, and S. Zhou, "The challenges of building mobile underwater wireless networks for aquatic applications," *IEEE Network*, vol. 20, no. 3, pp. 12–18, 2006.

[89] I. Vasilescu, K. Kotay, D. Rus, M. Dunbabin, and P. Corke, "Data collection, storage, and retrieval with an underwater sensor network," in *Proceedings of the 3rd international conference on Embedded networked sensor systems*. ACM, 2005, pp. 154–165.

[90] A. P. Shirodkar and S. Borkar, "Autonomous Surface Craft and a Significant Operating System–an Overview," 2014.

[91] S. Brizzolara and R. A. Brizzolara, "Autonomous Sea Surface Vehicles," in *Springer Handbook of Ocean Engineering*. Springer, 2016, pp. 323–340.

[92] Z. Liu, Y. Zhang, X. Yu, and C. Yuan, "Unmanned surface vehicles: An overview of developments and challenges," *Annual Reviews in Control*, vol. 41, pp. 71–93, 2016.

[93] F. García-Córdova and A. Guerrero-González, "Intelligent navigation for a solar powered unmanned underwater vehicle," *International Journal of Advanced Robotic Systems*, vol. 10, no. 4, p. 185, 2013.

[94] A. Bahr, J. J. Leonard, and M. F. Fallon, "Cooperative localization for autonomous underwater vehicles," *The International Journal of Robotics Research*, vol. 28, no. 6, pp. 714–728, 2009.

[95] M. F. Fallon, G. Papadopoulos, and J. J. Leonard, "Cooperative AUV navigation using a single surface craft," in *Field and service robotics*. Springer, 2010, pp. 331–340.

[96] S. E. Webster, L. L. Whitcomb, and R. M. Eustice, "Preliminary results in decentralized estimation for single-beacon acoustic underwater navigation," *Robotics: Science and Systems VI*, pp. 1–8, 2010.

[97] J. Curcio, J. Leonard, and A. Patrikalakis, "SCOUT-a low cost autonomous surface platform for research in cooperative autonomy," in *OCEANS, 2005. Proceedings of MTS/IEEE*. IEEE, 2005, pp. 725–729.

[98] E. Desa, P. K. Maurya, A. Pereira, A. M. Pascoal, R. Prabhudesai, A. Mascarenhas, R. Madhan, S. Matondkar, G. Navelkar, S. Prabhudesai, and S. Afzulpurkar, "A small autonomous surface vehicle for ocean color remote sensing," *IEEE Journal of Oceanic Engineering*, vol. 32, no. 2, pp. 353–364, 2007.

[99] *A Low Cost System for Autonomous Surface Vehicle based Hydrographic Survey*, March 16 - 19 2015.

[100] T. C. O'Reilly, B. Kieft, and M. Chaffey, "Communications relay and autonomous tracking applications for Wave Glider," in *OCEANS 2015-Genova*. IEEE, 2015, pp. 1–6.

[101] J. B. de Sousa, J. Pereira, J. Alves, M. Galocha, B. Pereira, C. Lourenço, and M. Portuguesa, "Experiments in multi-vehicle operations: The Rapid Environmental Picture Atlantic exercise 2014," in *OCEANS 2015-Genova*. IEEE, 2015, pp. 1–7.

[102] "Multi-domain autonomous mobile network for Sensing, author=Taher, Tawfiq and Viswanathan, Vinothkumar and Varghese, Tony and Jiang, Hongchuan and Patrikalakis, Nicholas and Cloitre, Audren," in *OCEANS 2016 MTS/IEEE Monterey*. IEEE, 2016, pp. 1–6.

[103] M. Sasano, S. Inaba, A. Okamoto, T. Seta, K. Tamura, T. Ura, S. Sawada, and T. Suto, "Development of a regional underwater positioning and communication system for control of multiple autonomous underwater vehicles," in *Autonomous Underwater Vehicles (AUV), 2016 IEEE/OES*. IEEE, 2016, pp. 431–434.

[104] M. R. Benjamin, H. Schmidt, P. M. Newman, and J. J. Leonard, "Nested autonomy for unmanned marine vehicles with MOOS-IvP," *Journal of Field Robotics*, vol. 27, no. 6, pp. 834–875, 2010.

[105] T. Schneider and H. Schmidt, "Unified command and control for heterogeneous marine sensing networks," *Journal of Field Robotics*, vol. 27, no. 6, pp. 876–889, 2010.

[106] I. Couzin, J. Krause, N. Franks, and S. Levin, "Effective leadership and decision-making in animal groups on the move," *Nature*, vol. 433 (7025), pp. 513–516, 2005.

[107] I. D. Couzin, J. Krause, R. James, G. D. Ruxton, and N. R. Franks, "Collective memory and spatial sorting in animal groups," *Journal of theoretical biology*, vol. 218, no. 1, pp. 1–11, 2002.

[108] FreeWave, http://www.freewave.com/wp-content/uploads/LDS0001HTE_Rev_A_HT_PE.pdf, 2017, accessed: Mar 4, 2018.

[109] A. F. Harris III and M. Zorzi, "Modeling the underwater acoustic channel in ns2," in *Proceedings of the 2nd international conference on Performance evaluation methodologies and tools*. ICST (Institute for Computer Sciences, Social-Informatics and Telecommunications Engineering), 2007, p. 18.

[110] Y. Guan, C.-C. Shen, and J. Yackoski, "MAC scheduling for high throughput underwater acoustic networks," in *Wireless Communications and Networking Conference (WCNC), 2011 IEEE*. IEEE, 2011, pp. 197–202.

[111] J.-H. Cui, J. Kong, M. Gerla, and S. Zhou, "The challenges of building mobile underwater wireless networks for aquatic applications," *Ieee Network*, vol. 20, no. 3, pp. 12–18, 2006.

[112] S. Climent, A. Sanchez, J. V. Capella, N. Meratnia, and J. J. Serrano, "Underwater acoustic wireless sensor networks: advances and future trends in physical, MAC and routing layers," *Sensors*, vol. 14, no. 1, pp. 795–833, 2014.

[113] D. Pompili, T. Melodia, and I. F. Akyildiz, "A CDMA-based medium access control for underwater acoustic sensor networks," *IEEE Transactions on Wireless Communications*, vol. 8, no. 4, 2009.

[114] G. Fan, H. Chen, L. Xie, and K. Wang, "An improved CDMA-based MAC protocol for underwater acoustic wireless sensor networks," in *Wireless Communications, Networking and Mobile Computing (WiCOM), 2011 7th International Conference on*. IEEE, 2011, pp. 1–4.

[115] L. Hong, F. Hong, Z. Guo, and Z. Li, "ECS: Efficient communication scheduling for underwater sensor networks," *Sensors*, vol. 11, no. 3, pp. 2920–2938, 2011.

[116] C.-C. Hsu, K.-F. Lai, C.-F. Chou, and K.-J. Lin, "ST-MAC: Spatial-temporal MAC scheduling for underwater sensor networks," in *INFOCOM 2009, IEEE*. IEEE, 2009, pp. 1827–1835.

[117] W. van Kleunen, N. Meratnia, and P. J. Havinga, "A set of simplified scheduling constraints for underwater acoustic mac scheduling," in *Advanced Information Networking and Applications (WAINA), 2011 IEEE Workshops of International Conference on*. IEEE, 2011, pp. 902–907.

[118] A. A. Syed, W. Ye, and J. Heidemann, "T-Lohi: A new class of MAC protocols for underwater acoustic sensor networks," in *INFOCOM 2008. The 27th Conference on Computer Communications. IEEE*. IEEE, 2008, pp. 231–235.

[119] P. Xie and J.-H. Cui, "R-MAC: An energy-efficient MAC protocol for underwater sensor networks," in *International Conference on Wireless Algorithms, Systems and Applications (WASA 2007)*. IEEE, 2007, pp. 187–198.

[120] J. Yackoski and C.-C. Shen, "UW-FLASHR: Achieving high channel utilization in a time-based acoustic MAC protocol," in *Proceedings of the third ACM international workshop on Underwater Networks*. ACM, 2008, pp. 59–66.

[121] G. Fan, H. Chen, L. Xie, and K. Wang, "A hybrid reservation-based MAC protocol for underwater acoustic sensor networks," *Ad Hoc Networks*, vol. 11, no. 3, pp. 1178–1192, 2013.

[122] A. A. Syed, J. S. Heidemann *et al.*, "Time Synchronization for High Latency Acoustic Networks."

[123] N. Chirdchoo, W.-S. Soh, and K. C. Chua, "MU-Sync: a time synchronization protocol for underwater mobile networks," in *Proceedings of the third ACM international workshop on Underwater Networks*. ACM, 2008, pp. 35–42.

[124] Y. Noh, U. Lee, S. Han, P. Wang, D. Torres, J. Kim, and M. Gerla, "DOTS: A propagation delay-aware opportunistic MAC protocol for mobile underwater networks," *IEEE Transactions on Mobile Computing*, vol. 13, no. 4, pp. 766–782, 2014.

[125] C. Li, Y. Xu, Q. Wang, B. Diao, Z. An, Z. Chen, and Z. Luo, "FDCA: A Full-Duplex Collision Avoidance MAC Protocol for Underwater Acoustic Networks," *IEEE Sensors Journal*, vol. 16, no. 11, pp. 4638–4647, 2016.

[126] M. Molins and M. Stojanovic, "Slotted FAMA: a MAC protocol for underwater acoustic networks," in *OCEANS 2006-Asia Pacific*. IEEE, 2007, pp. 1–7.

[127] C. L. Fullmer and J. Garcia-Luna-Aceves, "Solutions to hidden terminal problems in wireless networks," in *ACM SIGCOMM Computer Communication Review*, vol. 27, no. 4. ACM, 1997, pp. 39–49.

[128] M. Stojanovic, "Optimization of a data link protocol for an underwater acoustic channel," in *Europe Oceans 2005*, vol. 1. IEEE, 2005, pp. 68–73.

[129] W. W. Au, "Characteristics of dolphin sonar signals," in *The sonar of dolphins*. Springer, 1993, pp. 115–139.

[130] L. Li, S. Salehi, C.-C. Shen, L. J. Cimini, and J. Graybeal, "Multi-Carrier LAA with Adaptive Energy Detection and Carrier Selection," in *2019 IEEE 90th Vehicular Technology Conference (VTC2019-Fall)*. IEEE, 2019, pp. 1–5.

[131] S. Salehi, A. Song, and C.-C. Shen, "Hybrid Infrastructure for AUV Operations," in *Magnetic Communications: From Theory to Practice*, F. Hu, Ed. CRC Press, 2018, ch. 9, pp. 151–169.

Appendix

PERMISSIONS

Chapter 2 is published in IEEE 88th Vehicular Technology Conference (VTC-fall), 2018 [31]. The obtained permission is shown below.

Figure A.1: Permission from IEEE to include the paper in the dissertation document.

Chapter 6 is published as a book chapter in [131], the permission obtained from CRC press is included as follows.

PLS Clear

PARTIES:

1. **Taylor and Francis Group LLC (Books) US** [CompanyNumber] (Licensor); and
2. **Seyedmohammad Salehi** (Licensee).

Thank you for your recent permission request. Some permission requests for use of material published by the Licensor, such as this one, are now being facilitated by PLSclear.

Set out in this licence cover sheet (the **Licence Cover Sheet**) are the principal terms under which Licensor has agreed to license certain Licensed Material (as defined below) to Licensee. The terms in this Licence Cover Sheet are subject to the attached General Terms and Conditions, which together with this Licence Cover Sheet constitute the licence agreement (the **Licence**) between Licensor and Licensee as regards the Licensed Material. The terms set out in this Licence Cover Sheet take precedence over any conflicting provision in the General Terms and Conditions.

Free Of Charge Licence Terms

Licence Date:	28/01/2020
PLSclear Ref No:	33097

The Licensor

Company name:	Taylor and Francis Group LLC (Books) US
Address:	711 3rd Avenue New York 10017 United States US

The Licensee

Licensee Contact Name:	Seyedmohammad Salehi
Licensee Address:	18 Amstel Ave Smith 214 Newark 19716 United States

Licensed Material

title:	Magnetic Communications: From Theory to Practice
ISBN:	9781498799751
publisher:	Taylor and Francis Group LLC (Books) US

chapter name	Hybrid Infrastructure for AUV Operations
chapter number	9
Number of words	2000
page range	151-169
total number of pages	19
Are you requesting permission to reuse your own work?	Yes. I am the author

For Use In Licensee's Publication(s)

usage type	Book, Journal, Magazine or Academic Paper...-Thesis
distribution	5
estimated publication date	March 2020
language	English
number of pages	145
publication title	Delay and Collision Reduction in Wireless Networks
type of document	PhD dissertation

Rights Granted

Exclusivity:	Non-Exclusive
Format:	Thesis
Language:	English
Territory:	
Duration:	Lifetime of Licensee's Edition
Maximum Circulation:	5

GENERAL TERMS AND CONDITIONS

1. Definitions and Interpretation

1.1 Capitalised words and expressions in these General Terms and Conditions have the meanings given to them in the Licence Cover Sheet.

1.2 In this Licence any references (express or implied) to statutes or provisions are references to those statutes or provisions as amended or re-enacted from time to time. The term including will be construed as illustrative, without limiting the sense or scope of the words preceding it. A reference to in writing or written includes faxes and email. The singular includes the plural and vice versa.